

DETERMINING AND MODULATING E2-HECT
BINDING AFFINITY AND SPECIFICITY

by
Ziad Moustafa Eletr

A dissertation submitted to the faculty of the University of North Carolina at Chapel Hill in partial fulfillment of the requirements for the degree of Doctor of Philosophy in the Department of Biochemistry and Biophysics (Program in Molecular and Cellular Biophysics).

Chapel Hill
2007

Approved by

Advisor: Brian Kuhlman

Reader: Henrik Dohlman

Reader: Nikolay Dokholyan

Reader: Gary Pielak

Reader: Matt Redinbo

© 2007
Ziad Moustafa Eletr
ALL RIGHTS RESERVED

ABSTRACT

ZIAD MOUSTAFA ELETR: Deciphering and Modulating the Determinants of
E2–HECT Binding and Specificity
(Under the direction of Brian Kuhlman)

The ubiquitin pathway regulates nearly all cellular processes in eukaryotes and consequently aberrations within the pathway can lead to a diversity of human diseases and disorders. Ubiquitin is a 76 residue protein that is conjugated to specific protein substrates via a cascade of enzymatic reactions that require an activating enzyme (E1), conjugating enzymes (E2s), and ligases (E3s). In humans there is a single E1, roughly 30 E2s, and hundreds of E3s. There are two main types of E3s that are structurally and functionally unrelated. RING E3s catalyze the direct transfer of ubiquitin from E2 to substrate while HECT E3s form a thioester intermediate with ubiquitin prior to transfer. In most cases E2s function with many E3s while E3s function with one or few homologous E2s. The study of diseases and disorders stemming from the ubiquitin pathway is complicated by the E1–E2–E3 hierarchy and by elusive E3 substrates. An attractive method to identify E3 substrates is to isolate specific E2–E3 interactions in the cell. One means to isolate E2–E3 interactions is to create altered specificity E2–E3 pairs that function with each other but not their wild type precursors nor other natural partners. The ability to create altered specificity E2–E3 pairs hinges on our understanding of the amino acid residues that dictate binding affinity and specificity. The intent of the work in this dissertation is to identify these determinants of binding affinity and specificity and rationally manipulate them. We have focused on the HECT class of E3s and began with the UbcH7–E6AP interaction as a model system. We used a combination of quantitative binding assays, mutagenesis, and ubiquitin transfer assays as well as rational and computation protein engineering to elucidate and manipulate the amino acid residues that govern E2–HECT binding affinity and specificity.

ACKNOWLEDGEMENTS

First and foremost I would like to thank Brian for the opportunity to pursue my doctoral dissertation under his direction. Throughout my dissertation challenging obstacles were encountered which would seemingly prevent the pursuit of our goals. Brian was always able to conceive creative and non-conventional experiments to overcome these barriers. Second I would like to thank Barry Lentz for the opportunity to join the Molecular and Cellular Biophysics Training Program. The first semester in the program was an intense journey best remembered and appreciated in retrospect. I would like to thank the faculty of the Department of Biochemistry and Biophysics for the training and education I received. I was exposed to many excellent courses which significantly influenced the work in this dissertation. My comrades in Biophysics Group II, Deanne Sammond and Gottfried Schroeder, deserve acknowledgement for the common anguish we shared and the moral support they provided. Last but not least I acknowledge my mother Zeinab and my father Moustafa. I am grateful for having them as parents as they taught me many invaluable lessons on life and helped me persevere during difficult times. Most influential is their hard work ethic which I've always admired and tried to emulate.

TABLE OF CONTENTS

	Page
LIST OF FIGURES	viii
LIST OF TABLES	x
LIST OF ABBREVIATIONS	xi
Chapter	
I INTRODUCTION TO THE UBIQUITIN PATHWAY	1
EARLY HISTORY OF THE UBIQUITIN PATHWAY	2
THE UBIQUITIN PATHWAY	3
E2 CONJUGATING ENZYMES	5
HECT E3 UBIQUITIN LIGASES	6
UBIQUITIN AND DISEASE	8
TOWARDS A NEW METHOD OF IDENTIFYING E3 SUBSTRATES	9
REFERENCES	11
II SEQUENCE DETERMINANTS OF E2–E6AP BINDING AFFINITY	
AND SPECIFICITY	16
ABSTRACT	17
INTRODUCTION	18
RESULTS	21

DISCUSSION	27
FIGURES	30
TABLES	36
MATERIALS AND METHODS.....	38
SUPPLEMENTARY DATA	41
REFERENCES	43
III INSIGHTS INTO E2–HECT BINDING AFFINITY AND SPECIFICITY	45
ABSTRACT	46
INTRODUCTION	47
RESULTS	49
DISCUSSION.....	54
FIGURES.....	57
TABLES	62
MATERIALS AND METHODS.....	64
SUPPLEMENTARY DATA	66
REFERENCES	68
IV MODULATING E2–HECT BINDING AND SPECIFICITY	71
ABSTRACT	72
INTRODUCTION	73
RESULTS	75
DISCUSSION.....	80
FIGURES.....	81
TABLES	82
MATERIALS AND METHODS.....	83
REFERENCES	84
V E2 CONJUGATING ENZYMES MUST DISENGAGE FROM	

THEIR E1 ENZYME BEFORE E3-DEPENDENT UBIQUITIN AND UBIQUITIN-LIKE TRANSFER	87
ABSTRACT	88
MAIN TEXT	89
FIGURES.....	93
SUPPLEMENTARY METHODS	95
SUPPLEMENTARY DATA	102
REFERENCES	105
VI CONCLUSIONS AND FUTURE DIRECTIONS	107
APPENDIX I: PHYLOGENETIC TREE OF HUMAN E2s	111
APPENDIX II: PHYLOGENETIC TREE OF HUMAN HECT E3s.....	112

LIST OF FIGURES

Figure	Page
2.1. Cartoon representation of the UbcH7–E6AP crystal structure.....	29
2.2. E6AP selectively interacts with UbcH7 and UbcH8	30
2.3. Mapping $\Delta\Delta G^{\circ}_{\text{bind}}$ from alanine scan studies onto the UbcH7–E6AP structure	31
2.4. <i>In vitro</i> activity of E6AP mutant proteins	32
2.5. UbcH7 and UbcH8 form nearly identical interactions with E6AP.....	33
2.6. Rationally manipulating UbcH5b to enhance binding to E6AP.....	34
2.7. Multiple sequence alignment of the E2-binding subdomain of Rsp5 family members and E6AP.....	35
2.8. Isothermal titration calorimetry of unmodified UbcH7 with E6AP	41
2.9. Duplicate ubiquitin transfer assay with E6AP mutants	42
3.1. E1–E2 transthiolation assay	57
3.2. The Nedd4L HECT domain selectively interacts with E2s from the UBC4/5 and E2-E subfamilies	58
3.3. E6AP weakly interacts with the UBC4/5 and E2-E subfamily members.....	59
3.4. Multiple sequence alignment of the E3-binding residues of the 15 E2s used in this study.....	60
3.5. E2–Nedd4L specificity determining residues.....	61
3.6. Sequence alignment of the 15 E2s used in this study.....	66
3.7. Sequence alignment of the four HECT E3s used in this study.....	67
4.1. Binding results from orthogonal and rational designs of the UbcH7–E6AP complex.....	81
5.1. An E2 binding to E1 and a to HECT E3 are mutually exclusive	93
5.2. E2s binding to E1s and to RING E3s is mutually exclusive	94
5.3. Enhanced affinity UbcH7-E6AP-HECT pair inhibits E1-mediated transthiolation at lower E6AP concentrations	102

5.4. Kinetics of E1-mediated UbcH7~[³² P]-ubiquitin formation in the presence	
and absence of high concentrations of E6AP-HECT	103

LIST OF TABLES

Table	Page
2.1. Measured dissociation constants for UbcH7 and E6AP(HECT) mutants	36
2.2. Measured $\Delta\Delta G^{\circ}_{\text{bind}}$ (kcal/mol) of UbcH7–E6AP hot spots in UbcH8(C97S)	37
3.1. Measured dissociation constants (in μM) for E2–HECT interactions.....	62
3.2. Measured dissociation constants (in μM) of E6AP and Nedd4L HECT domains for UbcH7 mutants.....	63
4.1. Measured dissociation constants for mutant UbcH7–E6AP interactions	82
5.1. Measured dissociation and inhibition constants for wild type and mutant UbcH7–E6AP-HECT interactions.....	104

LIST OF ABBREVIATIONS

APF-1: ATP dependent proteolysis factor I

ATP: adenosine triphosphate

β -ME: β -mercaptoethanol

CAND1: cullin associated and neddylation dissociated 1

E6AP: E6 associated protein

FP: fluorescence polarization

GLB: SDS-PAGE gel loading buffer

HECT: homology to E6AP carboxy-terminus

HPV: human papillomavirus

ISG15: IFN-stimulatory gene factor 15

PHD: plant homeodomain

RING: really interesting new gene

SDS-PAGE: sodium dodecyl sulfate-polyacrylamide gel electrophoresis

SUMO: small ubiquitin-like modifier

UBL: ubiquitin-like protein

WT: wild type

CHAPTER I

INTRODUCTION TO THE UBIQUITIN PATHWAY

EARLY HISTORY OF THE UBIQUITIN PATHWAY

The ubiquitin protein was discovered by Goldstein and colleagues in 1975 and named so because it was thought to be ubiquitously present in all living cells¹. A few years later, a unique protein structure was observed when modified histone H2A protein was found to have two N-termini but just one C-terminus². This branched protein structure was generated by an isopeptide bond between the ϵ -amino group of a histone H2A lysine and a glycine residue of the smaller polypeptide² which was shortly thereafter identified as ubiquitin³. The cellular role of protein modification by ubiquitin was largely discovered by Avram Hershko, his graduate student Aaron Ciechanover, and their collaborator Irwin Rose. In studying ATP-dependent protein degradation, Hershko and Ciechanover were able to fractionate rabbit reticulocyte lysates into two components: fraction I which contained a small thermostable protein they called APF-1 (subsequently identified as ubiquitin⁴) was void of proteolytic activity, but when combined with fraction II and ATP was able to reconstitute proteolysis⁵. Two years later in collaboration with Rose's lab, it was shown that ubiquitin is conjugated to reticulocyte proteins when fractions I and II were combined with ATP, suggesting that ubiquitination is a pre-requisite for degradation. Their results also suggested and that ubiquitin conjugation was likely carried out by an enzyme because conjugation activity was dependent on time and temperature⁶. The following report by Hershko, Ciechanover, Rose and co-workers showed that multiple ubiquitin molecules are conjugated in a processive manner (poly-ubiquitination) and that depletion of ATP results in liberation of ubiquitin molecules⁷. From this groundbreaking study, the authors predicted the activity of three components of the pathway; a factor promoting processive ubiquitin conjugation (E3 ligases), a factor with amidase activity (deubiquitinating enzymes), and a protease specific for ubiquitin conjugated proteins (26S proteasome)⁸. In an effort to isolate all components necessary for ubiquitination activity, Hershko and Ciechanover soon thereafter discovered the E1, E2, and E3 enzymes^{9; 10}. In 2004, the Nobel Prize in Chemistry was awarded to Ciechanover, Hershko, and Rose for their pioneering work in the discovery of the ubiquitin pathway.

THE UBIQUITIN PATHWAY

We now know that the ubiquitin pathway regulates virtually all cellular process in eukaryotes by targeting proteins for degradation by the 26S proteasome¹¹. A requirement for proteolysis via the 26S proteasome is a polymer of four or more ubiquitin molecules linked together via isopeptide bonds between the C-terminal glycine (G76) and lysine 48 (K48)¹². Ubiquitin has six other lysine residues (K6, K11, K27, K29, K33, and K63) all of which are capable of forming isopeptide linkages with G76 of a second ubiquitin molecule¹³. Less is known about the cellular fate of such modifications, but G76–K63 ubiquitin polymers are thought to serve a non-proteolytic role¹⁴. In addition, mono-ubiquitination of cell membrane receptors can trigger their internalization and degradation in the lysosome¹⁵. The hydrolysis of G76-mediated isopeptide bonds, or deubiquitination, adds an additional means to regulate the process of ubiquitination and is carried out by ~60 different proteins in humans¹⁶.

The tethering of ubiquitin to itself and to proteins substrates is achieved by E1, E2, and E3 enzymes. The E1 activating enzyme uses ATP to adenylate the C-terminus of ubiquitin to form a reactive ubiquitin molecule. Following adenylation, the E1 uses a cysteine residue to form a thioester intermediate with G76 of ubiquitin. The E1 then binds to an E2 conjugating enzyme, transferring ubiquitin to the E2 active-site cysteine to form a second thioester intermediate. E3 ligases are responsible for binding to E2 and substrate and these two binding events are carried out by distinct domains in a protein or by multiple proteins in a multisubunit E3 complex. Catalysis can proceed in two mechanisms and is dependent on the type E2-binding domain. Ubiquitin can be transferred directly from E2 to substrate (RING, PHD, and U-box E3s) or by first forming a third thioester with E3 prior to transfer to substrate (HECT E3s). In humans there is a single E1, ~33 E2s, and hundreds of E3s. Not all E2s and E3s can functionally interact. In general E2s function with many E3s while E3s only function with one or few E2s¹¹. This E2–E3 specificity is important for maintaining proper spatial and temporal degradation of specific proteins.

Ubiquitin-like proteins (UBLs) share homology with the ubiquitin protein. Like ubiquitin, UBLs are conjugated to lysine residues of a protein substrate using an E1–E2–E3 cascade. The roles of such modifications are diverse in function but do not lead to degradation. UBL pathways have dedicated E1, E2, and E3 enzymes that in general do function in the ubiquitin pathway. The best studied UBLs in humans are Nedd8, SUMO, and ISG15¹⁷. The Nedd8 modification functions to upregulate the cullin family of E3 ligases by relieving inhibition imposed by the CAND1 protein^{18; 19} and/or by recruiting the E2s to E3 complex^{20; 21; 22}. The SUMO modification can serve various functions such as preventing ubiquitination and degradation, localization to nuclear pores, and upregulating protein activity²³. Though the SUMO pathway has dedicated E3s²⁴, the SUMO E2 can directly bind and sumoylate substrates bearing the consensus sequence [I/V/L]-K-X-[D/E]^{17; 23}. The ISG15 UBL is likely involved in the innate immune response and recently a myriad of cellular proteins were shown to bear this modification upon stimulation with IFN- β ²⁵.

E2 CONJUGATING ENZYMES

In humans there are ~33 E2 enzymes all of which share a conserved catalytic core domain of ~150 amino acids. Some E2s have N- and C-terminal extensions that confer these E2s with diverse functions. For example the Nedd8 E2 Ubc12 possesses a unique N-terminal extension that is required for an optimal interaction with its cognate E1²⁶. Roughly fifty structures of E2s have been deposited in the RCSB protein databank. The E2 catalytic core domain is composed of a four-stranded β -sheet, four α -helices, and a 3_{10} helix proceeding to the active-site cysteine. The E2 catalytic core remains relatively unchanged when interacting with E1, E3s, and ubiquitin as evidenced from structures of E2s in complex with these proteins^{27; 28; 29; 30; 31}. These structures also suggested that the E1-binding and E3-binding sites of E2s partially overlap. This is indeed the case as a series of competitive binding experiments showed that E1 and E3 compete for E2 and that a ternary E1–E2–E3 complex is not formed³².

Crystal structures of the E2 UbcH7 in complex with a HECT E3²⁷ and a RING E3²⁸ revealed that E2s use similar residues to contact both types of E3s. In both structures the primary interface contact was contributed by the loop 4-Phe63 side-chain of UbcH7 (L4-Phe) which buries into hydrophobic grooves created by the E3s. Other contacts from UbcH7 were contributed from the N-terminal helix (H1), loop 4 (L4), loop 7 (L7) and to a lesser extent loop 2 (L2). In our studies on E2–E6AP specificity, we found that an L4-Phe is necessary for interacting with E6AP and that mutation to alanine reduced binding by 3 kcal/mol³³. This L4-Phe can also be considered a primary specificity determinant as all E2s that have been shown to function with HECT E3s possess a phenylalanine at this position³⁴. Amino acids within H1 and L7 are more varied across E2s and thought to dictate the specificity of E2–HECT interactions²⁷. Sequence alignment and phylogenetic analysis of the 33 human E2s shows that some share high sequence identity within and beyond the catalytic core (**Appendix I**). Additionally, these E2s paralogs are highly conserved within the E3-binding positions suggesting that these E2s will display similar specificities for E3s.

HECT E3 UBIQUITIN LIGASES

The first HECT domain characterized resided within the E6AP protein. E6AP was initially identified as a protein that cooperates with the E6 protein from oncogenic forms of the human papillomavirus to destabilize cellular levels of the p53 tumor suppressor protein³⁵. The conserved HECT domain is ~350 amino acids and always found at the C-terminus of E3s. Four crystal structures of HECT domains are now deposited in the RCSB protein databank^{27; 36; 37; 38}. The HECT domain adopts a bilobal structure with N-terminal lobe harboring the ~80 residue E2-binding subdomain and the C-terminal lobe containing the catalytic cysteine. A three residue hinge connects the two lobes which interact to form a conserved interface²⁷. Superimposition of the E2-binding domain of the four HECT crystal structures reveals that the orientations of the two are markedly different in each structure. Conformational flexibility of the HECT domain is known to be important for catalysis as mutations to the hinge and the interface of the two lobes have been shown to reduce ligase activity^{37; 39; 40}.

Different HECT E3s are capable of synthesizing different types of poly-ubiquitin chains (K48, K29, and K63) using distinct mechanisms suggesting additional roles for HECT E3s in non-proteolytic regulation of proteins^{13; 41}. The residues N-terminal to the HECT domain are responsible for substrate interactions. In humans there are at least 27 HECT E3s, of which nine are similar in their N-terminal domain architecture (**Appendix II**). These E3s represent the C2-WW-HECT superfamily of E3s and contain an N-terminal C2 domain (phospholipid binding) followed by 2-4 WW domains (poly-proline binding). Within this C2-WW-HECT superfamily are four HECT subfamilies (HERCW, AIP, Smurf, and Nedd4). These HECT paralogs share high identity throughout the C2, WW, and HECT domains. Though the superfamily is similar in domain architecture, the four subfamilies have subtle amino acid differences in their HECT domains which results in dissimilar preferences for E2s. For example the Nedd4 subfamily functionally interacts with the UBC4/5 E2s whereas the Smurf subfamily does not efficiently function with any E2s^{38; 42; 43}. To induce a functional E2 interaction, the Smurf2 protein must bind an additional protein Smad7

which specifically recruits UbcH7 to the HECT domain. HECT E3s from the same subfamily share high sequence identity within their E2-binding residues suggesting they function with similar E2 subfamilies. Indeed this has been observed for the Nedd4 and Nedd4L proteins⁴³.

UBIQUITIN AND DISEASE

It is well established that various human diseases and disorders are consequences of E3s improperly regulating their substrates^{44; 45}. For example, inherited disorders such as Angelman's syndrome, Liddle's syndrome, and autosomal recessive Parkinson's disease (AR-PD) have been linked to E3s with dysfunctional interactions with their substrates^{46; 47; 48; 49; 50}. In the case of Liddle's syndrome, the HECT E3 Nedd4 no longer binds to or ubiquitinates the epithelial Na⁺ channel (ENaC) ultimately resulting in stabilization of ENaC, increased Na⁺ uptake and hypertension^{51; 52}. In approximately 75% of patients with Angelman's syndrome, the maternal copy of the gene encoding the HECT E3 E6AP has been entirely deleted or has acquired mutations⁵³ that have been shown to reduce ligase activity^{39; 40}. Though a handful of E6AP substrates have been identified^{35; 39; 54; 55; 56}, none have been implicated in the pathogenesis of Angelman's syndrome. Similarly, approximately 50% of patients with AR-PD have acquired mutations to the gene encoding a RING E3 Parkin⁵⁷ but the link between Parkin substrates and the etiology of AR-PD remains unclear^{58; 59}.

In addition to inherited disorders, idiopathic diseases can arise from aberrant regulation of substrate ubiquitination. The pathology of sporadic neurodegenerative disorders like Parkinson's disease and Alzheimer's disease are partially the result of a dysfunctional ubiquitin pathway; the hallmark of these diseases is the accumulation of ubiquitinated proteins and inclusion bodies⁴⁵. Cervical carcinomas caused by human papillomavirus (HPV) are a result of a viral protein E6 hijacking E6AP to degrade the p53 tumor suppressor protein³⁵. Increased degradation of the cyclin dependent kinase inhibitor p27 has been linked to carcinomas of the colon, prostate, and breast⁶⁰. Given the breadth of the ubiquitin pathway, it is not surprising that a plethora of malignancies arise from dysregulation within the pathway. The identification of all the substrates of a given E3 would aid in the study and treatment of diseases stemming from the ubiquitin pathway

TOWARDS A NEW METHOD OF IDENTIFYING E3 SUBSTRATES

The identification of all the substrates of a given E3 is a challenging but very important task. Previous methods have relied on a variety of techniques including two-hybrid screens and coimmunoprecipitations. Though both approaches have led to the identification of numerous E3 substrates, both are inherently limited when applied to detecting E3–substrate interactions. The two-hybrid screen is usually performed in a host system so E3 substrates that require phosphorylation or other post-translational modifications prior to recognition by E3 may not bind E3 with sufficient affinity for detection. Coimmunoprecipitations are limited by the stability of the ubiquitinated substrate as deubiquitinating enzymes and the 26S proteasome function to remove ubiquitin and degraded the substrate. Inhibitors of the proteasome and deubiquitinating enzymes can be useful but again the context of the interaction has been altered. Clearly a better approach is needed. An ideal method would allow for the detection of low affinity E3–substrate interactions without significantly perturbing the cellular environment. One way to craft such a tool is by creating altered specificity E2–E3 pairs. Altered specificity pairs would allow a specific E2–E3 interaction to be isolated in the cell so that downstream events can be examined.

The manipulation of an E2–E3 pair has been demonstrated previously⁶¹. A charge swap interaction was generated across the UbcH5b-CNOT4 interface to create a mutant pair that no longer interacted with the WT precursors⁶¹. In this study the authors claim to have generated an altered specificity pair but the mutant proteins were not tested against other natural partners. A *bona fide* altered specificity E2–E3 pair must display two characteristics. First, the redesigned E2 and E3 proteins must interact favorably with one another but not with their wild-type precursors. Redesigned E2–E3 pairs displaying this property will be referred to as orthogonal E2–E3 pairs. Second, the redesigned E2–E3 pair should no longer interact favorably with other naturally occurring partners. This property is most important for E2s because each E2 usually interacts with multiple E3s. Since hundreds of proteins are ubiquitinated in the cell, the substrates of a specific E2–E3 pairs may remain difficult to detect. To circumvent this obstacle, instead of altered specificity pairs passing ubiquitin they could be

engineered to pass the UBL Nedd8 which has ~10 known substrates. To achieve a method like this, the following challenges must be resolved. (1) All the natural E2–E3 pairs that yield functional interactions must be identified. (2) A method to generate orthogonal E2–E3 pairs must be developed. Furthermore, orthogonal E2–E3 pairs must be screened against natural partners to test whether they are *bona fide* altered specificity pairs. (3) Engineered E2s must be able to bind to the Nedd8 E1 and form a Nedd8-E2 thioester intermediate. (4) The Nedd8-charged E2 must be able to pass Nedd8 to E3 and/or substrate. (5) A method to express altered specificity E2–E3 pairs in the cell must be developed. (6) Finally a method to detect and identify Nedd8-modified proteins must be developed. The work in this dissertation has focused on challenges (1) and (2). To simply matters we have chosen to restrict our characterization and engineering of E2–E3 interactions to the HECT family of E3 enzymes.

REFERENCES

1. Goldstein, G., Scheid, M., Hammerling, U., Schlesinger, D. H., Niall, H. D. & Boyse, E. A. (1975). Isolation of a polypeptide that has lymphocyte-differentiating properties and is probably represented universally in living cells. *Proc Natl Acad Sci U S A* **72**, 11-5.
2. Goldknopf, I. L. & Busch, H. (1977). Isopeptide linkage between nonhistone and histone 2A polypeptides of chromosomal conjugate-protein A24. *Proc Natl Acad Sci U S A* **74**, 864-8.
3. Hunt, L. T. & Dayhoff, M. O. (1977). Amino-terminal sequence identity of ubiquitin and the nonhistone component of nuclear protein A24. *Biochem Biophys Res Commun* **74**, 650-5.
4. Wilkinson, K. D., Urban, M. K. & Haas, A. L. (1980). Ubiquitin is the ATP-dependent proteolysis factor I of rabbit reticulocytes. *J Biol Chem* **255**, 7529-32.
5. Ciechanover, A., Hod, Y. & Hershko, A. (1978). A heat-stable polypeptide component of an ATP-dependent proteolytic system from reticulocytes. *Biochem Biophys Res Commun* **81**, 1100-5.
6. Ciechanover, A., Heller, H., Elias, S., Haas, A. L. & Hershko, A. (1980). ATP-dependent conjugation of reticulocyte proteins with the polypeptide required for protein degradation. *Proc Natl Acad Sci U S A* **77**, 1365-8.
7. Hershko, A., Ciechanover, A., Heller, H., Haas, A. L. & Rose, I. A. (1980). Proposed role of ATP in protein breakdown: conjugation of protein with multiple chains of the polypeptide of ATP-dependent proteolysis. *Proc Natl Acad Sci U S A* **77**, 1783-6.
8. Wilkinson, K. D. (2005). The discovery of ubiquitin-dependent proteolysis. *Proc Natl Acad Sci U S A* **102**, 15280-2.
9. Ciechanover, A., Heller, H., Katz-Etzion, R. & Hershko, A. (1981). Activation of the heat-stable polypeptide of the ATP-dependent proteolytic system. *Proc Natl Acad Sci U S A* **78**, 761-5.
10. Hershko, A., Heller, H., Elias, S. & Ciechanover, A. (1983). Components of ubiquitin-protein ligase system. Resolution, affinity purification, and role in protein breakdown. *J Biol Chem* **258**, 8206-14.
11. Hershko, A. & Ciechanover, A. (1998). The ubiquitin system. *Annu Rev Biochem* **67**, 425-79.
12. Chau, V., Tobias, J. W., Bachmair, A., Marriott, D., Ecker, D. J., Gonda, D. K. & Varshavsky, A. (1989). A multiubiquitin chain is confined to specific lysine in a targeted short-lived protein. *Science* **243**, 1576-83.
13. Kim, H. T., Kim, K. P., Lledias, F., Kisselev, A. F., Scaglione, K. M., Skowyra, D., Gygi, S. P. & Goldberg, A. L. (2007). Certain E2-E3 pairs synthesize nondegradable forked ubiquitin chains containing all possible isopeptide linkages. *J Biol Chem*.
14. Pickart, C. M. (2001). Mechanisms underlying ubiquitination. *Annu Rev Biochem* **70**, 503-33.

15. Hicke, L. (1999). Gettin' down with ubiquitin: turning off cell-surface receptors, transporters and channels. *Trends Cell Biol* **9**, 107-12.
16. Wilkinson, K. D. (1997). Regulation of ubiquitin-dependent processes by deubiquitinating enzymes. *Faseb J* **11**, 1245-56.
17. Kerscher, O., Felberbaum, R. & Hochstrasser, M. (2006). Modification of proteins by ubiquitin and ubiquitin-like proteins. *Annu Rev Cell Dev Biol* **22**, 159-80.
18. Liu, J., Furukawa, M., Matsumoto, T. & Xiong, Y. (2002). NEDD8 modification of CUL1 dissociates p120(CAND1), an inhibitor of CUL1-SKP1 binding and SCF ligases. *Mol Cell* **10**, 1511-8.
19. Zheng, J., Yang, X., Harrell, J. M., Ryzhikov, S., Shim, E. H., Lykke-Andersen, K., Wei, N., Sun, H., Kobayashi, R. & Zhang, H. (2002). CAND1 binds to unneddylated CUL1 and regulates the formation of SCF ubiquitin E3 ligase complex. *Mol Cell* **10**, 1519-26.
20. Kawakami, T., Chiba, T., Suzuki, T., Iwai, K., Yamanaka, K., Minato, N., Suzuki, H., Shimbara, N., Hidaka, Y., Osaka, F., Omata, M. & Tanaka, K. (2001). NEDD8 recruits E2-ubiquitin to SCF E3 ligase. *Embo J* **20**, 4003-12.
21. Zheng, N., Schulman, B. A., Song, L., Miller, J. J., Jeffrey, P. D., Wang, P., Chu, C., Koepp, D. M., Elledge, S. J., Pagano, M., Conaway, R. C., Conaway, J. W., Harper, J. W. & Pavletich, N. P. (2002). Structure of the Cul1-Rbx1-Skp1-F boxSkp2 SCF ubiquitin ligase complex. *Nature* **416**, 703-9.
22. Sakata, E., Yamaguchi, Y., Miyauchi, Y., Iwai, K., Chiba, T., Saeki, Y., Matsuda, N., Tanaka, K. & Kato, K. (2007). Direct interactions between NEDD8 and ubiquitin E2 conjugating enzymes upregulate cullin-based E3 ligase activity. *Nat Struct Mol Biol* **14**, 167-8.
23. Yeh, E. T., Gong, L. & Kamitani, T. (2000). Ubiquitin-like proteins: new wines in new bottles. *Gene* **248**, 1-14.
24. Jackson, P. K. (2001). A new RING for SUMO: wrestling transcriptional responses into nuclear bodies with PIAS family E3 SUMO ligases. *Genes Dev* **15**, 3053-8.
25. Zhao, C., Denison, C., Huibregtse, J. M., Gygi, S. & Krug, R. M. (2005). Human ISG15 conjugation targets both IFN-induced and constitutively expressed proteins functioning in diverse cellular pathways. *Proc Natl Acad Sci U S A* **102**, 10200-5.
26. Huang, D. T., Miller, D. W., Mathew, R., Cassell, R., Holton, J. M., Roussel, M. F. & Schulman, B. A. (2004). A unique E1-E2 interaction required for optimal conjugation of the ubiquitin-like protein NEDD8. *Nat Struct Mol Biol* **11**, 927-35.
27. Huang, L., Kinnucan, E., Wang, G., Beaudenon, S., Howley, P. M., Huibregtse, J. M. & Pavletich, N. P. (1999). Structure of an E6AP-UbcH7 complex: insights into ubiquitination by the E2-E3 enzyme cascade. *Science* **286**, 1321-6.
28. Zheng, N., Wang, P., Jeffrey, P. D. & Pavletich, N. P. (2000). Structure of a c-Cbl-UbcH7 complex: RING domain function in ubiquitin-protein ligases. *Cell* **102**, 533-9.

29. Hamilton, K. S., Ellison, M. J., Barber, K. R., Williams, R. S., Huzil, J. T., McKenna, S., Ptak, C., Glover, M. & Shaw, G. S. (2001). Structure of a conjugating enzyme-ubiquitin thiolester intermediate reveals a novel role for the ubiquitin tail. *Structure* **9**, 897-904.
30. Pickart, C. M. & Eddins, M. J. (2004). Ubiquitin: structures, functions, mechanisms. *Biochim Biophys Acta* **1695**, 55-72.
31. Huang, D. T., Paydar, A., Zhuang, M., Waddell, M. B., Holton, J. M. & Schulman, B. A. (2005). Structural basis for recruitment of Ubc12 by an E2 binding domain in NEDD8's E1. *Mol Cell* **17**, 341-50.
32. Eletr, Z. M., Huang, D. T., Duda, D. M., Schulman, B. A. & Kuhlman, B. (2005). E2 conjugating enzymes must disengage from their E1 enzymes before E3-dependent ubiquitin and ubiquitin-like transfer. *Nat Struct Mol Biol* **12**, 933-4.
33. Eletr, Z. M. & Kuhlman, B. (2007). Sequence Determinants of E2-E6AP Binding Affinity and Specificity. *J Mol Biol* **369**, 419-28.
34. Nuber, U. & Scheffner, M. (1999). Identification of determinants in E2 ubiquitin-conjugating enzymes required for hec E3 ubiquitin-protein ligase interaction. *J Biol Chem* **274**, 7576-82.
35. Scheffner, M., Huibregtse, J. M., Vierstra, R. D. & Howley, P. M. (1993). The HPV-16 E6 and E6-AP complex functions as a ubiquitin-protein ligase in the ubiquitination of p53. *Cell* **75**, 495-505.
36. Walker, J. R., Avvakumov, G.V., Xue, S., Butler-Cole, C., Weigelt, J., Sundstrom, M., Arrowsmith, C.H., Edwards, A.M., Bochkarev, A., Dhe-Paganon, S. Catalytic Domain of the Human NEDD4-like E3 Ligase *To be published*.
37. Verdecia, M. A., Joazeiro, C. A., Wells, N. J., Ferrer, J. L., Bowman, M. E., Hunter, T. & Noel, J. P. (2003). Conformational flexibility underlies ubiquitin ligation mediated by the WWP1 HECT domain E3 ligase. *Mol Cell* **11**, 249-59.
38. Ogunjimi, A. A., Briant, D. J., Pece-Barbara, N., Le Roy, C., Di Guglielmo, G. M., Kavsak, P., Rasmussen, R. K., Seet, B. T., Sicheri, F. & Wrana, J. L. (2005). Regulation of Smurf2 ubiquitin ligase activity by anchoring the E2 to the HECT domain. *Mol Cell* **19**, 297-308.
39. Nawaz, Z., Lonard, D. M., Smith, C. L., Lev-Lehman, E., Tsai, S. Y., Tsai, M. J. & O'Malley, B. W. (1999). The Angelman syndrome-associated protein, E6-AP, is a coactivator for the nuclear hormone receptor superfamily. *Mol Cell Biol* **19**, 1182-9.
40. Cooper, E. M., Hudson, A. W., Amos, J., Wagstaff, J. & Howley, P. M. (2004). Biochemical analysis of Angelman syndrome-associated mutations in the E3 ubiquitin ligase E6-associated protein. *J Biol Chem* **279**, 41208-17.
41. Wang, M. & Pickart, C. M. (2005). Different HECT domain ubiquitin ligases employ distinct mechanisms of polyubiquitin chain synthesis. *Embo J* **24**, 4324-33.
42. Anan, T., Nagata, Y., Koga, H., Honda, Y., Yabuki, N., Miyamoto, C., Kuwano, A., Matsuda, I., Endo, F., Saya, H. & Nakao, M. (1998). Human ubiquitin-protein ligase Nedd4:

- expression, subcellular localization and selective interaction with ubiquitin-conjugating enzymes. *Genes Cells* **3**, 751-63.
43. Fotia, A. B., Cook, D. I. & Kumar, S. (2006). The ubiquitin-protein ligases Nedd4 and Nedd4-2 show similar ubiquitin-conjugating enzyme specificities. *Int J Biochem Cell Biol* **38**, 472-9.
 44. Schwartz, A. L. & Ciechanover, A. (1999). The ubiquitin-proteasome pathway and pathogenesis of human diseases. *Annu Rev Med* **50**, 57-74.
 45. Glickman, M. H. & Ciechanover, A. (2002). The ubiquitin-proteasome proteolytic pathway: destruction for the sake of construction. *Physiol Rev* **82**, 373-428.
 46. Shimkets, R. A., Warnock, D. G., Bositis, C. M., Nelson-Williams, C., Hansson, J. H., Schambelan, M., Gill, J. R., Jr., Ulick, S., Milora, R. V., Findling, J. W. & et al. (1994). Liddle's syndrome: heritable human hypertension caused by mutations in the beta subunit of the epithelial sodium channel. *Cell* **79**, 407-14.
 47. Kishino, T., Lalande, M. & Wagstaff, J. (1997). UBE3A/E6-AP mutations cause Angelman syndrome. *Nat Genet* **15**, 70-3.
 48. Matsuura, T., Sutcliffe, J. S., Fang, P., Galjaard, R. J., Jiang, Y. H., Benton, C. S., Rommens, J. M. & Beaudet, A. L. (1997). De novo truncating mutations in E6-AP ubiquitin-protein ligase gene (UBE3A) in Angelman syndrome. *Nat Genet* **15**, 74-7.
 49. Kitada, T., Asakawa, S., Hattori, N., Matsumine, H., Yamamura, Y., Minoshima, S., Yokochi, M., Mizuno, Y. & Shimizu, N. (1998). Mutations in the parkin gene cause autosomal recessive juvenile parkinsonism. *Nature* **392**, 605-8.
 50. Shimura, H., Hattori, N., Kubo, S., Mizuno, Y., Asakawa, S., Minoshima, S., Shimizu, N., Iwai, K., Chiba, T., Tanaka, K. & Suzuki, T. (2000). Familial Parkinson disease gene product, parkin, is a ubiquitin-protein ligase. *Nat Genet* **25**, 302-5.
 51. Staub, O., Dho, S., Henry, P., Correa, J., Ishikawa, T., McGlade, J. & Rotin, D. (1996). WW domains of Nedd4 bind to the proline-rich PY motifs in the epithelial Na⁺ channel deleted in Liddle's syndrome. *Embo J* **15**, 2371-80.
 52. Staub, O., Gautschi, I., Ishikawa, T., Breitschopf, K., Ciechanover, A., Schild, L. & Rotin, D. (1997). Regulation of stability and function of the epithelial Na⁺ channel (ENaC) by ubiquitination. *Embo J* **16**, 6325-36.
 53. Laan, L. A., v Haeringen, A. & Brouwer, O. F. (1999). Angelman syndrome: a review of clinical and genetic aspects. *Clin Neurol Neurosurg* **101**, 161-70.
 54. Kuhne, C. & Banks, L. (1998). E3-ubiquitin ligase/E6-AP links multicopy maintenance protein 7 to the ubiquitination pathway by a novel motif, the L2G box. *J Biol Chem* **273**, 34302-9.
 55. Kumar, S., Talis, A. L. & Howley, P. M. (1999). Identification of HHR23A as a substrate for E6-associated protein-mediated ubiquitination. *J Biol Chem* **274**, 18785-92.

56. Oda, H., Kumar, S. & Howley, P. M. (1999). Regulation of the Src family tyrosine kinase Blk through E6AP-mediated ubiquitination. *Proc Natl Acad Sci U S A* **96**, 9557-62.
57. Lucking, C. B., Durr, A., Bonifati, V., Vaughan, J., De Michele, G., Gasser, T., Harhangi, B. S., Meco, G., Deneffe, P., Wood, N. W., Agid, Y. & Brice, A. (2000). Association between early-onset Parkinson's disease and mutations in the parkin gene. *N Engl J Med* **342**, 1560-7.
58. Kahle, P. J. & Haass, C. (2004). How does parkin ligate ubiquitin to Parkinson's disease? *EMBO Rep* **5**, 681-5.
59. Mata, I. F., Lockhart, P. J. & Farrer, M. J. (2004). Parkin genetics: one model for Parkinson's disease. *Hum Mol Genet* **13 Spec No 1**, R127-33.
60. Loda, M., Cukor, B., Tam, S. W., Lavin, P., Fiorentino, M., Draetta, G. F., Jessup, J. M. & Pagano, M. (1997). Increased proteasome-dependent degradation of the cyclin-dependent kinase inhibitor p27 in aggressive colorectal carcinomas. *Nat Med* **3**, 231-4.
61. Winkler, G. S., Albert, T. K., Dominguez, C., Legtenberg, Y. I., Boelens, R. & Timmers, H. T. (2004). An altered-specificity ubiquitin-conjugating enzyme/ubiquitin-protein ligase pair. *J Mol Biol* **337**, 157-65.

CHAPTER II

SEQUENCE DETERMINANTS OF E2–E6AP BINDING AFFINITY AND SPECIFICITY

Ziad M Eletr¹ and Brian Kuhlman^{1*}

¹Department of Biochemistry and Biophysics,
University of North Carolina, Chapel Hill, NC 27599-7260, USA

*Corresponding Author

Keywords: Ubiquitin; UbcH7; E6AP; HECT; E2-E3 Specificity

This work was published in the Journal of Molecular Biology (2007) 369, 419–428.

Reproduced with permission from Elsevier.

ABSTRACT

The conjugation of ubiquitin to substrates requires a series of enzymatic reactions consisting of an activating enzyme (E1), conjugating enzymes (E2) and ligases (E3). Tagging the appropriate substrate with ubiquitin is achieved by specific E2–E3 and E3–substrate interactions. E6AP, a member of the HECT family of E3s, has been previously shown to bind and function with the E2s UbcH7 and UbcH8. To decipher the sequence determinants of this specificity we have developed a quantitative E2–E3 binding assay based on fluorescence polarization and used this assay to measure the affinity of wild-type and mutant E2–E6AP interactions. Alanine scanning of the E6AP–UbcH7 binding interface identified four side-chains on UbcH7 and six side-chains on E6AP that contribute more than 1 kcal /mol to the binding free energy. Two of the hot spot residues from UbcH7 (K96 and K100) are conserved in UbcH8 but vary across other E2s. To determine if these are key specificity determining residues, we attempted to induce a tighter association between the E2 UbcH5b and E6AP by mutating the corresponding positions in UbcH5b to lysine residues. Surprisingly, the mutations had little effect, but rather a mutation at UbcH7 position 4, which is not at a hot spot on the UbcH7–E6AP interface, significantly strengthened UbcH5bs affinity for E6AP. This result indicates that E2–E3 binding specificities are a function of both favorable interactions that promote binding, and unfavorable interactions that prevent binding with unwanted partners.

INTRODUCTION

Protein ubiquitination is an essential eukaryotic pathway that influences nearly all cellular processes¹. The conjugation of ubiquitin to a protein substrate requires a cascade of enzymatic reactions beginning with the ubiquitin activating enzyme (E1). The E1 uses ATP to form a thioester bond between the carboxyl terminus of ubiquitin and the E1 active site cysteine. The E1 then binds a ubiquitin conjugating enzyme (E2) and transfers ubiquitin to the E2 active site cysteine. The next step in the pathway requires a ubiquitin ligase (E3) which utilizes distinct domains to bind both E2 and substrate. The two major classes of E3s bind E2s using either a RING (*really interesting gene*) domain or a HECT (*homology to E6AP carboxy terminus*) domain. E3s containing a HECT domain form a third thioester intermediate with ubiquitin prior to transfer to substrate². E3s that contain a RING domain do not form a covalent intermediate with ubiquitin, but rather bring the substrate in proximity of the E2 whereby transfer of ubiquitin proceeds directly from E2 to substrate.

The importance of specific E3–substrate interactions is apparent as aberrations can lead to improper substrate regulation and severe physiological consequences^{3; 4}. Often overlooked is the specificity of E2–E3 interactions as similar outcomes could potentially arise. The hierarchical nature of the ubiquitin pathway presents a formidable task in dissecting all E2–E3 and E3–substrate interactions. For example in humans there is a single E1, ~30 E2s and hundreds of potential E3s. In general, a given E2 will interact with multiple E3s while E3s only function with a limited subset of E2s⁴. Additionally, a given E3 may have more than one substrate and some substrates can be recognized by multiple E3s⁴. One possible method to dissect the network of interactions is to design altered specificity E2-E3 pairs that will function together but not with their wild-type partners. Such an approach has been taken by Marc Timmers and colleagues who used a charge swap interaction across the UbCH5b–cNOT4 interface to create an altered specificity E2-RING pair⁵. The Timmers study, as well as others, have helped map the determinants of E2-RING specificity^{5; 6; 7; 8; 9}. Here, we examine the sequence determinants of E2-HECT specificity. In particular, we focus on the HECT domain protein, E6AP.

E6AP is the founding member of the HECT domain class of E3s. It was first identified as a protein that cooperates with the E6 protein from oncogenic forms of the human papillomavirus to down regulate the p53 tumor suppressor¹⁰. The conserved ~350 amino acid residue HECT domain adopts a bilobal structure and is always found at the C-terminus of E3s. A three residue hinge connects the N-terminal E2 binding lobe with the catalytic C-terminal lobe and the interface created by the two lobes forms a highly conserved cleft containing the catalytic cysteine¹¹ (**Figure 2.1(a)**). Three crystal structures of HECT domains have revealed significantly different orientations of the two lobes, implying that conformational changes are necessary for catalysis^{11; 12; 13}. Hinge mutations to proline that restrict the conformational flexibility of the HECT domain result in impaired E3 activity¹². Also, some patients with Angelman syndrome (AS), a severe neurological disorder linked to E6AP, have acquired mutations within the conserved cleft that have been shown to reduce E6AP ligase activity^{14; 15}. Despite the significant progress on AS associated E6AP mutations, none of the identified E6AP substrates have been directly linked to the disorder¹⁶. A better understanding of HECT domains as well as their E2s and substrates may help combat such E3 associated diseases.

All E2 enzymes possess a conserved catalytic core domain of approximately 150 amino acid residues though some E2s also contain N- and C-terminal extensions which serve diverse functions¹⁶. The E2 core domain contains the residues responsible for catalysis as well as binding E1 and E3s. Crystal structures of the E2 UbCH7 bound to a HECT E3, E6AP¹¹, and a RING E3, c-Cbl¹⁷, revealed that E2s utilize similar residues to bind both classes of E3s. The majority of E3 binding residues are contained within the N-terminal helix (helix 1) as well as loops 4 and 7^{11; 17} (**Figure 2.1(b)**). In both E2-E3 structures, the primary contact at the interface arises from F63 on loop 4 of UbCH7 which is buried in a hydrophobic groove created by the E3^{11; 17}. This phenylalanine is present in all E2s that have been shown to function with HECT E3s^{11; 18}. The sequences of helix 1 and loop 7 of HECT binding E2s are more varied, and it has been proposed that these regions of the interface determine which HECT domains an E2 will bind¹¹. HECT E3s have been shown to form selective interactions with at least three distinct E2 subfamilies^{19; 20; 21; 22}. To decipher the sequence determinants of E2-

E6AP specificity, we have performed a variety of mutagenesis experiments to map out which E2 and E6AP residues are important for E2-E6AP affinity, and have used this information along with multiple sequence alignments to rationally perturb E2-E6AP binding preferences.

RESULTS

E6AP selectivity for UbcH7 and UbcH8

Previous two-hybrid studies and activity assays indicate that E6AP binds and functions with the E2s UbcH7 and UbcH8, and to a lesser extent UbcH5a^{19; 20}. To more precisely quantify these preferences and test a larger set of E2s, we measured the binding affinity of E6AP for nine E2s using a fluorescence polarization (FP) assay that we previously used to measure UbcH7-E6AP binding²³. E2s were selectively labeled at cysteine side-chains using a thiol-reactive bodipy dye, and fluorescence polarization of the modified E2 was monitored as a function of E3 concentration. To ensure that the bodipy labeling of the E2s was not influencing binding, we measured the binding affinity of unmodified UbcH7 for E6AP using isothermal titration calorimetry (ITC) (**Supplementary Data, Figure 2.8**). The two experiments yielded similar measures of the UbcH7-E6AP dissociation constant (K_D of 5.0 μ M from FP and 2.2 μ M from ITC). Of the E2s tested only UbcH8 contained a cysteine near the HECT-binding interface and for this reason we used a C97S UbcH8 mutant in our FP assays.

Four of the E2s (Ubc9, UbcH10, Rad6b, and Ubc12) lack a phenylalanine at position 63 (F63) and were not expected to bind E6AP (**Figure 2.2(a)**). The E2s with a F63 represent three distinct E2 subfamilies according to a recent phylogenetic analysis of E2 enzymes²⁴. Representatives of the UBC4/5 subfamily include yeast UBC4 and its human homolog UbcH5b (UbcH5a paralog). The human UbcH2 protein belongs to the UBC8 subfamily while human UbcH7 and UbcH8 represent the UbcH7/8 subfamily. The binding assays show that only UbcH7 and UbcH8(C97S) bind to E6AP with low micromolar affinity (**Figure 2.2(b)**). The other E2s with a phenylalanine at position 63 (UBC4, UbcH5b, and UbcH2) bind E6AP with affinities less than 200 μ M. Of the E2s lacking F63, UbcH10, Rad6b, and Ubc12 did not bind E6AP. Ubc9, the SUMO-conjugating enzyme, was able to weakly interact with E6AP. These results are consistent with previous findings that show that HECT E3s preferentially interact with E2s containing a phenylalanine at position 63^{11; 18}.

Identifying hot spot residues at the UbchH7–E6AP interface

Having confirmed the importance of F63 to binding E6AP, we next set out to identify secondary determinants that provide E6AP selectivity for the UbchH7/8 subfamily. We used alanine scanning of the E6AP–UbchH7 interface followed by binding measurements to determine which side-chains contribute most to binding. A total of 36 residues at the interface were mutated to either alanine or glycine. The mutants were expressed in *Escherichia coli* and binding affinities were measured with the FP binding assay.

The free energy of binding for the wild-type UbchH7–E6AP interaction was measured at 7.2 kcal/mol ($K_D = 5.0 \mu\text{M}$). As expected, the mutation resulting in the largest loss of binding energy was F63A ($\Delta\Delta G^\circ_{\text{bind}} = 3.0$ kcal/mol). None of the other mutants tested lost more than 2 kcal/mol, but nine mutants lost greater than 1 kcal/mol. Together with F63 these residues will be referred to as hot spots (**Table 2.1**). Of these nine mutants, four are hydrophobic E6AP residues (L635A, L639A, L642A, and F690A) that form van der Waals contacts with F63 (**Figure 2.3**). An unexpected finding was that two UbchH7 loop 7 lysine residues, K96 and K100, were binding hot spots. In the crystal structure, K96 forms a salt bridge with D641 of E6AP while the K100 hydrogen bonds with the D652 backbone carbonyl of E6AP. Hot spots were also observed at a completely conserved proline preceding F63 as well as M653 and Y645 of E6AP. The latter two residues form van der Waals contacts with P97 and A98 of UbchH7 loop 7. Of the remaining mutants we found 16 to be moderately destabilizing ($\Delta\Delta G^\circ_{\text{bind}}$ of 0.25 to 1.0 kcal/mol). These residues are a mixture of polar, charged, and hydrophobic amino acids. Interestingly these residues form a shell around the hydrophobic hot spot residues of UbchH7 and E6AP (**Figure 2.3**). Like the reciprocating hydrophobic hot spots, moderately destabilizing residues of UbchH7 interact with moderately destabilizing residues of E6AP. The final ten mutants exhibited either neutral ($\Delta\Delta G^\circ_{\text{bind}}$ of -0.25 to 0.25 kcal/mol) or stabilizing ($\Delta\Delta G^\circ_{\text{bind}} < -0.25$ kcal/mol) effects on the binding free energy. These residues cluster further from the hot spots and outside the shell of moderately destabilizing residues (**Figure 2.3**). The observed pattern of an

energetically important hydrophobic interface core surrounded by a shell of energetically less important residues is not uncommon to protein–protein interfaces^{25; 26}.

Other mutations were made to UbchH7 and E6AP to serve as controls. In the UbchH7–E6AP crystal structure, R52 of UbchH7 is solvent exposed and situated opposite the binding interface. Mutation of this residue to alanine resulted in wild-type binding affinity (**Table 2.1**). Similarly, no change in binding free energy was observed upon mutating the E6AP catalytic cysteine to alanine (C820A) (**Table 2.1**). Previous studies on the WWP1 HECT domain found that a double proline mutation in the hinge connecting the N and C lobes resulted in reduced ligase activity¹². To confirm that the impaired activity arises from restricted conformational flexibility and not perturbed binding, the analogous positions in E6AP were mutated to proline (S739P N741P). The resulting mutant bound UbchH7 with wild-type affinity (**Table 2.1**).

Charge swap mutations at the UbchH7–E6AP interface

To identify charged amino acids engaged in electrostatic interactions across the interface we measured binding affinities of ten UbchH7–E6AP charge swap mutants (**Table 2.1**). The binding affinities from the charge swap experiments were grouped into the same categories as the alanine mutant affinities. Six of the mutants lost > 1.0 kcal/mol of binding free energy. These include UbchH7 helix 1 mutants R5E, R6E, and K9E as well as loop 7 charge swaps K96E and K100E. The helix 1 mutants form inter-chain (R5 and R6) and intra-chain (K9) hydrogen bonds to backbone oxygen atoms. The D652R mutation was also largely destabilizing, possibly because of a loss of interaction with K100. Three of the remaining charge swap mutants displayed less significant losses in binding energy (E60R, K64E, and D641K). The E93R mutant displayed a large gain in binding energy that may be the result of a new hydrogen bond with the Q637 E6AP side-chain.

Only two side-chain–side-chain charged interactions are present across the interface, K100–D652 and K96–D641. We proceeded to test the mutant pairs for an altered specificity interaction. The effects from K100E–D652R interaction were as unfavorable as the effects of either single mutant

($\Delta\Delta G_{bind}$ of 1.6 kcal/mol). In contrast, the K96E–D641K mutant pair displayed a charge swap interaction that was more favorable than the wild-type interaction ($\Delta\Delta G_{bind}$ of -0.8 kcal/mol). For the purpose of creating an altered specificity UbcH7–E6AP pair, the K96–D641K mutant pair would only achieve specificity towards E3s because the D641K mutant displays no defects in binding wild-type UbcH7. A sub-optimal K96–D641K salt-bridge in the wild-type interaction could give rise to such results. These findings suggest that creating an altered specificity UbcH7–E6AP pair using a charge swap interaction may prove difficult.

Ubiquitin transfer rates correlate with UbcH7–E6AP binding affinity

Ubiquitin transfer assays were used to assess if changes in UbcH7–E6AP binding affinity influence the rate ubiquitin is transferred to E6AP. Activity assays were not performed with mutant UbcH7 proteins because of potential complications from altered E1-UbcH7 activity. All E6AP mutants were tested in reactions containing radiolabeled ubiquitin, E1, UbcH7, ATP and an ATP regenerating system. Each reaction was quenched in SDS-PAGE loading buffer lacking β -mercaptoethanol (β -ME), separated by SDS-PAGE, and ubiquitin-modified proteins were visualized using a phosphorimager (**Figure 2.4(a)**). Ubiquitin-modified E6AP appears as two bands and UbcH7 as a single band. The wild-type reaction quenched in loading buffer containing β -ME demonstrates that the ubiquitin modifications to both UbcH7 and the faster migrating E6AP band are mediated via thioester linkages (denoted with \sim). The slower migrating E6AP band that is resistant to treatment with β -ME likely represents ubiquitin modification via an isopeptide bond (denoted with $-$). No ubiquitin-modified E6AP is observed in reactions using the catalytic cysteine mutant (C820A) or the control lacking E6AP.

Phosphorimaging software was used to quantify the total amount of Ub~E6AP formed in each reaction as well as the amount of Ub~UbcH7 (**Figure 4(b)**). Ub-UbcH7 levels were not constant between the various reactions, indicating that the rates of Ub~E6AP formation were partially limited

by the E1/UbcH7 reaction rates. Indeed, in reactions with the tighter binding E2–E3 pairs the Ub~UbcH7 band was very weak, suggesting that the rate of Ub~E6AP formation depended almost entirely on the E1/UbcH7 reaction rate. Previously, we have shown that E3 and E1 binding to UbcH7 are mutually exclusive and that saturating amounts of E3 can inhibit the E1/E2 transfer step²³. We do not believe that is occurring in this case as the E3 concentrations are well below saturating levels. Despite being partially limited by the E1/E2 transfer step, there is still a correlation between the amount of Ub~E6AP formed and the E2/E3 binding affinities (correlation coefficient = 0.58). E6AP hot spot mutants Y645A, D652R, F690A, and M653A as well as Y694L, M654A, and S739P N741P formed less than 55% of the ubiquitin-E6AP observed in the wild-type reactions. All the E6AP mutants displaying enhanced binding affinity resulted in an increase in the formation of ubiquitin-E6AP. There are a few outliers. L639A and L635A weaken binding by > 1 kcal/mol, but do not show a reduced amount of Ub~E6AP formed. However, there is a greater build up of Ub~UbcH7 for these two reactions than for the wild-type reaction. Overall, the results indicate that E2/E3 binding affinity does affect E2/E3 ubiquitin transfer rates, but that there could be additional important factors such as on and off rates, rate of transfer within the bound complex and the affinity of ubiquitin charged E2 for the E3.

UbcH7–E6AP hot spots are essentially conserved in the UbcH8–E6AP interaction

The hot spot residues in UbcH7, F63, K96 and K100, are conserved in UbcH8 (F62, K95 and K99). To confirm that these residues are playing the same role at the UbcH8–E6AP interface we mutated them to alanine and measured affinity for E6AP. The UbcH8 F62A mutation abolished binding to E6AP. The K95A and K99A mutations proved to be destabilizing with losses in binding energy of 0.9 and 1.3 kcal/mol respectively (**Table 2.2**). In both E2s, the double loop 7 mutants show nearly additive effects from the single mutants, but still the combined destabilization is less than the loop 4 phenylalanine mutation. We also tested our panel of E6AP mutants with UbcH8 in binding assays. There is a striking similarity in the binding affinities of UbcH7 and UbcH8 for E6AP mutants

(**Figure 5**). Only two significant discrepancies are observed and these are L639A and D641K; both are stabilizing with UbchH8 yet destabilizing with UbchH7. These results show that hot spots at the UbchH7–E6AP interface are also hot spots at the UbchH8–E6AP interface.

Redesigning UbchH5b to bind E6AP

To further explore the determinants of E2-E6AP binding specificity we characterized a set of mutations that were rationally designed to induce UbchH5b to bind more tightly to E6AP. Our first design strategy was to mutate residues in UbchH5b that map to hot spot positions in UbchH7. We made the S94K and T98K single and double mutants in UbchH5b and measured binding to E6AP (**Figure 2.6**). The S94K mutant destabilized binding by 0.5 kcal/mol while the T98K strengthened binding by 0.4 kcal/mol. The double mutant bound weaker than wild-type UbchH5b but stronger than the S94K single mutant. A possible explanation for this result is that the extra residue present in UbchH7/8 loop 7 (**Figure 2.2(a)**) may lead to different loop 7–E6AP interactions in UbchH5b. From these results it is clear that conserving the hot spot residues from UbchH7 is not sufficient to induce low micromolar binding with E6AP.

To further search for UbchH5b mutations that could increase affinity for E6AP we examined the E2 multiple sequence alignment for residues that were not conserved between UbchH7 and UbchH5b but were located at the E6AP–UbchH7 interface. The only residue that differs between the proteins and had an affect on UbchH7–E6AP affinity is serine 4 on UbchH7, which is a leucine in UbchH5b. Somewhat surprisingly, mutating this leucine on UbchH5b to serine (L3S) resulted in a significant gain of 1.2 kcal/mol in binding energy (K_D of 23 μ M) (**Figure 2.6**). This mutation was tested in conjunction with the S94K and T98K mutants mentioned above, and the L3S T98K double mutant bound E6AP with UbchH7/8-like affinity. So although the serine at residue 4 in UbchH7 is not making strong favorable interactions with E6AP, the residue located at this position can have a significant impact on E2-E6AP binding specificity. The leucine at this position in UbchH5b is dictating specificity by disfavoring interactions with E6AP.

DISCUSSION

The sequence determinants of E2–E6AP binding affinity and specificity have been studied by mutational analysis. The major findings can be summarized as follows. (1) A F63 in loop 4 of an E2 is necessary but not sufficient for tight E2–E6AP binding affinity as the five E2s that were characterized with this phenylalanine bind with affinities ranging from 5–180 μ M. Of these E2s only UbcH7 and UbcH8 bind E6AP with low micromolar affinity. (2) In addition to F63, three side-chains on UbcH7 contribute > 1 kcal/mol to the binding free energy between UbcH7 and E6AP. Two of these (K96 and K100) are located on the periphery of the interface and are not conserved in other E2 subfamilies that bind more weakly to E6AP. (3) The E6AP side-chains that contribute most to binding UbcH7 are hydrophobic and surround the F63 binding cleft. (4) Residues that are not hot spots for the UbcH7–E6AP interaction can contribute significantly to E2–E6AP binding specificity. Mutating L3 of UbcH5b to a serine led to a \sim tenfold increase in UbcH5b–E6AP affinity.

An important question that remains is whether the interactions that determine E6AP-E2 specificity will translate to other E2-HECT interfaces. Much of the initial work on E2-HECT specificity focused on E6AP and *Saccharomyces cerevisiae* Rsp5. Different techniques yielded conflicting results as to which E2s these E3s preferred. Studies using the yeast two-hybrid method showed that E6AP selectively interacts with UbcH7 and UbcH8 while Rsp5 prefers UbcH5a and UbcH6²⁰. Other results using substrate or E3 ubiquitination assays show that UbcH5a and UbcH7 support equal E6AP activity or that Rsp5 is not active with UbcH6^{18; 19; 22}. One consistent finding was that Rsp5 prefers UbcH5a. Many human HECT E3s are closely related to yeast Rsp5 in their HECT domain as well as N-terminal substrate binding domains (Nedd4, Nedd4L, Smurf1/2, WWP1/2 and AIP4 in humans)²⁷. A sequence alignment of the E2 binding region of HECT E3s (**Figure 2.7**) shows that within the Rsp5 subfamily there are conserved residues not present in E6AP. Some of these differences map to a loop that is one to three residues shorter than E6AP in the Rsp5 subfamily. In more structurally defined positions notable differences are observed at E6AP residues D641 (W in Rsp5 subfamily), V634 (D/E), and Y645 (N), and F690 (Y). In an attempt to optimize the UbcH7–Smurf2 interaction,

Ogunjimi et al. found two mutations to Smurf2 that were capable of enhancing catalytic activity *in vitro* and *in vivo*¹³. These mutations, H547I and Y581F, replaced polar groups in the binding groove with hydrophobic residues observed in E6AP (I655 and F690). Other Rsp5 family members maintain the hydrophobic nature of I655. Whether subtle differences within other Rsp5 family members will drive specificity towards the UBC4/5 family or towards other E2 families with an F63 remains undetermined. Our results show that a subtle difference between UbcH7 and UbcH5b indeed affects binding to E6AP.

Our *in vitro* ubiquitination assays with E6AP mutants demonstrate that E2–E3 affinity influences the rate ubiquitin~HECT thioesters can be formed. *In vivo* there will be the added complexity that a variety of E3s will be competing for E2 binding sites, which could make E3 conjugation rates more sensitive to E2–E3 affinity. Additionally, the study by Ogunjimi et al. found that an auxiliary protein Smad7 was able to bind both UbcH7 and the Smurf2 E3 via its WW domain and effectively enhance the activity of Smurf2¹³. This finding suggests that in some cases the specificity of E2–E3 interactions may reside in a tertiary protein. Discovering which E2–E3 pairs functionally interact in the cell is a challenging problem. Introducing E2s and E3s with redesigned binding specificities into the cell may provide one route for deciphering the importance of specific interactions. Our study (and others like it) on the determinants of E2–E3 specificity lays the foundation for such efforts.

FIGURES

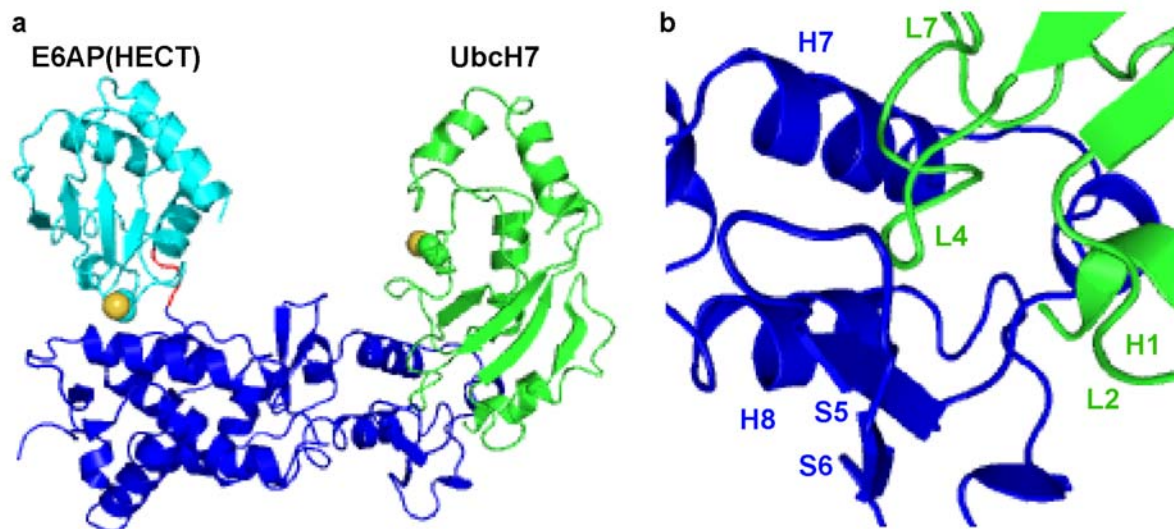


Figure 2.1. Cartoon representation of the Ubch7–E6AP crystal structure¹¹. (a) The E6AP N-terminal lobe (blue) and C-terminal lobe (cyan) are connected by a three residue hinge (red). E6AP uses an ~80 amino acid residue subdomain in the N-terminal lobe to bind Ubch7 (green). Catalytic cysteine side-chains of Ubch7 and E6AP are shown as van der Waals radii. (b) Close up of the Ubch7–E6AP interface. The most significant contacts arise from Ubch7 helix 1 (H1) as well as loops 4 and 7 (L4 and L7), which interact with E6AP helices 7 and 8 (H7 and H8) and the H7-S5 loop. The Figure was generated using PDB 1C4Z¹¹ and PYMOL [<http://www.pymol.org>].

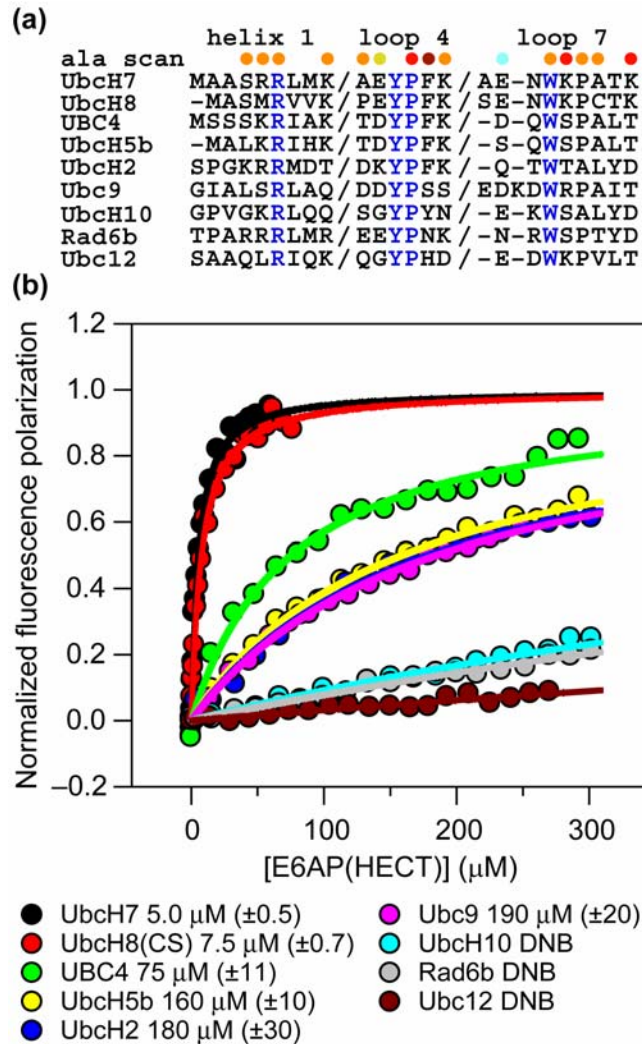


Figure 2.2. E6AP selectively interacts with UbcH7 and UbcH8. (a) Sequence alignment of the E3 binding regions of a subset of E2 enzymes. The dots indicate UbcH7 residues used to bind E6AP and are colored by the change in UbcH7–E6AP binding energy associated with mutating the side-chain to alanine (or glycine) according to Figure 3. (b) Fluorescence polarization binding assays of E6AP (HECT) with each of the E2s listed in (a). The results show that only UbcH7 and UbcH8 interact with low micromolar affinity and that UBC4 and UbcH5b of the closely related UBC4/5 subfamily bind E6AP significantly weaker. Aside from UbcH7 and UbcH8, all E2s have sub-optimal amino acids at hot spots for E6AP.

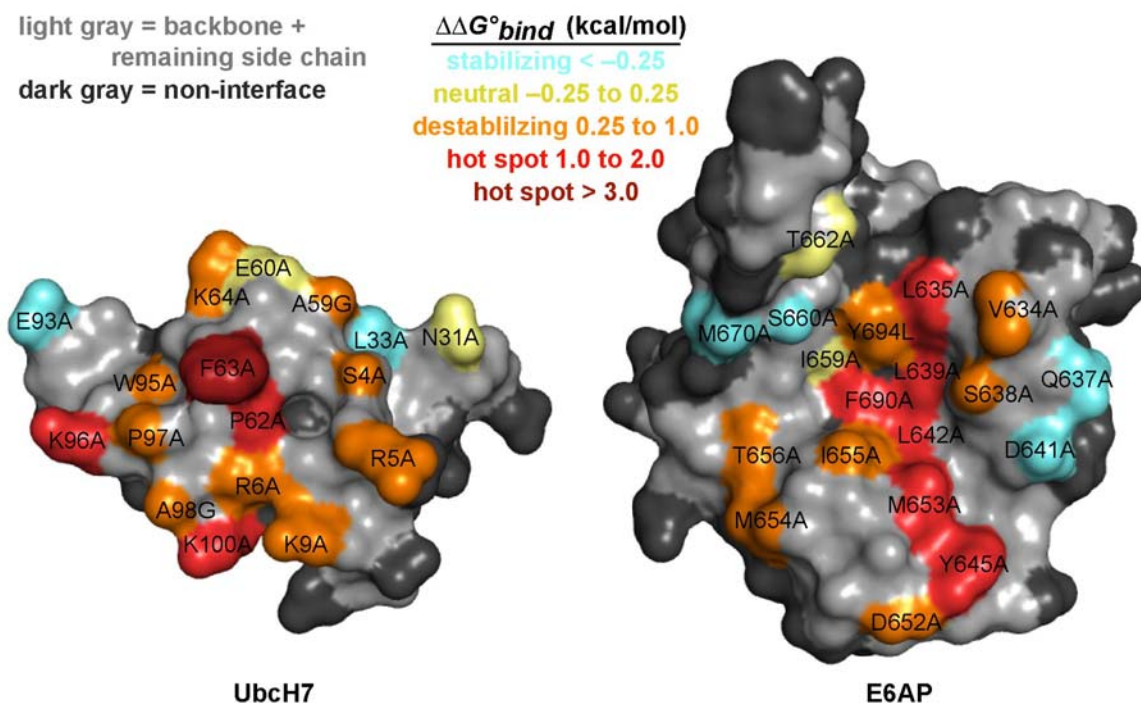


Figure 2.3. Mapping $\Delta\Delta G^{\circ}_{bind}$ from alanine scan studies onto the UbchH7–E6AP structure. The interface view was obtained by rotating UbchH7 180° about the y-axis. Individual amino acid residues are colored by the change in binding free energy observed upon making the indicated mutation. F63 of UbchH7 is the most important residue for binding. Other hot spots include E6AP residues lining the hydrophobic groove that contacts F63 as well as K96 and K100 of UbchH7. Residues with smaller contributions to binding form a shell around F63 and the hydrophobic E6AP groove. The Figure was generated using PDB 1C4Z¹¹ and PYMOL.

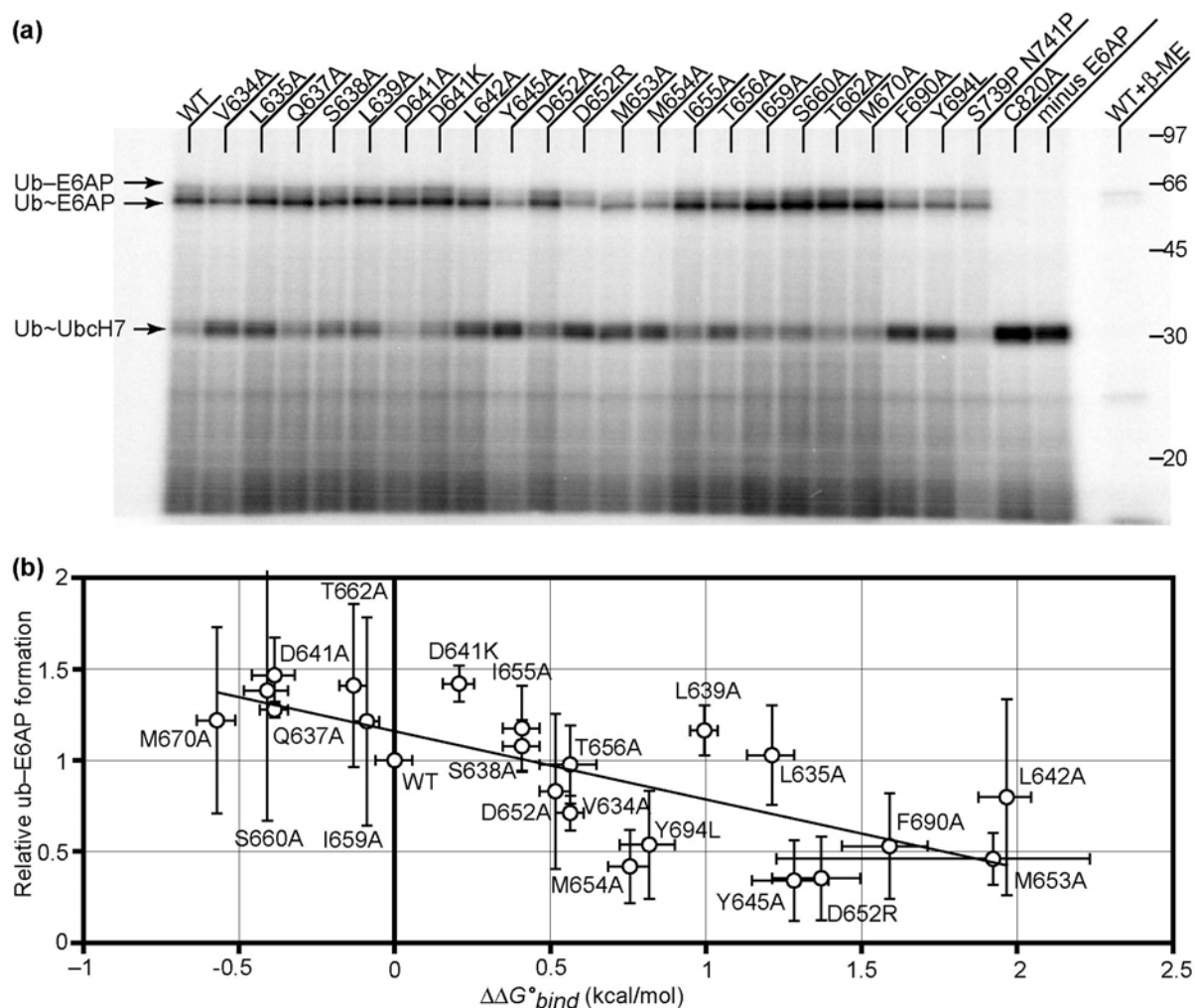


Figure 2.4. *In vitro* activity of E6AP mutant proteins. (a) A ubiquitin transfer assay was used to detect the formation of ubiquitin-E6AP thioester in reactions containing 5 μ M [32 P]ubiquitin, 50 nM E1, 1 μ M wild-type UbchH7 and 1 μ M wild-type or mutant E6AP and an ATP regenerating buffer. The ubiquitin-E6AP thioester (Ub~E6AP) is reduced in the control reaction quenched in β -ME while the isopeptide-linked ubiquitin (Ub-E6AP) is retained. (b) For each reaction the total ubiquitin-E6AP formed was quantified and normalized to the wild-type reaction. The assay was repeated (**Supplementary Data, Figure 2.9**) and the averaged counts for each mutant is plotted versus the experimentally determined $\Delta\Delta G^{\circ}_{\text{bind}}$. Error bars represent standard deviation of relative ub-E6AP formed and the standard error of $\Delta\Delta G^{\circ}_{\text{bind}}$.

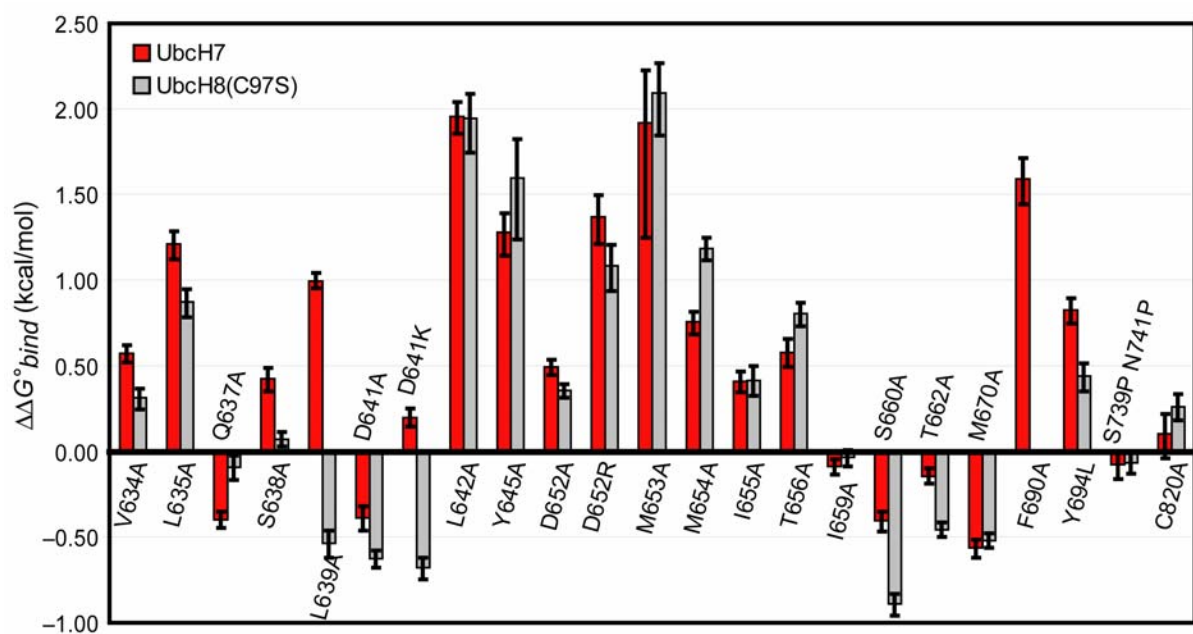


Figure 2.5. UbchH7 and UbchH8 form nearly identical interactions with E6AP. Bar graph comparing the observed change in binding free energy of E6AP mutants for UbchH7 and UbchH8(C97S). Nearly all E6AP interface residues contribute similar energy to binding UbchH7 and UbchH8(C97S). The two significant differences (L639A and the charge swap D641K) may arise from a slight difference in loop L7 of UbchH7 and UbchH8. The F690A mutant was not tested with UbchH8.

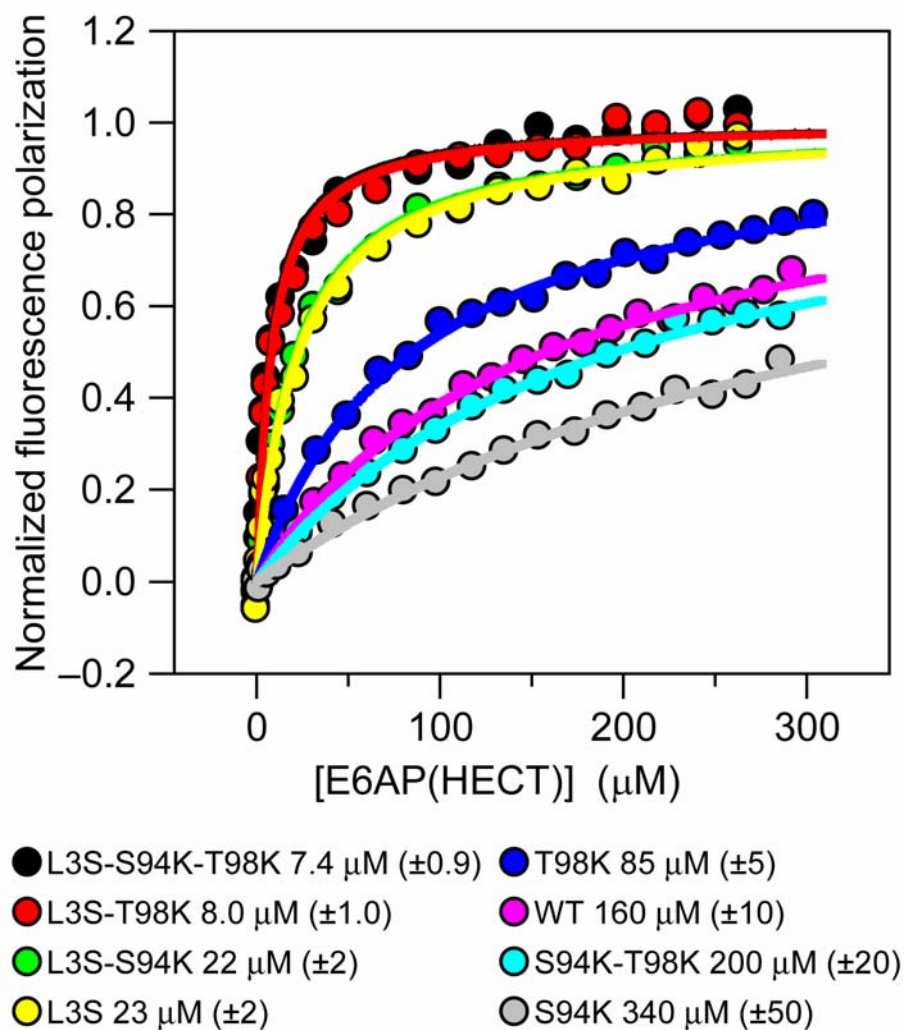


Figure 2.6. Rationally manipulating Ubch5b to enhance binding to E6AP. Three Ubch5b positions were mutated and tested for their contribution to binding E6AP. Ubch5b mutants containing the Ubch7 hot spot lysine(s) (S94K and T98K) alone were not able to significantly enhance binding. The L3 Ubch5b residue is a serine in UBC4, Ubch7 and Ubch8, and the L3S mutation resulted in a large increase in binding affinity for E6AP. The L3S T98K double mutant was capable of binding E6AP with Ubch7/8-like affinity. Interestingly the S94K mutation is destabilizing except when present with the L3S mutation.

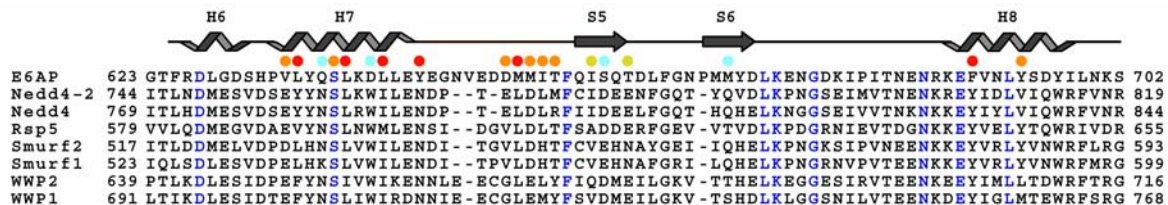


Figure 2.7. Multiple sequence alignment of the E2-binding subdomain of Rsp5 family members and E6AP. The dots are colored by the change in UbC7–E6AP binding energy associated with mutating the E6AP side-chain to alanine according to **Figure 2.3**. Amino acids lining the hydrophobic groove that interacts with F63 of E2s are generally hydrophobic and/or aromatic in the Rsp5 family of E3s. The Rsp5 family members have a one to three residue deletion in the H7-S5 loop and numerous non-conservative substitutions at E6AP residues. Both of these differences likely play a role in dictating E2-HECT specificity.

TABLES

Table 2.1. Measured dissociation constants for UbcH7 and E6AP(HECT) mutants.

UbcH7	K_D (μ M)	$\Delta\Delta G^\circ_{bind}$ (kcal/mol)	E6AP	K_D (μ M)	$\Delta\Delta G^\circ_{bind}$ (kcal/mol)
WT	5.0 ± 0.5	0	WT	5.0 ± 0.5	0
S4A	13 ± 1	0.54	V634A	13 ± 1	0.57
R5A	12 ± 2	0.51	L635A	39 ± 5	1.2
R5E	44 ± 10	1.3	Q637A	2.6 ± 0.2	-0.40
R6A	11 ± 2	0.46	S638A	10 ± 1	0.42
R6E	37 ± 8	1.2	L639A	27 ± 2	1.0
K9A	14 ± 2	0.62	D641A	2.6 ± 0.3	-0.39
K9E	69 ± 22	1.6	D641K	7.1 ± 0.6	0.20
N31A	3.7 ± 0.3	-0.18	L642A	140 ± 20	2.0
L33A	2.8 ± 0.7	-0.36	Y645A	44 ± 9	1.3
R52A	4.9 ± 0.5	-0.02	D652A	12 ± 1	0.49
A59G	13 ± 2	0.54	D652R	51 ± 12	1.4
E60A	5.8 ± 0.7	0.09	M653A	130 ± 90	1.9
E60R	5.6 ± 1.2	0.06	M654A	18 ± 2	0.76
P62A	54 ± 10	1.4	I655A	10 ± 1	0.41
F63A	810 ± 550	3.0	T656A	13 ± 2	0.58
K64A	8.2 ± 1.1	0.29	I659A	4.3 ± 0.3	-0.09
K64E	17 ± 3	0.71	S660A	2.5 ± 0.3	-0.41
E93A	2.4 ± 0.3	-0.43	T662A	4.0 ± 0.3	-0.14
E93R	0.92 ± 0.09	-1.0	M670A	1.9 ± 0.2	-0.56
W95A	20 ± 2	0.83	F690A	74 ± 17	1.6
K96A	34 ± 6	1.1	Y694L	20 ± 3	0.83
K96E	36 ± 13	1.2	S739P N741P	4.4 ± 0.6	-0.07
P97A	21 ± 2	0.85	C820A	6.0 ± 1.3	0.10
A98G	10 ± 1	0.41			
K100A	45 ± 15	1.3			
K100E	55 ± 26	1.4			

Table 2.2. Measured $\Delta\Delta^\circ G_{bind}$ (kcal/mol) of UbcH7–E6AP hot spots in UbcH8(C97S)

UbcH7		UbcH8(C97S)	
F63A	3.0	F62A	DNB
K96A	1.1	K95A	0.9
K100A	1.3	K99A	1.3
K96A K100A	2.1	K95A K99A	2.1
DNB, does not bind in our assay.			

MATERIALS AND METHODS

Protein purification

UbcH7, ubiquitin, and E6AP expression plasmids have been described²³. All other clones were obtained in or subcloned into pGEX vectors with N-terminal GST-tags followed by a thrombin recognition sequence. Vectors harboring *S. cerevisiae* UBC4 and human UbcH5b, UbcH8, UbcH10, Rad6b, and UbcH2 were kindly provided by Marc Timmers. Human Ubc12 and Ubc9 were kindly provided by Brenda Schulman and Jon Huibgretse respectively. Point mutations were introduced using the QuickChange® site-directed mutagenesis protocol (Stratagene). All vectors were verified by DNA sequencing.

Proteins were expressed overnight at 25° C with 0.3 mM IPTG in the BL21(DE3) strain of *E. coli*. Cells were disrupted by sonication and the resulting lysates were cleared by ultracentrifugation. UbcH7 was purified by metal chelating Sepharose followed by cation exchange and gel filtration. Ubiquitin was purified by metal chelating Sepharose followed by thrombin cleavage and gel filtration. The HECT domain of E6AP and all other E2s were purified by glutathione Sepharose followed by thrombin cleavage, anion exchange and gel filtration. For the Y694A E6AP mutant we were not able to purify a sufficient amount of protein, so instead we tested the Y694L mutation. Proteins were concentrated using Centricon® and Centriprep® centrifugal concentrators. Extinction coefficients used to determine protein concentrations were calculated using the method described by Gill and von Hippel²⁸.

Isothermal titration calorimetry binding assay

A Microcal-VP-ITC was used to measure the binding thermodynamics of unmodified UbcH7 for E6AP (**Supplementary Data, Figure 2.8**). The experiment was performed at 25° C using 700 µM UbcH7 in the sample syringe and 1.45 ml of 35 µM E6AP in the sample cell. A total of 41 5 µl injections of UbcH7 were performed at 5 min intervals. The heat of dilution of UbcH7 was

calculated as the average of the final three titrations and this value was subtracted from the dataset.

Origin software was used to fit the data to a single-site binding model and determine the stoichiometry (N) and thermodynamic parameters of binding ΔH_{bind} , ΔG_{bind} and ΔS_{bind} .

Fluorescence polarization binding assays

Binding assays, data analysis, and labeling of the E2 enzymes with bodipy (507/545)-iodoacetamide (Molecular Probes) has been described²³. Starting concentrations for bodipy-E2 depended on the extent of conjugated fluorophore and typically fell in the range of 0.5–2.0 μ M. Manual titrations were performed using wild-type and mutant E6AP(HECT) stock solutions that varied based on yield and strength of the interaction. All binding assays were performed at room temperature in 20 mM KH_2PO_4 (pH 7.0), 150 mM NaCl, 5 mM β -ME. For each binding experiment, nine polarization readings were collected and averaged at 20 concentrations of E6AP(HECT). Data were fit to a single-site binding model using non-linear regression with SigmaPlot software to yield parameters for P_{min} (starting polarization), P_{max} (maximum polarization), and K_D (dissociation constant).

***In vitro* ubiquitin transfer assay**

Isotopic labeling of ubiquitin with ^{32}P was carried out using the PKAce™ kit (Novagen) according to the manufacturer's protocol. The labeling reaction was quenched with a tenfold molar excess of protein kinase A inhibitor (PKI 6–22 Amide, EMD Biosciences). Assays were carried out at 4 °C for 20 min in 50 μ l volumes containing 20 mM Tris (pH 7.5), 50 mM NaCl, 10 mM MgCl_2 , 0.2 mM β -ME, 2 mM ATP, 10 mM creatine phosphate, ten U/ml creatine kinase, 5 μ M [^{32}P]ubiquitin, 50 nM human E1 (Boston Biochem), 1 μ M UbcH7, and 1 μ M wild-type or mutant E6AP(HECT). Reactions were initiated with the addition of [^{32}P]ubiquitin and terminated with 2X SDS-PAGE loading buffer with or without 200 mM β -ME. SDS-PAGE was used to separate 30 μ l of the final reactions and

gels were then dried and exposed to a phosphor screen. A phosphorimager and ImageQuant 5.0 software (GE Healthcare) were used to detect and quantify [^{32}P]ubiquitin bands. The experiment was performed in duplicate (**Supplementary Data, Figure 2.9**).

SUPPLEMENTARY DATA

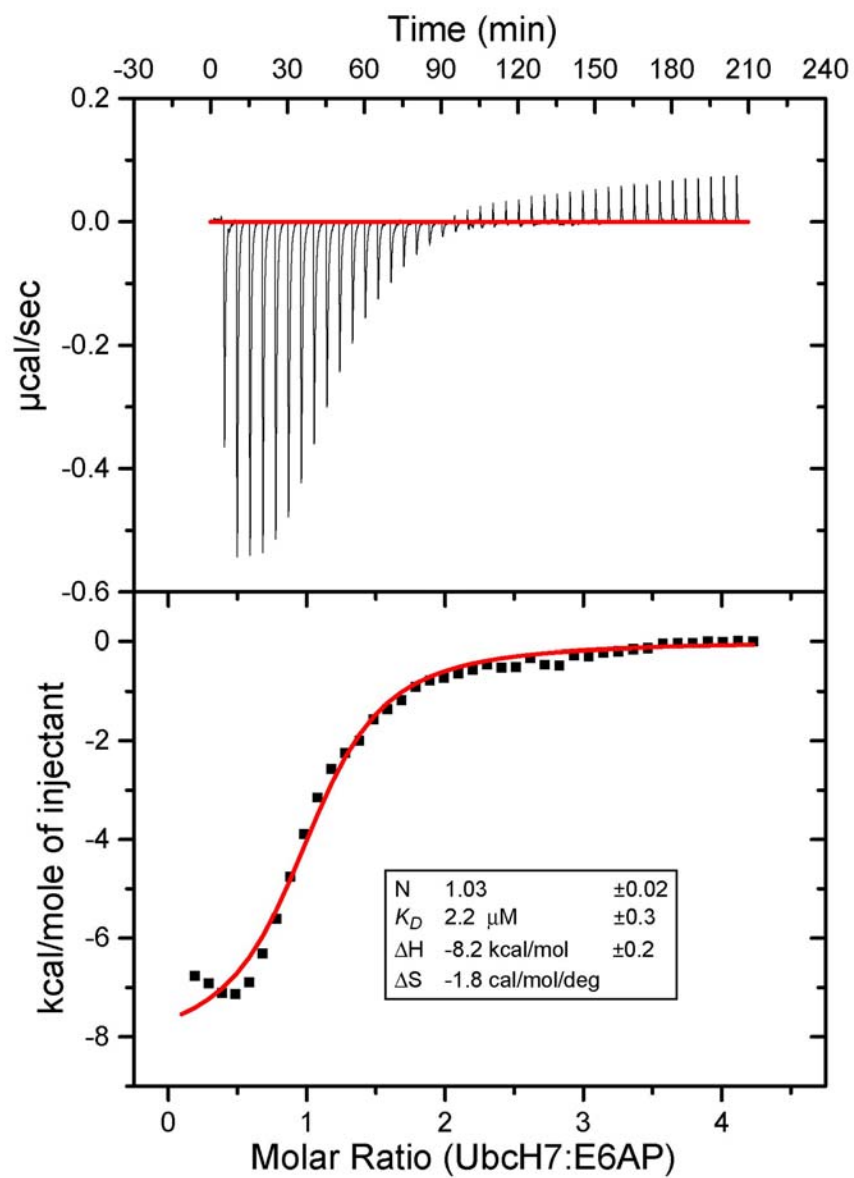


Figure 2.8. Isothermal titration calorimetry of unmodified Ubch7 with E6AP.

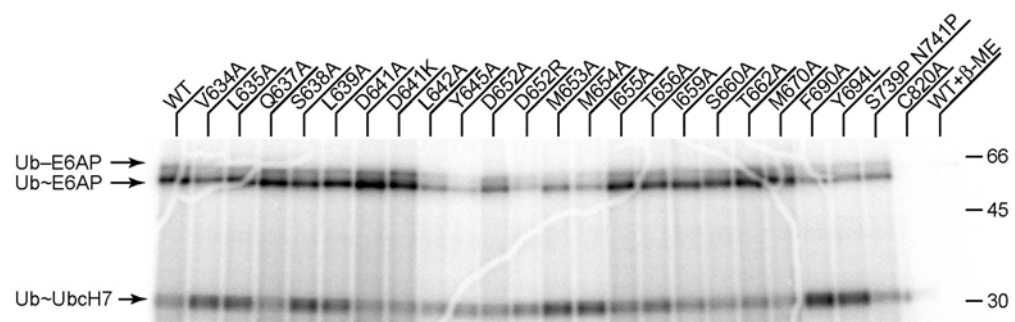


Figure 2.9. Duplicate ubiquitin transfer assay with E6AP mutants.

REFERENCES

1. Hershko, A. & Ciechanover, A. (1998). The ubiquitin system. *Annu Rev Biochem* **67**, 425-79.
2. Scheffner, M., Nuber, U. & Huibregtse, J. M. (1995). Protein ubiquitination involving an E1-E2-E3 enzyme ubiquitin thioester cascade. *Nature* **373**, 81-3.
3. Schwartz, A. L. & Ciechanover, A. (1999). The ubiquitin-proteasome pathway and pathogenesis of human diseases. *Annu Rev Med* **50**, 57-74.
4. Glickman, M. H. & Ciechanover, A. (2002). The ubiquitin-proteasome proteolytic pathway: destruction for the sake of construction. *Physiol Rev* **82**, 373-428.
5. Winkler, G. S., Albert, T. K., Dominguez, C., Legtenberg, Y. I., Boelens, R. & Timmers, H. T. (2004). An altered-specificity ubiquitin-conjugating enzyme/ubiquitin-protein ligase pair. *J Mol Biol* **337**, 157-65.
6. Martinez-Noel, G., Muller, U. & Harbers, K. (2001). Identification of molecular determinants required for interaction of ubiquitin-conjugating enzymes and RING finger proteins. *Eur J Biochem* **268**, 5912-9.
7. Zheng, N., Schulman, B. A., Song, L., Miller, J. J., Jeffrey, P. D., Wang, P., Chu, C., Koepp, D. M., Elledge, S. J., Pagano, M., Conaway, R. C., Conaway, J. W., Harper, J. W. & Pavletich, N. P. (2002). Structure of the Cul1-Rbx1-Skp1-F boxSkp2 SCF ubiquitin ligase complex. *Nature* **416**, 703-9.
8. Ulrich, H. D. (2003). Protein-protein interactions within an E2-RING finger complex. Implications for ubiquitin-dependent DNA damage repair. *J Biol Chem* **278**, 7051-8.
9. Katoh, S., Tsunoda, Y., Murata, K., Minami, E. & Katoh, E. (2005). Active site residues and amino acid specificity of the ubiquitin carrier protein-binding RING-H2 finger domain. *J Biol Chem* **280**, 41015-24.
10. Scheffner, M., Huibregtse, J. M., Vierstra, R. D. & Howley, P. M. (1993). The HPV-16 E6 and E6-AP complex functions as a ubiquitin-protein ligase in the ubiquitination of p53. *Cell* **75**, 495-505.
11. Huang, L., Kinnucan, E., Wang, G., Beaudenon, S., Howley, P. M., Huibregtse, J. M. & Pavletich, N. P. (1999). Structure of an E6AP-UbcH7 complex: insights into ubiquitination by the E2-E3 enzyme cascade. *Science* **286**, 1321-6.
12. Verdecia, M. A., Joazeiro, C. A., Wells, N. J., Ferrer, J. L., Bowman, M. E., Hunter, T. & Noel, J. P. (2003). Conformational flexibility underlies ubiquitin ligation mediated by the WWPI HECT domain E3 ligase. *Mol Cell* **11**, 249-59.
13. Ogunjimi, A. A., Briant, D. J., Pece-Barbara, N., Le Roy, C., Di Guglielmo, G. M., Kavsak, P., Rasmussen, R. K., Seet, B. T., Sicheri, F. & Wrana, J. L. (2005). Regulation of Smurf2 ubiquitin ligase activity by anchoring the E2 to the HECT domain. *Mol Cell* **19**, 297-308.

14. Nawaz, Z., Lonard, D. M., Smith, C. L., Lev-Lehman, E., Tsai, S. Y., Tsai, M. J. & O'Malley, B. W. (1999). The Angelman syndrome-associated protein, E6-AP, is a coactivator for the nuclear hormone receptor superfamily. *Mol Cell Biol* **19**, 1182-9.
15. Cooper, E. M., Hudson, A. W., Amos, J., Wagstaff, J. & Howley, P. M. (2004). Biochemical analysis of Angelman syndrome-associated mutations in the E3 ubiquitin ligase E6-associated protein. *J Biol Chem* **279**, 41208-17.
16. Pickart, C. M. (2001). Mechanisms underlying ubiquitination. *Annu Rev Biochem* **70**, 503-33.
17. Zheng, N., Wang, P., Jeffrey, P. D. & Pavletich, N. P. (2000). Structure of a c-Cbl-UbcH7 complex: RING domain function in ubiquitin-protein ligases. *Cell* **102**, 533-9.
18. Nuber, U. & Scheffner, M. (1999). Identification of determinants in E2 ubiquitin-conjugating enzymes required for hect E3 ubiquitin-protein ligase interaction. *J Biol Chem* **274**, 7576-82.
19. Nuber, U., Schwarz, S., Kaiser, P., Schneider, R. & Scheffner, M. (1996). Cloning of human ubiquitin-conjugating enzymes UbcH6 and UbcH7 (E2-F1) and characterization of their interaction with E6-AP and RSP5. *J Biol Chem* **271**, 2795-800.
20. Kumar, S., Kao, W. H. & Howley, P. M. (1997). Physical interaction between specific E2 and Hect E3 enzymes determines functional cooperativity. *J Biol Chem* **272**, 13548-54.
21. Anan, T., Nagata, Y., Koga, H., Honda, Y., Yabuki, N., Miyamoto, C., Kuwano, A., Matsuda, I., Endo, F., Saya, H. & Nakao, M. (1998). Human ubiquitin-protein ligase Nedd4: expression, subcellular localization and selective interaction with ubiquitin-conjugating enzymes. *Genes Cells* **3**, 751-63.
22. Schwarz, S. E., Rosa, J. L. & Scheffner, M. (1998). Characterization of human hect domain family members and their interaction with UbcH5 and UbcH7. *J Biol Chem* **273**, 12148-54.
23. Eletr, Z. M., Huang, D. T., Duda, D. M., Schulman, B. A. & Kuhlman, B. (2005). E2 conjugating enzymes must disengage from their E1 enzymes before E3-dependent ubiquitin and ubiquitin-like transfer. *Nat Struct Mol Biol* **12**, 933-4.
24. Winn, P. J., Religa, T. L., Battey, J. N., Banerjee, A. & Wade, R. C. (2004). Determinants of functionality in the ubiquitin conjugating enzyme family. *Structure* **12**, 1563-74.
25. Clackson, T. & Wells, J. A. (1995). A hot spot of binding energy in a hormone-receptor interface. *Science* **267**, 383-6.
26. Bogan, A. A. & Thorn, K. S. (1998). Anatomy of hot spots in protein interfaces. *J Mol Biol* **280**, 1-9.
27. Ingham, R. J., Gish, G. & Pawson, T. (2004). The Nedd4 family of E3 ubiquitin ligases: functional diversity within a common modular architecture. *Oncogene* **23**, 1972-84.
28. Gill, S. C. & von Hippel, P. H. (1989). Calculation of protein extinction coefficients from amino acid sequence data. *Anal Biochem* **182**, 319-26.

CHAPTER III

INSIGHTS INTO E2-HECT BINDING AFFINITY AND SPECIFICITY

ABSTRACT

It is well established that conjugation of ubiquitin to a protein substrate requires the sequential action of E1, E2, and E3 enzymes. In humans a hierarchy of a single E1, roughly thirty E2s and hundreds of E3s allows for targeting specific protein substrates for ubiquitination. Inherent to this hierarchy is the requirement for E2s to interact with multiple E3s. Indeed this is the case for most E2s which can function with E3s that possess different E2-binding domains. In contrast, a given E3 will selectively function with E2s from one or few E2 subfamilies. Selective E2–E3 interactions are important in ensuring that substrate ubiquitination is highly specific. In humans, improper substrate ubiquitination can have severe consequences resulting in inherited disorders as well as acquired diseases and cancers. In this study we have attempted to gain insights into E2–E3 specificity by identifying high affinity E2–HECT E3 interactions. Using a quantitative binding assay we measured the affinity of HECT domains from Nedd4L, Smurf2, and Huwe1 proteins for fifteen E2s representing 11 E2 subfamilies. Our results with Nedd4L support previous findings that have demonstrated HECT domains selectively interact with subfamilies of E2s. The Nedd4L protein formed high affinity interactions with E2s from the UBC4/5 and E2-E subfamilies but Smurf2 did not display high affinity interactions with any E2s tested. Interestingly, the Huwe1 protein did not bind any E2s tightly suggesting it may act in a mechanism similar to Smurf2 whereby a tertiary protein provides affinity and selectivity for E2s. A better understanding of E2–E3 specificity will help in the development of new methods to study the pathology of ubiquitin related diseases.

INTRODUCTION

Ubiquitin conjugation to a substrate requires the sequential action of E1, E2, and E3 enzymes. In humans there is a hierarchy of a single ubiquitin E1, roughly 30 E2s, and hundreds of E3s. The activating enzyme (E1) uses ATP to adenylate the carboxyl terminus of ubiquitin and subsequently forms a thioester intermediate with ubiquitin via its active-site cysteine residue. Ubiquitin conjugating enzymes (E2s) bind to the E1 and form a second cysteine-mediated thioester bond with ubiquitin prior to binding a ubiquitin ligase (E3). Ubiquitin ligases (E3s) are proteins or protein complexes that catalyze ubiquitination by selectively binding both substrate and E2. These two binding events are carried out by distinct domains within a protein or by separate proteins within a multisubunit protein complex. E3s enzymes can be classified by the type of E2-binding domain they harbor. RING (really interesting new gene), PHD (plant homeodomain), and U-box domain E3s facilitate the direct transfer of ubiquitin from E2 to substrate^{1; 2; 3; 4} while HECT (homology to E6AP carboxy terminus) domain E3s form a third thioester-intermediate with ubiquitin prior to transfer to substrate⁵.

Much of our understanding of E2–E3 interactions at the molecular level is owed to two crystal structures of E2–E3 complexes. The first structure solved was that of the E2 Ubch7 in complex with the HECT domain of E6AP⁶. This most significant contact at the interface comes from a phenylalanine residue of Ubch7 that is situated at the tip of loop 4 (L4-Phe) and packs into a hydrophobic groove created by E6AP⁶. Additional contacts from Ubch7 came mostly from helix 1 (H1) and loop 7 (L7) with fewer contributions from loop 2 (L2)⁶. The RING E3 c-Cbl was later crystallized in complex with the same E2 Ubch7⁷. This structure showed that E2s use similar residues to bind both RING and HECT domain E3s and that the L4-Phe again forms the most extensive interface contacts⁷. Mounting evidence from biochemical and biophysical data suggests that a phenylalanine amino acid at this position is absolutely necessary for a functional E2–HECT interaction^{6; 8; 9; 10; 11}. In contrast, RING domain E3s are more tolerable to different amino acids at this position as functional E2–RING pairs have been identified with Asn, Tyr, His, and Leu at this

position. In humans there are approximately 33 E3s of which 14 have an L4-Phe. Nine of these E2s can be grouped into the UBC4/5, E2-E, and E2-L subfamilies which have all been shown to function with HECT E3s. It is yet to be determined whether the five remaining E2s (UbcH2, HIP-2, NCUBE2, E2-T, and E2-W) will also function with HECT domain E3s.

The hierarchical nature of the ubiquitin pathway imposes a requirement that at least some E2s must function with multiple E3s. Indeed this is the case as most E2s are capable of functioning with multiple E3s¹². In most cases, a given E3 selectively functions with only one or few E2s. This E2–E3 specificity was first demonstrated with the HECT E3s Rsp5 and E6AP¹³. Specific E2–E3 and E3–substrate interactions are critical for maintaining the high specificity of ubiquitin-dependent protein degradation. Dysregulation of ubiquitin substrates when E3s gain or lose function can have severe consequences in humans. Inherited neurological disorders like Angelman’s syndrome and autosomal-recessive Parkinson’s disease have been linked to the E3s E6AP^{14; 15} and Parkin^{16; 17}, but the substrates responsible for the pathology of these diseases remain elusive^{12; 18; 19}. One method to identify the substrates of a given E3s is to isolate specific E2–E3 interactions in the cell and study the downstream events. Isolating a specific E2–E3 pair in the cell could be achieved by redesigning E2–E3 interfaces to create altered specificity E2–E3 pairs that function with one another but no longer with their wild-type precursors or other E2 and E3 proteins. The E2–RING pair UbcH5b–CNOT4 has been successfully redesigned to interact with one another but not their wild-type precursors²⁰. The ability to rationally create altered specificity E2–E3 pairs rests on our understanding of the determinants of E2–E3 specificity. In this study we have expanded upon previous work that utilized a quantitative binding assay to show that the HECT domain from E6AP selectively binds to the UbcH7/8 subfamily of E2s with high affinity¹¹. We have employed the same assay to measure the binding affinity of fifteen E2s for HECT domains from human Nedd4L, Smurf2, and Huwe1 proteins. Our findings provide insight into high affinity E2–HECT pairs and the residues that dictate E2–HECT specificity.

RESULTS

Recombinant ubiquitin E2 enzymes are capable of forming ubiquitin-thioester intermediates

The E2s used in our binding assays are human proteins (except *Saccharomyces cerevisiae* UBC4) that represent 11 different E2 subfamilies (**Supplementary Data, Figure 3.6**). Three of the E2s are conjugating enzymes dedicated to ubiquitin-like pathways. The Ubc9 protein functions in the SUMO pathway, Ubc12 in the Nedd8 pathway, and UbcH8 in the ISG15 pathway. Full length proteins for all fifteen E2s were purified from *Escherichia coli* lysates and tested for their ability to form a thioester intermediate with ubiquitin. Transthioylation reactions were performed using [³²P]-ubiquitin, E1, ATP, and an ATP regenerating system. Separate reactions containing equal concentrations of E2s were allowed to proceed for 30 minutes before quenching in SDS-PAGE gel loading buffer (GLB) with and without β -mercaptoethanol (β -ME). The reactions were separated by SDS-PAGE and [³²P]-ubiquitin bands were visualized using a phosphorimager. The results for reactions quenched in GLB lacking β -ME show that all E2s except the those involved in ubiquitin-like protein conjugation (Ubc9, Ubc12, and UbcH8) were capable of forming thioester intermediates with ubiquitin (**Figure 3.1(a)**). Some E2s displayed robust transthioylation activity while others like HIP-2 and UbcH2 were much less active under our conditions. Poly-ubiquitinated E2s were not observed but some E2s did display a second band at the expected change in MW for a second ubiquitin (~11.5 kDa). The E1-ubiquitin thioester seen at the top of each lane is constant in all reactions indicating that the ATP-dependent activation step is not rate-limiting. Transthioylation reactions were also quenched in buffer containing β -ME to break thioester bonds and detect isopeptide linkages (**Figure 3.1(b)**). Interestingly, the three class III E2s with N-terminal extensions (UbcH10, UbcH8*, and UbcH9) all displayed β -ME resistant E2-ubiquitin bands suggesting these E2s possess autoubiquitination activity. Also prominent in a few reactions is a β -ME resistant diubiquitin band (E2-G2 and Cdc34) that runs at ~23 kDa. Our results show that our ubiquitin E2s are active and that E1-E2 transthioylation reactions proceed with differing kinetics and yield different ubiquitination activity. These differences were not accounted for in

studies by other groups addressing E2–E3 specificity and may have led to the conflicting results that were often observed^{8; 9; 10; 13; 21; 22}.

The Nedd4L HECT domain selectively binds to E2s from the UBC4/5 and E2-E subfamilies

The human Nedd4 and Nedd4L paralogs are ~80% identical in amino acid sequence across the E2-binding region of their HECT domains suggesting that both E3s will display similar E2-binding preferences. Indeed this was observed in a previous study that found both E3s preferred UbcH5a, UbcH5b, and UbcH7 followed by UbcH6 and UbcH9 in a substrate ubiquitination assays¹⁰. In a prior study, Nedd4 autoubiquitination activity was greatest with UbcH6 and UbcH7 followed by UbcH5b and UbcH5c⁸. Also, the UbcH9–Nedd4L interaction was identified in a two-hybrid screen and validated *in vitro* and *in vivo*²³. In conclusion these findings suggested that these E2s will display high affinity interactions with Nedd4L in our binding assay. To monitor HECT binding to E2s we covalently labeled each E2 with a thiol-reactive fluorophore. The labeling of UbcH7 with the identical fluorophore was previously shown to have little effect on UbcH7 binding to E6AP¹¹. The UbcH8 protein is the only E2 with a cysteine at the E3-binding interface and for this reason we tested the C97S mutant in our FP binding assays. All HECT domains examined in this study (**Supplementary Data, Figure 3.7**) were purified from *E.coli* lysates.

The Nedd4L HECT domain (residues 596-975) bound to five of the E2s tested with a dissociation constant (K_D) below 50 μ M (**Figure 3.2**). These five E2s are members of the UBC4/5 subfamily (UbcH5a, UbcH5b, and yUbc4) and the E2-E subfamily (UbcH8* and UbcH9). The UbcH5a and UbcH9 proteins formed the highest affinity interactions exhibiting K_D values of 4.6 μ M and 8.4 μ M respectively. Interestingly the UbcH7 and UbcH8(C97S) proteins weakly bound to Nedd4L with affinities of 370 μ M and 490 μ M respectively (**Figure 3.2**). The six E2s that lack a L4-Phe (Rad6b, Cdc34, E2-G2, Ubc9, UbcH10, and Ubc12) all failed to bind Nedd4L HECT with a measurable affinity. The HIP-2 protein also failed to bind while UbcH2 bound Nedd4L

weakly ($K_D = 340 \mu\text{M}$). Our finding that Nedd4L selectively binds E2s from the UBC4/5 and E2-E subfamilies is consistent with previous studies^{10; 23}. An unexpected finding was that the E2-L family members UbcH7 and UbcH8 failed to bind with high affinity despite displaying similar conjugating activity as UbcH5a and UbcH5b¹⁰. One explanation is that substrate ubiquitination assays are an indirect measure of E2–E3 binding and are less sensitive in detecting small differences in E2–E3 affinity because the E1–E2 reaction slow and rate-limiting¹¹.

The E6AP HECT domain weakly binds E2s from the E2-E subfamily

In our previous study on E2–E6AP specificity we measured E6AP binding affinity for nine of the E2s used in this study¹¹. Of the six additional E2s used in this study, two are members of the E2-E subfamily (UbcH8* and UbcH9) which are class III E2s with N-terminal extensions. These E2s are most similar to the UBC4/5 subfamily in residues responsible for E3 binding. Given our finding that the UBC4/5 and E2-E subfamilies bound Nedd4L with similar affinity, we expected that E6AP would weakly interact with these E2s. Indeed this was the case as we measured UbcH9 affinity at $140 \mu\text{M}$ and UbcH8* affinity at $290 \mu\text{M}$ (**Figure 3.3**). We also measured E6AP affinity for the other new E2s (HIP-2, Cdc34, UbcH5a, and E2-G2) and found that only UbcH5a bound with detectable affinity ($K_D = 80 \mu\text{M}$). This value is similar to previously measured affinities for other E2s from the UBC4/5 subfamily (**Table 3.1**)¹¹. These findings support our previous results on E2–E6AP specificity that showed E6AP only bound the E2-L subfamily (UbcH7 and UbcH8) with high affinity¹¹.

Smurf2 and Huwe1 HECT domains do not form high affinity E2 interactions

A new twist on E2–E3 specificity was revealed when Ogunjimi *et al* showed the Smad7 protein was capable of recruiting UbcH7 to the Smurf2 HECT domain by directly binding to both proteins²⁴. This interaction was specific for UbcH7 as the Smad7 protein was not able enhance other E2–Smurf2

interactions²⁴. The Ogunjimi *et al* study also showed that two Smurf2 residues (H547 and Y581) were disfavoring UbcH7 binding and that mutating these residues to E6AP amino acids (H547I and Y581F) significantly enhanced the affinity UbcH7–Smurf2 interaction²⁴. We tested the Smurf2 HECT domain (residues 371-748) in our FP binding assay against our panel of E2s and found that it did not bind any E2s with moderate affinity except UbcH2 ($K_D = 320 \mu\text{M}$). To better estimate the affinity of Smurf2 for UbcH5b and UbcH7 we performed FP binding assays in which the final concentration of Smurf2 was increased from 250 μM to $\sim 800 \mu\text{M}$. In these experiments the UbcH7 dissociation constant was measured at $\sim 1.4 \text{ mM}$ while UbcH5b binding was still undetected (data not shown). We next measured the effects of the H547I and Y581F Smurf2 point mutants in our FP binding assay. Both Smurf2 mutants bound UbcH7 with improved affinities ($K_D \sim 0.5\text{--}1 \text{ mM}$), but given the weak affinity a precise measure of binding was not possible. Our results support the Ogunjimi *et al* finding that the Smurf2 E2-binding pocket contains amino acid residues that disfavor high affinity E2-interactions.

The Huwe1 protein (also called ARF-BP1/Mule/HectH9) has been shown to function *in vitro* with both UbcH5a and UbcH7^{25; 26; 27} but to our knowledge the E2 selectivity of Huwe1 has not been examined. In our FP binding assay the Huwe1 HECT domain (residues 3987-4374) was unable to interact favorably with UbcH5a nor UbcH7 (**Table 3.1**). The only E2 that formed an interaction with detectable affinity was UbcH2 which bound with a dissociation constant of 190 μM . The full length Huwe1 protein is $\sim 500 \text{ kDa}$ and contains many additional domains²⁷ that could potentially bind a tertiary protein and enhance an E2–Huwe1 interaction. These findings suggest that the like Smurf2, Huwe1 and possibly other HECT E3s have suboptimal E2-binding grooves necessitating a tertiary protein for high affinity E2-interactions.

Engineering a tight binding UbchH7–Nedd4L pair

An interesting question that remains is which E2 and Nedd4L amino acid side-chains are most responsible for forming high affinity interactions. We previously used alanine mutagenesis and our FP binding assay to measure the effects of 36 single mutations at the UbchH7–E6AP interface¹¹. In that study we found four UbchH7 side-chains (P62, F63, K96, and K100) contributed more than 1 kcal/mol to the free energy of binding and that two mutations to UbchH5b (L3S and T98K) were able to enhance UbchH5b–E6AP affinity from 160 μ M down to 7.4 μ M¹¹. We aligned the primary sequences of the 15 E2s used in this study (**Supplementary Data, Figure 3.6**) and analyzed the subset of residues that interact E3s (**Figure 3.4**). We first mutated the L7-UbchH7 lysines to the corresponding amino acids found in the UBC4/5 and E2-E subfamilies (K96S and K100T). We measured binding of these UbchH7 mutant proteins against both E6AP and Nedd4L. The K96S mutation had little impact on E6AP binding yet was able to promote a tighter UbchH7–Nedd4L interaction ($\Delta\Delta G^{\circ}_{\text{bind}} = -0.5$ kcal/mol) (**Table 3.2**). In contrast the K100T mutation showed reduced binding to E6AP ($\Delta\Delta G^{\circ}_{\text{bind}} = 0.8$ kcal/mol) while binding Nedd4L with wild-type affinity. We also tested the A59T UbchH7 mutation because threonine is seen at this position in the UBC4/5 subfamily. We found that E6AP disfavored this mutation ($\Delta\Delta G^{\circ}_{\text{bind}} = 0.7$ kcal/mol) while Nedd4L preferred a threonine ($\Delta\Delta G^{\circ}_{\text{bind}} = -0.4$ kcal/mol). We next tested if the A59T–K96S double mutant would display an additive enhancement to binding Nedd4L. To our surprise the effects on binding were non-additive as the double mutant bound Nedd4L no tighter than either single mutation. This observation was not observed for E6AP which bound A59T–K96S with additive effects of each single mutant ($\Delta\Delta G^{\circ}_{\text{bind}} = 0.8$ kcal/mol). The S4L mutation is yet to be tested and may be necessary for obtaining a high affinity UbchH7–Nedd4L pair.

DISCUSSION

In this study we measured the dissociation constant for fifty E2–HECT interactions in an effort to better understand amino acid residues that dictate E2–HECT specificity. The importance of a L4-Phe residue for HECT binding is demonstrated again as none of the E2s lacking this phenylalanine bound to any HECT with detectable affinity. We have found that like E6AP, the HECT domain of Nedd4L selectively forms high affinity E2 interactions. Unlike E6AP which prefers the E2-L subfamily, Nedd4L preferentially bound E2s from UBC4/5 and E2-E subfamilies. The E2–Nedd4L interactions displaying tightest binding were UbcH9 and UbcH5a with dissociation constants below 10 μ M and quite similar to values of those measured for E6AP binding to UbcH7 and UbcH8¹¹. The binding of Nedd4L to UbcH7 and UbcH8 (370–490 μ M) was weaker than E6AP binding to UBC4/5 and E2-E subfamily members (80–290 μ M). The Smurf2 and Huwe1 HECT domains exhibited similar behavior in that neither bound any E2s with high affinity. The only E2 that bound with detectable affinity was the UbcH2 protein which formed weak interactions with both HECT domains. The Smurf2 protein has been shown to have a non-optimal E2-binding site and to function in conjunction with Smad7 to selectively bind UbcH7²⁴. Though the effects of Smad7 on the UbcH7–Smurf2 interaction has not been addressed in this work, a ~1000-fold increase in binding affinity would be necessary to approach the affinity of tight binding E2–HECT pairs. Our findings with the Huwe1 HECT domain suggest that it also requires an additional protein factor for tight E2-binding. It is possible that an untested human E2 with a L4-Phe could form favorable interactions with Smurf2 or Huwe1, but we do not believe this will be the case as Nedd4L and E6AP both maintain weak affinity for non-preferred E2s.

In a previous work on UbcH7–E6AP specificity, we measured the change in UbcH7 affinity for E6AP upon mutating 18 individual side-chains to alanine¹¹. To map these positions on other HECT domains we performed a structure-guided alignment of the HECT domains examined in this study. Crystal structures of the HECT domains of Smurf2²⁴, Nedd4L²⁸, and E6AP⁶ were used to perform a

structural alignment of their ~80 amino acid E2-binding domains. The structurally defined portions of the E2-binding domains aligned well allowing us to translate E6AP residues to the other HECT domains with confidence. The alignment (**Figure 3.5(a)**) shows that the loop connecting H7 and S5 is 1–3 residues longer in E6AP and the S5-S6 hairpin in E6AP has a leucine insertion. The 18 interface positions mutated to alanine in our previous work were mapped onto the aligned HECT structures (**Figure 3.5(b)**). We first looked for differences in Huwe1 relative to E6AP in effort to identify residues that potentially disfavor binding to all E2s. Some of the differences are common to Nedd4L suggesting that they are not responsible for disfavoring all E2 interactions. For example the F690 E6AP side-chain is present as a tyrosine in the other E3s; we have measured the effects of the F690Y E6AP mutation on binding UbcH7 and found that though destabilizing, the interaction was not abolished ($K_D = 53 \pm 12 \mu\text{M}$, unpublished results). The Huwe1 HECT has unique substitutions that are seemingly destabilizing at E6AP residues V634(H), S638(G), D652(G), and M653(Y). The H547 position in Smurf2 is a leucine in Huwe1 suggesting that the two HECT disfavor binding E2s using different side-chains.

In this study we also found that two mutations to UbcH7 that were able to provide marginal improvements to Nedd4L binding affinity. It is likely that the threonine side-chain in the A59T-UbcH7 protein is forming a hydrogen bond with the D778 Nedd4L side-chain. This hydrogen bond would be absent in the wild-type UbcH7–E6AP interaction because E6AP has a serine amino acid at this position. In support of this potential hydrogen bond interaction is our finding that the A59T-UbcH7 mutant bound E6AP with reduced affinity. The K96S-UbcH7 protein is likely enhancing affinity by relieving a steric clash imposed by the wild-type lysine with the Nedd4L W762 side-chain. Our findings with E6AP suggest that a serine residue at this position in UbcH7 may be capable of retaining a hydrogen bond with the D641 E6AP side-chain. The K100T mutant bound both E6AP and Nedd4L with reduced affinity suggesting that this threonine is too distant from the HECT domains to form interactions. We observed that the double mutant A59T–K96S did not bind Nedd4L with additive effects of both mutations. This was similarly observed when reengineering the

UbcH5b–E6AP interaction as the S94K UbcH5b mutation reduced binding alone or in the presence of T98K, but had no effect in the presence of the L3S mutation¹¹. This suggests that optimizing a cluster of interacting residues at a given E2–HECT interface may alter interface interactions at distal positions. Other mutations to UbcH7 that have not been tested but may prove important for UbcH7–Nedd4L affinity are S4L and R5K. The R5K mutant may allow for a hydrogen bond with Nedd4L D772, which is a methionine residue in E6AP (M654). The results from this work will aid efforts attempting to redesign E2–E3 interactions to better understand the pathology of ubiquitin-related diseases.

FIGURES

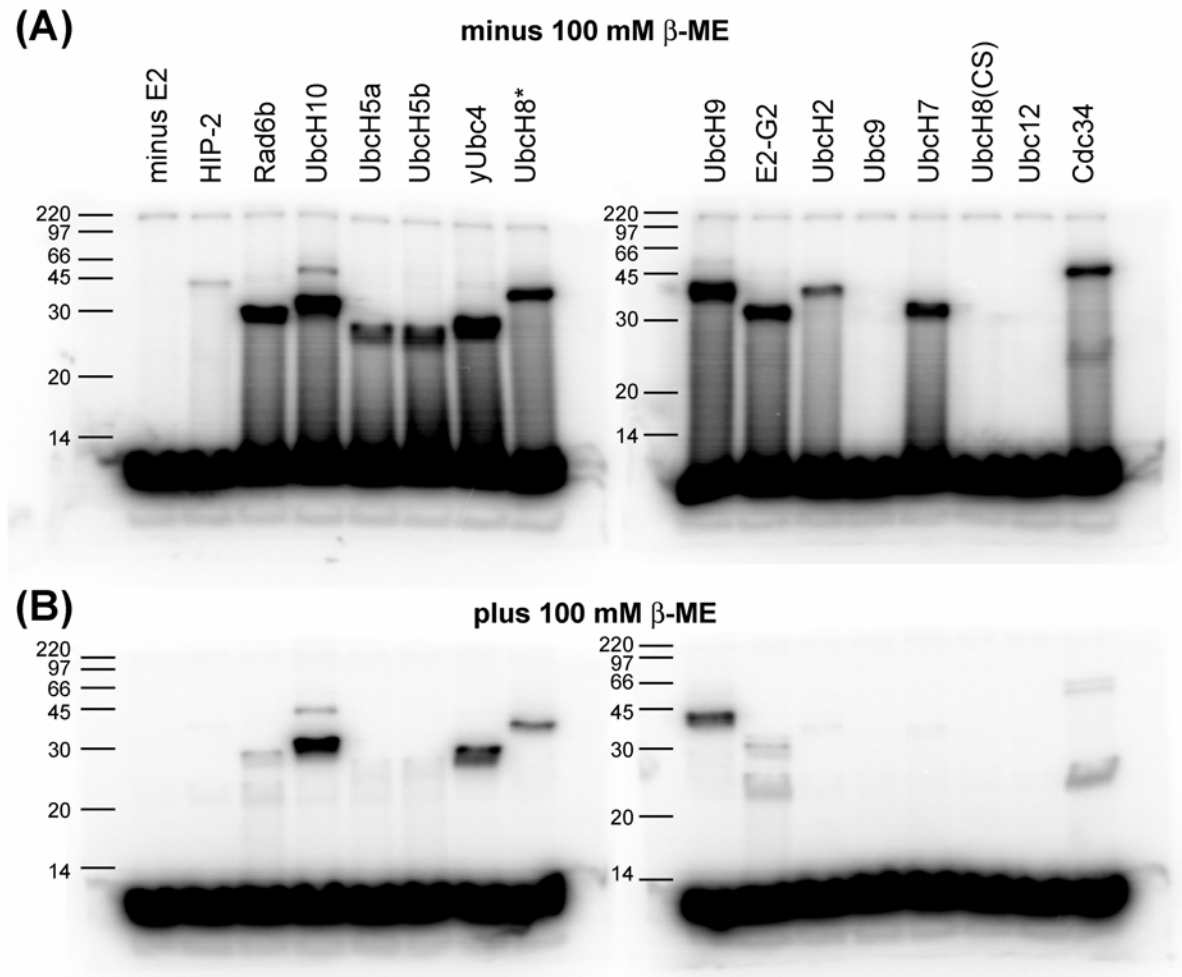


Figure 3.1. E1–E2 transthiolation assay. The 15 recombinant E2s were tested for their ability form ubiquitin thioester intermediates. Equal concentrations of each E2 were incubated with E1, [32 P]-ubiquitin, ATP, and an ATP regenerating system and allowed to proceed for 30 minutes at 25° C. Reactions were quenched in SDS-PAGE gel loading buffer without (A) and with 100 mM β -ME (B). All ubiquitin E2s were capable of forming thioester intermediates while E2s belonging to the Nedd8 (Ubc12), SUMO (Ubc9), and ISG15 (UbcH8) pathways were not.

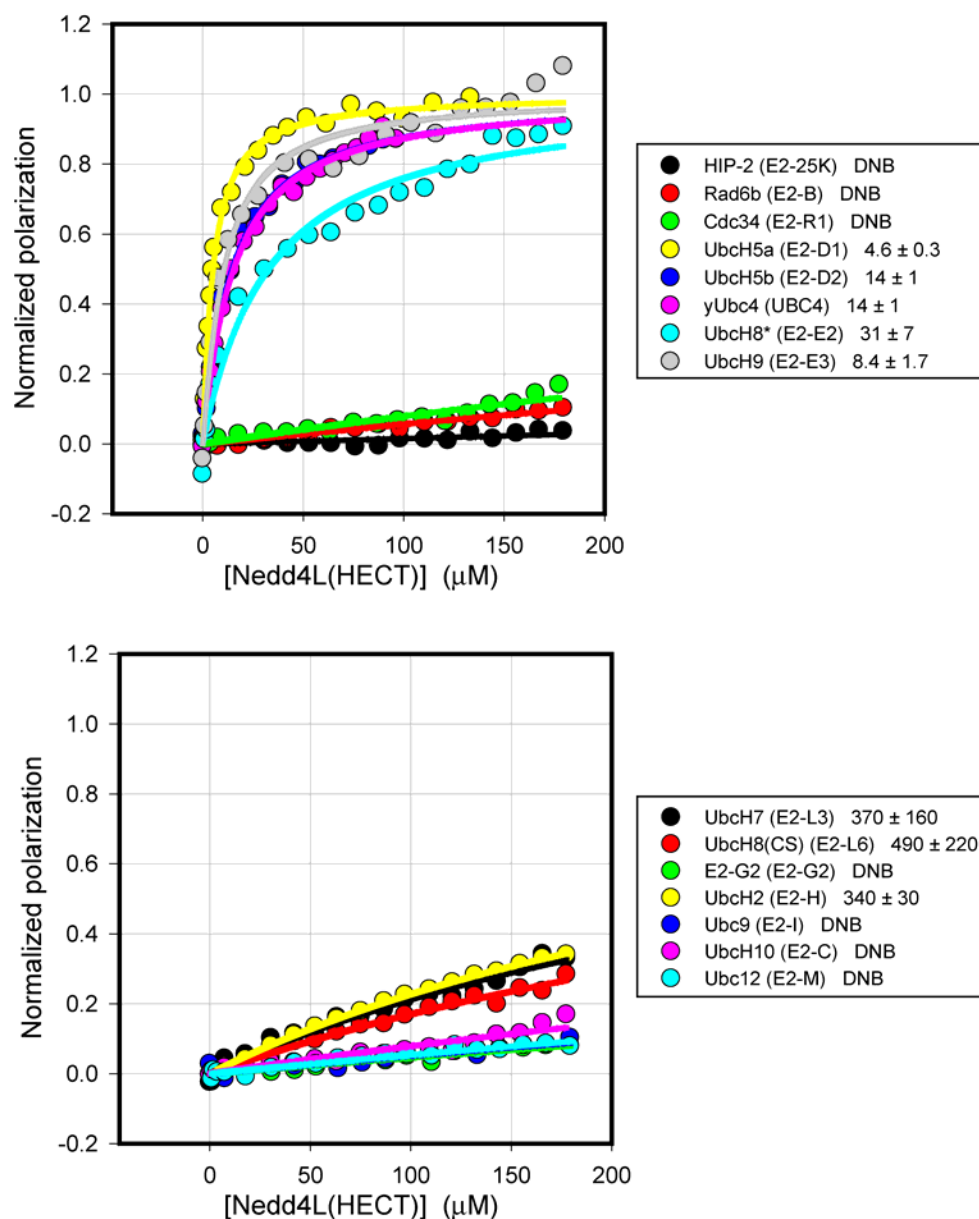


Figure 3.2. The Nedd4L HECT domain selectively interacts with E2s from the UBC4/5 and E2-E subfamilies. The Nedd4L HECT domain was tested in FP binding assays against the 15 E2s. UbcH5a and UbcH9, members of the UBC4/5 and E2-E subfamilies, bound Nedd4L with dissociation constant below $10 \mu\text{M}$. Other members of these subfamilies formed favorable interactions with Nedd4L (UbcH5b, yUbc4, and UbcH8*).

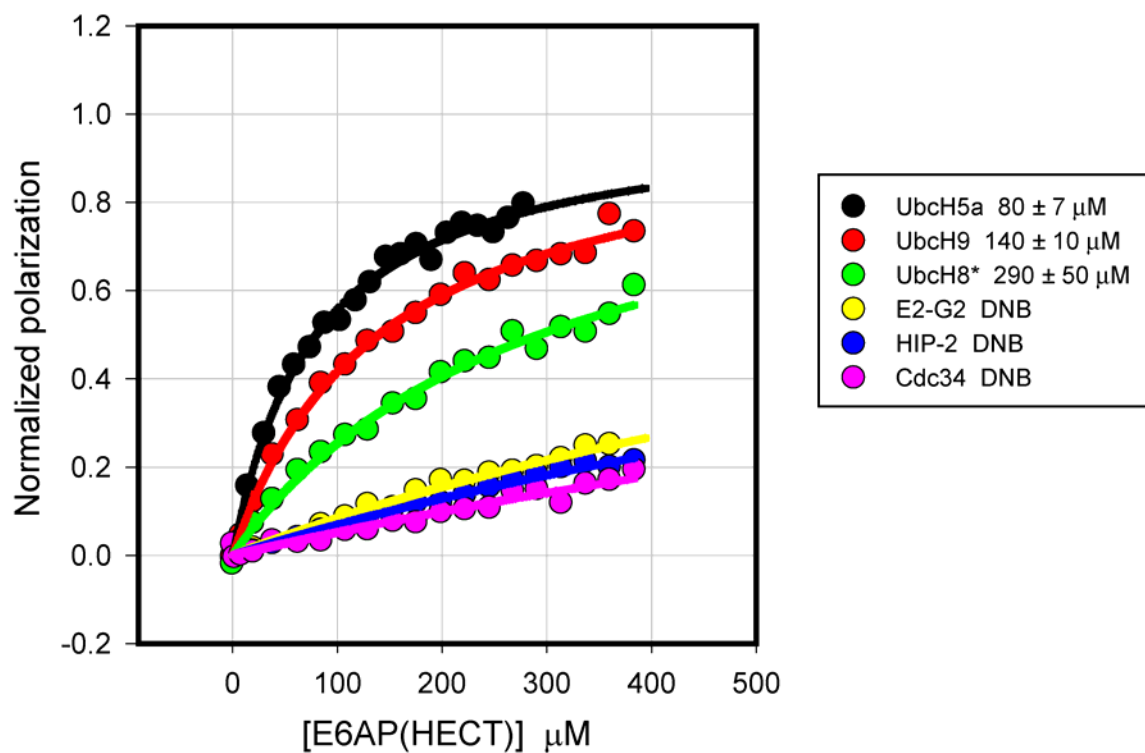


Figure 3.3. E6AP weakly interacts with the UBC4/5 and E2-E subfamily of E2s. The E6AP HECT domain was tested in the FP assay and found to weakly interact with UBC4/5 and E2-E subfamily members. This is in agreement with previous results that showed E6AP selectively binds the E2-L subfamily E2s Ubch7 and Ubch8¹¹.

	H1	L2	L4	L7	K_D for Nedd4L (μ M)
	●		● ●	● ●	
UbcH5a	LKRIQK	DLF	TDY P FK	S-Q W SPALT	4.6
UbcH9	AKRIQK	NIY	SDY P FK	D-N W SPALT	8.4
UbcH5b	LKRIHK	DMF	TDY P FK	S-Q W SPALT	14
yUbc4	SKRIAK	DLY	TDY P FK	D-Q W SPALT	14
UbcH8*	AKRIQK	NIY	PDY P FK	D-N W SPALT	31
UbcH2	KRRMDT	GLN	DKY P FK	Q-T W TALYD	340
UbcH7	SRRLMK	NLL	AEY P FK	E-N W KPATK	370
UbcH8	SMRVVK	NVL	PEY P FK	E-N W KPCTK	490
HIP-2	IKREFK	NFT	ETY P FN	D-Q W AAAMT	DNB
E2-G2	LKRLMA	NFF	LDY P LS	E-R W SPVQS	DNB
Cdc34	QKALLL	DLY	IDY P YS	E-R W NPTQN	DNB
Ubc9	LSRLAQ	NLM	DDY P SS	DKD W RPAIT	DNB
Rad6b	RRRLMR	NIM	EEY P NK	N-R W SPTYD	DNB
UbcH10	GKRLQQ	NLF	SGY P YN	E-K W SALYD	DNB
Ubc12	QLRIQK	-LL	QG Y PHD	E-D W KPVL	DNB

Figure 3.4. Multiple sequence alignment of the E3-binding residues of the 15 E2s used in this study. Red dots indicate positions that were previously found to be important for UbcH7–E6AP binding affinity and specificity¹¹. The E2s that interact most favorably with Nedd4L have an S/T at the first position in loop 4, a S at the fifth position in loop 7, and a T at the last position in loop 7..

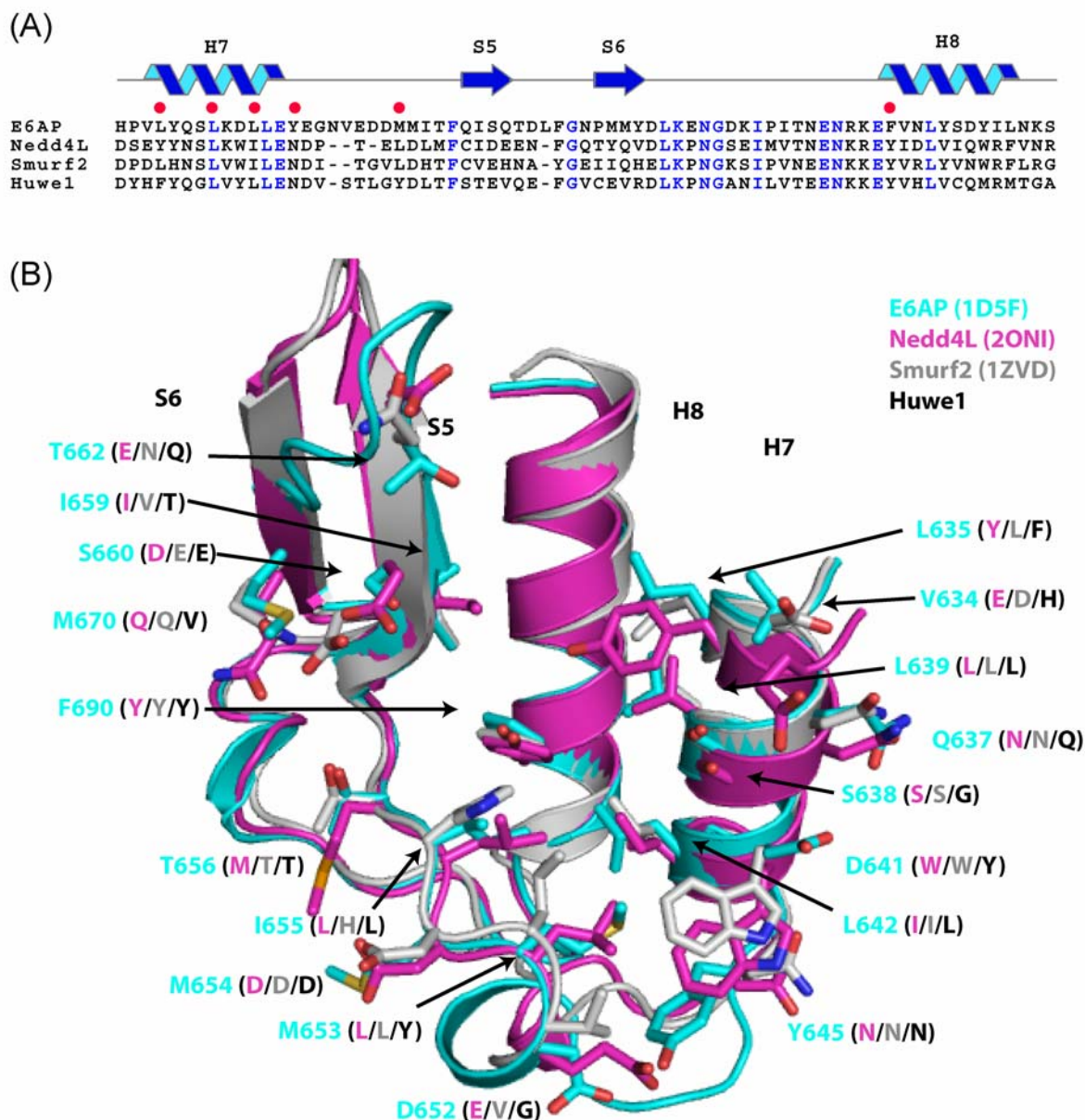


Figure 3.5. E2–Nedd4L specificity determining residues. (A) Multiple sequence alignment of the E2-binding domains of the 4 HECT E3s examined in this study. Red dots indicate residues that were previously shown to be important for Ubch7–E6AP binding affinity¹¹. (B) Superimposition of the E2-binding residues of the E6AP, Nedd4L, and Smurf2 HECT domains. Highlighted side-chains are interface residues that were previous analyzed by alanine mutagenesis and the FP assay¹¹.

TABLES

Table 3.1. Measured dissociation constants (in μM) for E2–HECT interactions.

E2	subfam	pos 63	E6AP	Nedd4L	Smurf2	Huwe1	K_D (μM)
HIP-2 (E2-25K)	UBC1	Phe	DNB	DNB	DNB	DNB	
Rad6b (E2-B)	UBC2	Asn	DNB [†]	DNB	DNB	DNB	
Cdc34 (E2-R1)	UBC3	Tyr	DNB	DNB	DNB	DNB	
UbcH5a (E2-D1)	UBC4/5	Phe	80 ± 7	4.6 ± 0.3	DNB	DNB	
UbcH5b (E2-D2)	UBC4/5	Phe	160 ± 10 [†]	14 ± 1	DNB	DNB	<div>< 50</div> <div>50 – 200</div> <div>200 – 500</div> <div>> 500</div>
yUbc4 (scUBC4)	UBC4/5	Phe	75 ± 11 [†]	14 ± 1	DNB	DNB	
UbcH8* (E2-E2)	E2-E	Phe	290 ± 50	31 ± 7	DNB	DNB	
UbcH9 (E2-E3)	E2-E	Phe	140 ± 10	8.4 ± 1.7	DNB	DNB	
UbcH7 (E2-L3)	E2-L	Phe	5.0 ± 0.5 [†]	370 ± 160	DNB	DNB	
UbcH8 (E2-L6)	E2-L	Phe	7.5 ± 0.7 [†]	490 ± 220	DNB	DNB	
E2-G2 (E2-G2)	UBC7	Leu	DNB	DNB	DNB	DNB	
UbcH2 (E2-H)	UBC8	Phe	180 ± 30 [†]	340 ± 30	320 ± 20	190 ± 20	
Ubc9 (E2-I)	UBC9	Ser	180 ± 20 [†]	DNB	DNB	DNB	
UbcH10 (E2-C)	UBC11	Tyr	DNB [†]	DNB	DNB	DNB	
Ubc12 (E2-M)	UBC12	His	DNB [†]	DNB	DNB	DNB	

[†]Reproduced from (11).

Table 3.2. Measured dissociation constants (in μM) of E6AP and Nedd4L HECT domains for UbcH7 mutants.

UbcH7	E6AP	Nedd4L
WT	$5.0 \pm 0.5^\dagger$	370 ± 160
A59T	15 ± 1	180 ± 40
K96S	5.5 ± 0.7	150 ± 30
K100T	20 ± 2	440 ± 280
A59T–K96S	19 ± 2	220 ± 60

† Reproduced from (11).

MATERIALS AND METHODS

Protein Purification

Expression plasmids and purification schemes for Rad6b, UbcH2, yUbc4, UbcH5b, UbcH7, UbcH8, UbcH10, Ubc9, Ubc12, E6AP(HECT), and ubiquitin have been described^{11; 29}. Expression plasmids for UbcH8*, E2-G2, HIP-2, and Cdc34 were subcloned from MGC clones (Open Biosystems) into the pGEX-4T-1 expression vector (GE Healthcare). Many groups kindly contributed plasmids used in this study. UbcH9 (from pGEX*, Marc Timmers), UbcH5a (from pET-3a, Jon Huibregtse), and Nedd4L (from pRK5, Fiona McDonald) were subcloned in pGEX-4T-1. Plasmids encoding Huwe1 HECT domain (pGEX-2TK, Jean Cook) and Smurf2 HECT domain (pGEX-4T-1, Tony Pawson) were in suitable vectors for bacterial expression. Single point mutations were generated using the QuickChange® site-directed mutagenesis protocol (Stratagene). All proteins were expressed in the BL21(DE3) strain of *E.coli* at 25° C for ~16 hours using 0.3 mM IPTG. Resuspended cells were disrupted by sonication and the resulting lysates was cleared by ultracentrifugation. All proteins were purified using glutathione Sepharose followed by thrombin cleavage to remove the GST-tag, anion exchange chromatography, and finally size-exclusion chromatography. Proteins were concentrated using Centriprep® and Centricon® concentrators and were quantified using extinction coefficients derived from the method describe by Gill and von Hippel³⁰.

E1–E2 transthiolation assay

Ubiquitin was expressed and purified with an N-terminal protein kinase A (PKA) recognition site. Isotopic labeling of ubiquitin with [³²P] was carried out using the PKAce™ kit (Novagen) according to the manufacturer's suggested protocol. A coomassie-stained SDS-PAGE gel was run to ensure equal concentrations of E2 were present in each reaction (data not shown). Reactions of 50 µl volumes containing 20 mM Tris (pH 7.5), 50 mM NaCl, 10 mM MgCl₂, 0.2 mM β-ME, 2 mM ATP,

10 mM creatine phosphate, 10 U/ml creatine kinase, 10 U/ml inorganic pyrophosphatase, 1 mM PMSF, 100 nM E1 (Boston Biochem), 13 μ M [32 P]-ubiquitin, and 5 μ M E2 were allowed to proceed for 30 min at 25°C. Reactions were initiated with [32 P]-ubiquitin and quenched in SDS-PAGE gel-loading buffer with and without 100 mM β -ME. Twenty microliters of each transthiolation reaction was separated by SDS-PAGE and the resulting gels were dried and exposed to a phosphor screen. Ubiquitin and ubiquitinated proteins were visualized using a phosphorimager (GE Healthcare).

Fluorescence polarization binding assay

A detailed method describing the E2 fluorophore-labeling reaction with bodipy (507/545)-iodoacetamide has been described²⁹. Binding assays were performed at room temperature in 20 mM KH_2PO_4 (pH 7.0), 150 mM NaCl, and 5 mM β -ME. For almost all binding measurements the HECT E3 stock solution was approximately 300 μ M. The starting concentration of each E2 varied from 0.5 μ M to 2 μ M and was dependent on the extent of labeling with bodipy. In each experiment, the polarization of bodipy-E2 was recorded at twenty concentrations of HECT domain. At each HECT concentration nine polarization readings were collected and averaged. Binding data were fit to a single-site binding model using non-linear regression in SigmaPlot as previously described²⁹. Data analysis in SigmaPlot yields parameters for P_{\min} (starting polarization) P_{\max} (maximum polarization) and K_D (dissociation constant). Weak E2–HECT interactions tended to fit to the maximum allowable P_{\max} (0.5) with micromolar K_D s and high standard errors. The P_{\min} for each E2 varied, but the change in polarization ($P_{\max} - P_{\min}$) observed for high affinity E2–HECT interactions typically fell in the range of 0.09 to 0.11. The UbcH2 protein, which bound all HECT domains tested with marginal affinity, is the only exception and it displayed a change in polarization of ~ 0.3 when bound to a HECT domain.

SUPPLEMENTARY DATA

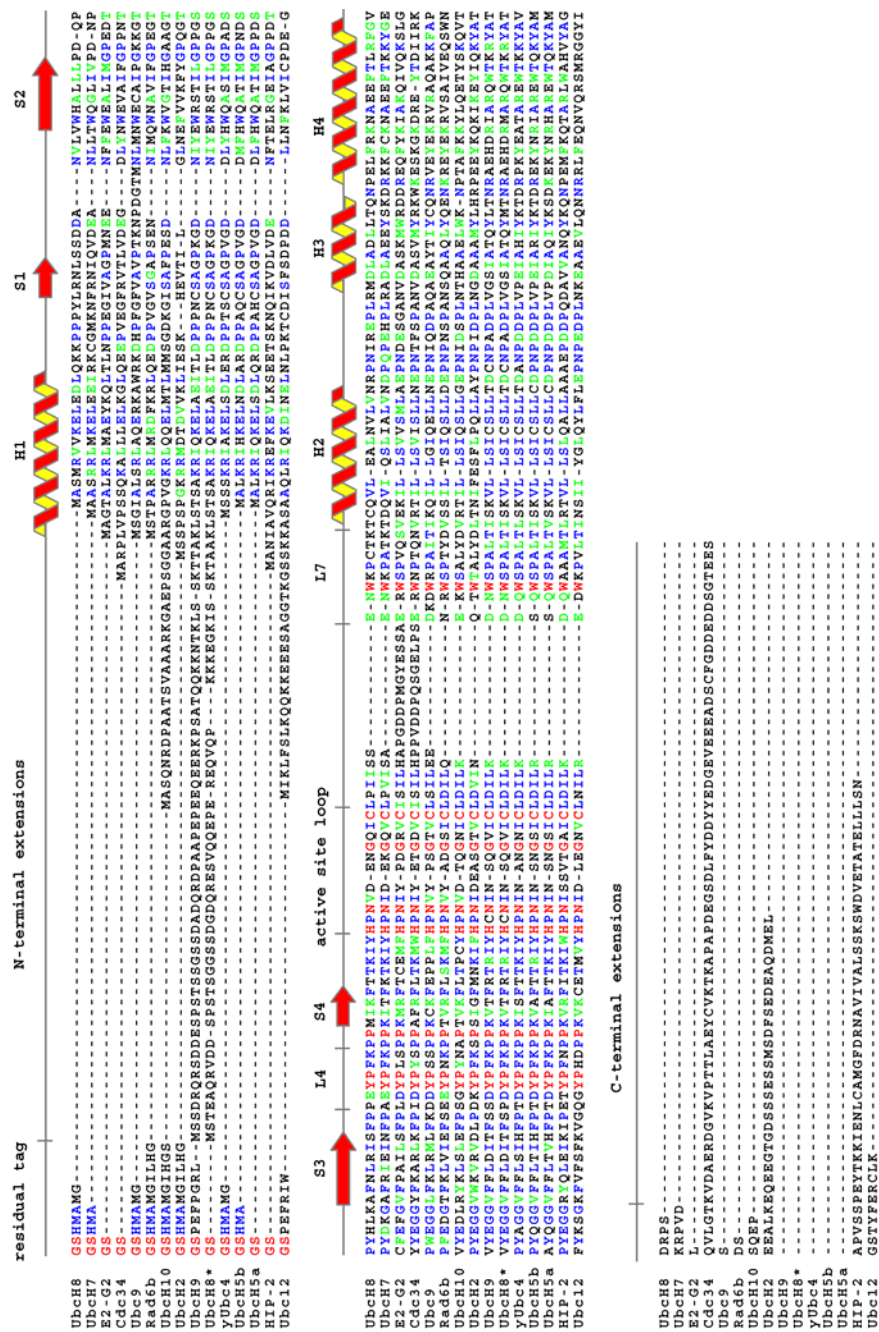


Figure 3.6. Sequence alignment of the 15 E2s used in this study.

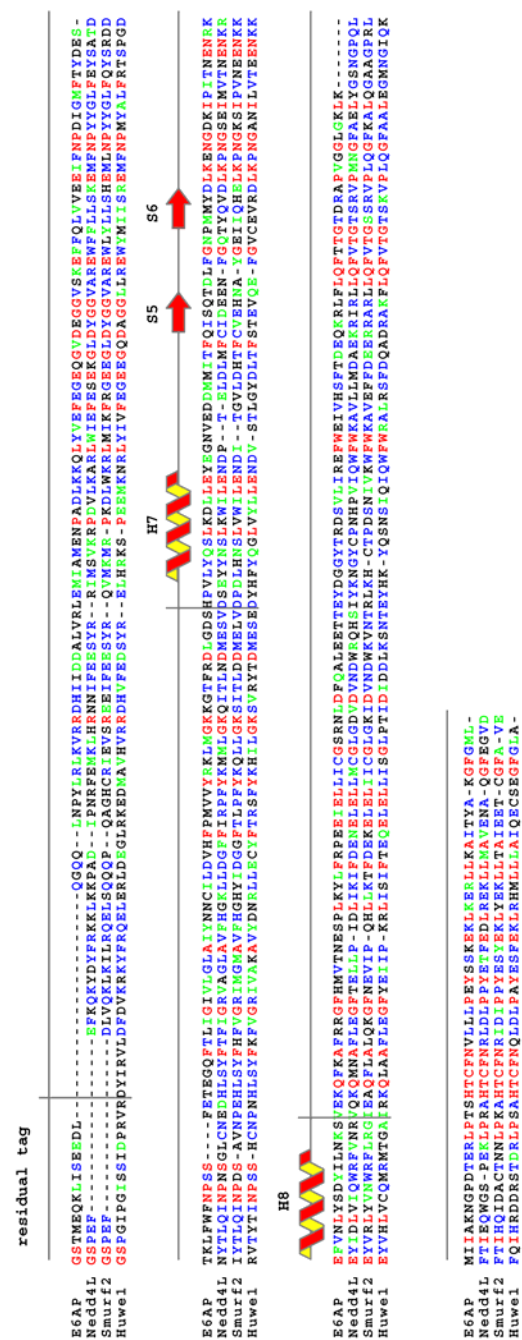


Figure 3.7. Sequence alignment of the four HECT E3s used in this study.

REFERENCES

1. Hatakeyama, S., Yada, M., Matsumoto, M., Ishida, N. & Nakayama, K. I. (2001). U box proteins as a new family of ubiquitin-protein ligases. *J Biol Chem* **276**, 33111-20.
2. Joazeiro, C. A. & Weissman, A. M. (2000). RING finger proteins: mediators of ubiquitin ligase activity. *Cell* **102**, 549-52.
3. Lorick, K. L., Jensen, J. P., Fang, S., Ong, A. M., Hatakeyama, S. & Weissman, A. M. (1999). RING fingers mediate ubiquitin-conjugating enzyme (E2)-dependent ubiquitination. *Proc Natl Acad Sci U S A* **96**, 11364-9.
4. Lu, Z., Xu, S., Joazeiro, C., Cobb, M. H. & Hunter, T. (2002). The PHD domain of MEKK1 acts as an E3 ubiquitin ligase and mediates ubiquitination and degradation of ERK1/2. *Mol Cell* **9**, 945-56.
5. Scheffner, M., Nuber, U. & Huibregtse, J. M. (1995). Protein ubiquitination involving an E1-E2-E3 enzyme ubiquitin thioester cascade. *Nature* **373**, 81-3.
6. Huang, L., Kinnucan, E., Wang, G., Beaudenon, S., Howley, P. M., Huibregtse, J. M. & Pavletich, N. P. (1999). Structure of an E6AP-UbcH7 complex: insights into ubiquitination by the E2-E3 enzyme cascade. *Science* **286**, 1321-6.
7. Zheng, N., Wang, P., Jeffrey, P. D. & Pavletich, N. P. (2000). Structure of a c-Cbl-UbcH7 complex: RING domain function in ubiquitin-protein ligases. *Cell* **102**, 533-9.
8. Anan, T., Nagata, Y., Koga, H., Honda, Y., Yabuki, N., Miyamoto, C., Kuwano, A., Matsuda, I., Endo, F., Saya, H. & Nakao, M. (1998). Human ubiquitin-protein ligase Nedd4: expression, subcellular localization and selective interaction with ubiquitin-conjugating enzymes. *Genes Cells* **3**, 751-63.
9. Nuber, U. & Scheffner, M. (1999). Identification of determinants in E2 ubiquitin-conjugating enzymes required for hec E3 ubiquitin-protein ligase interaction. *J Biol Chem* **274**, 7576-82.
10. Fotia, A. B., Cook, D. I. & Kumar, S. (2006). The ubiquitin-protein ligases Nedd4 and Nedd4-2 show similar ubiquitin-conjugating enzyme specificities. *Int J Biochem Cell Biol* **38**, 472-9.
11. Eletr, Z. M. & Kuhlman, B. (2007). Sequence Determinants of E2-E6AP Binding Affinity and Specificity. *J Mol Biol* **369**, 419-28.
12. Glickman, M. H. & Ciechanover, A. (2002). The ubiquitin-proteasome proteolytic pathway: destruction for the sake of construction. *Physiol Rev* **82**, 373-428.
13. Kumar, S., Kao, W. H. & Howley, P. M. (1997). Physical interaction between specific E2 and Hect E3 enzymes determines functional cooperativity. *J Biol Chem* **272**, 13548-54.
14. Kishino, T., Lalande, M. & Wagstaff, J. (1997). UBE3A/E6-AP mutations cause Angelman syndrome. *Nat Genet* **15**, 70-3.

15. Matsuura, T., Sutcliffe, J. S., Fang, P., Galjaard, R. J., Jiang, Y. H., Benton, C. S., Rommens, J. M. & Beaudet, A. L. (1997). De novo truncating mutations in E6-AP ubiquitin-protein ligase gene (UBE3A) in Angelman syndrome. *Nat Genet* **15**, 74-7.
16. Kitada, T., Asakawa, S., Hattori, N., Matsumine, H., Yamamura, Y., Minoshima, S., Yokochi, M., Mizuno, Y. & Shimizu, N. (1998). Mutations in the parkin gene cause autosomal recessive juvenile parkinsonism. *Nature* **392**, 605-8.
17. Shimura, H., Hattori, N., Kubo, S., Mizuno, Y., Asakawa, S., Minoshima, S., Shimizu, N., Iwai, K., Chiba, T., Tanaka, K. & Suzuki, T. (2000). Familial Parkinson disease gene product, parkin, is a ubiquitin-protein ligase. *Nat Genet* **25**, 302-5.
18. Kahle, P. J. & Haass, C. (2004). How does parkin ligate ubiquitin to Parkinson's disease? *EMBO Rep* **5**, 681-5.
19. Mata, I. F., Lockhart, P. J. & Farrer, M. J. (2004). Parkin genetics: one model for Parkinson's disease. *Hum Mol Genet* **13 Spec No 1**, R127-33.
20. Winkler, G. S., Albert, T. K., Dominguez, C., Legtenberg, Y. I., Boelens, R. & Timmers, H. T. (2004). An altered-specificity ubiquitin-conjugating enzyme/ubiquitin-protein ligase pair. *J Mol Biol* **337**, 157-65.
21. Nuber, U., Schwarz, S., Kaiser, P., Schneider, R. & Scheffner, M. (1996). Cloning of human ubiquitin-conjugating enzymes UbcH6 and UbcH7 (E2-F1) and characterization of their interaction with E6-AP and RSP5. *J Biol Chem* **271**, 2795-800.
22. Schwarz, S. E., Rosa, J. L. & Scheffner, M. (1998). Characterization of human hect domain family members and their interaction with UbcH5 and UbcH7. *J Biol Chem* **273**, 12148-54.
23. Debonneville, C. & Staub, O. (2004). Participation of the ubiquitin-conjugating enzyme UBE2E3 in Nedd4-2-dependent regulation of the epithelial Na⁺ channel. *Mol Cell Biol* **24**, 2397-409.
24. Ogunjimi, A. A., Briant, D. J., Pece-Barbara, N., Le Roy, C., Di Guglielmo, G. M., Kavsak, P., Rasmussen, R. K., Seet, B. T., Sicheri, F. & Wrana, J. L. (2005). Regulation of Smurf2 ubiquitin ligase activity by anchoring the E2 to the HECT domain. *Mol Cell* **19**, 297-308.
25. Adhikary, S., Marinoni, F., Hock, A., Hulleman, E., Popov, N., Beier, R., Bernard, S., Quarto, M., Capra, M., Goettig, S., Kogel, U., Scheffner, M., Helin, K. & Eilers, M. (2005). The ubiquitin ligase HectH9 regulates transcriptional activation by Myc and is essential for tumor cell proliferation. *Cell* **123**, 409-21.
26. Chen, D., Kon, N., Li, M., Zhang, W., Qin, J. & Gu, W. (2005). ARF-BP1/Mule is a critical mediator of the ARF tumor suppressor. *Cell* **121**, 1071-83.
27. Zhong, Q., Gao, W., Du, F. & Wang, X. (2005). Mule/ARF-BP1, a BH3-only E3 ubiquitin ligase, catalyzes the polyubiquitination of Mcl-1 and regulates apoptosis. *Cell* **121**, 1085-95.
28. Walker, J. R., Avvakumov, G.V., Xue, S., Butler-Cole, C., Weigelt, J., Sundstrom, M., Arrowsmith, C.H., Edwards, A.M., Bochkarev, A., Dhe-Paganon, S. Catalytic Domain of the Human NEDD4-like E3 Ligase *To be published*.

29. Eletr, Z. M., Huang, D. T., Duda, D. M., Schulman, B. A. & Kuhlman, B. (2005). E2 conjugating enzymes must disengage from their E1 enzymes before E3-dependent ubiquitin and ubiquitin-like transfer. *Nat Struct Mol Biol* **12**, 933-4.
30. Gill, S. C. & von Hippel, P. H. (1989). Calculation of protein extinction coefficients from amino acid sequence data. *Anal Biochem* **182**, 319-26.

CHAPTER IV

MODULATING E2-HECT BINDING AND SPECIFICITY

ABSTRACT

A variety of human disease and disorders stem from E3 improperly regulating the ubiquitination of substrate proteins. In some cases, like Angelman's syndrome and Liddle's syndrome, E3s or substrates acquire mutations that reduce or abolish ubiquitination resulting in stabilization of the substrate in the cell. In other cases like the human papillomavirus, E3s gain function and ubiquitinate improper substrates resulting in their degradation. Though direct links to E3s have been made, the substrates and pathology of some disease remain unclear. Detecting the substrates of a given E3 has proven to be a challenging task. The hierarchical nature of the ubiquitin pathway presents a formidable obstacle in detecting all E2-E3 and E3-substrate interactions. One approach to dissecting these interactions is to design altered specificity E2-E3 pairs that function with one another, but not other natural partners. In this fashion a particular E2-E3 interaction could be isolated in the cell so that the downstream consequences of this interaction can be studied. The creation of altered specificity E2-E3 pairs can be achieved by designing orthogonal E2-E3 interfaces. A given E2-E3 pair is redesigned so that they function well with each other but not their wild-type (WT) precursors. Orthogonal E2-E3 pairs have potential to be *bona fide* altered specificity pairs because interactions that disrupt binding to the WT precursors will likely disrupt binding to other natural partners. In this study we have used a combination of computational protein design and rational engineering to manipulate E2-E3 interactions. Combining results from both methods we created a UbcH7-E6AP pair that binds ~1000 times stronger than the WT interaction.

INTRODUCTION

It has become evident that ubiquitin-mediated protein degradation influences nearly all cellular processes and pathways¹. It is also well established that various human diseases and disorders are consequences of E3s improperly regulating their substrates^{2; 3}. For example, inherited disorders such as Angelman's syndrome, Liddle's syndrome, and autosomal recessive Parkinson's disease (AR-PD) have been linked to E3s that can no longer fulfill their cellular roles^{4; 5; 6; 7; 8}. In Liddle's syndrome, the HECT E3 Nedd4 no longer binds to or ubiquitinates the epithelial Na⁺ channel (ENaC) ultimately resulting in stabilization of ENaC, increased Na⁺ uptake and hypertension^{9; 10}. In approximately 75% of patients with Angelman's syndrome, the maternal copy of the gene encoding the HECT E3 E6AP has been entirely deleted or has acquired mutations¹¹ that have been shown to reduce ligase activity^{11; 12; 13}. Though a handful of E6AP substrates have been identified^{13; 14; 15; 16; 17; 18}, none have been implicated in the etiology of Angelman's syndrome. Similarly, approximately 50% of patients with AR-PD have acquired mutations to the gene encoding a RING E3 Parkin¹⁹ but the link between Parkin substrates and the etiology of AR-PD remains unclear^{20; 21}. The identification of all the substrates of a given E3 would aid in the study of diseases stemming from the ubiquitin pathway.

The identification of all the substrates of a given E3 is a challenging but very important task. Previous methods have relied on a variety of techniques including two-hybrid screens and coimmunoprecipitations. Though both approaches have led to the identification of numerous E3 substrates, both are inherently limited when applied to detecting interactions within the ubiquitin pathway. The two-hybrid screen is usually performed in a host system so E3 substrates that require phosphorylation or other post-translational modifications prior to recognition by E3 may not bind E3 with sufficient affinity for detection. Coimmunoprecipitations are limited by the stability of the ubiquitinated substrate as deubiquitinating enzymes and the 26S proteasome function to remove ubiquitin and degraded the substrate. Inhibitors of the proteasome and deubiquitinating enzymes can be useful but again the context of the interaction has been altered. The hierarchy of the ubiquitin pathway complicates matters because each E2 functions with many E3s³. While E3s can interact with

multiple E2s, these E2s are usually highly homologous and stem from similar E2 subfamilies.

Clearly a better approach to identifying E3 substrates is needed. An ideal method would allow for the detection of low-affinity E3–substrate interactions without significantly perturbing the cellular environment. One way to create such a tool is by creating altered specificity E2–E3 pairs.

The manipulation of an E2–E3 pair has been demonstrated previously²². A charge swap interaction was generated across the UbcH5b-CNOT4 interface to create a mutant pair that no longer interacted with the WT precursors²². In this study the authors claim to have generated an altered specificity pair but the mutant proteins were not tested against other natural partners. A *bona fide* altered specificity E2–E3 pair must display two characteristics. First, the redesigned E2 and E3 proteins must interact favorably with one another but not with their wild-type precursors. Redesigned E2–E3 pairs displaying this property will be referred to as orthogonal E2–E3 pairs. Second, the redesigned E2–E3 pair should no longer interact favorably with other naturally occurring partners. This property is most important for E2s because each E2 usually interacts with multiple E3s³. Orthogonal E2–E3 pairs have potential to be *bona fide* altered specificity pairs because interactions that disrupt binding to the WT precursors will likely disrupt binding to other natural partners. In this study we have used a computational protein design and rational engineering to generate orthogonal E2–E3 interfaces and to enhance E2–E3 affinity. We have used the UbcH7–E6AP interaction as a model system for these studies.

RESULTS

Manipulation of K96–D641 interaction

We previously found that the K96 residue of UbcH7 is important for E6AP binding and specificity²³. In the WT UbcH7–E6AP interaction this lysine, situated on loop 7, forms a salt-bridge interaction with D641 of E6AP. We previously used the interface design algorithm of RosettaDesign to create an enhanced affinity K96S-UbcH7–D641K-E6AP (K96S–D641K) pair²⁴. The K96S–D641K pair bound with a K_D of 100 nM, a significant enhancement relative to the WT interaction ($\Delta\Delta G^\circ_{\text{bind}}$ of -2.3 kcal/mol). We also tested the K96E–D641K pair for a charge swap interaction and again observed an improvement to binding ($\Delta\Delta G^\circ_{\text{bind}}$ of -0.8 kcal/mol)²³. The mutant proteins were also tested with their WT partners to test for orthogonal interfaces. The D641K and K96S proteins bind their WT partners with roughly the same affinity as the WT interaction whereas the K96E mutant was destabilizing ($\Delta\Delta G^\circ_{\text{bind}}$ of $+1.2$ kcal/mol)²³. The interface design protocol was again applied to the K96–D641 interaction to test for other mutations that may yield an orthogonal interface. RosettaDesign predicted that mutations to Trp or Tyr at both positions would generate an enhanced affinity interaction. An orthogonal interface was not predicted because the D641Y/W mutants were predicted to enhance affinity WT-UbcH7. We made the K96Y, K96W, D641Y, and D641W mutant proteins and tested them in our binding assay. Indeed all four mutant interactions were capable of enhancing affinity with similar gains in binding affinity ($K_D = 470\text{--}610$ nM) (**Figure 4.1**). We next tested the effects of the D641Y/W mutations on binding to WT-UbcH7 and found that these mutations indeed enhanced affinity ($K_D = 0.8\text{--}1.2$ μM)²⁵. The K96Y/W mutants bound WT-E6AP slightly weaker than WT-UbcH7 ($K_D = 7.2\text{--}8.7$ μM). The results from manipulating the K96–D641K interaction suggest that these positions may be amenable to manipulation in other E2–HECT pairs.

Redesigning other loop 7-UbcH7–E6AP interactions

Other loop 7-UbcH7 side-chains that interact with E6AP include E93, W95, P97, A98, and K100. The W95 residue is completely conserved in all E2s and P97 is highly conserved suggesting these residues are important for structural orientation of loop 7. We avoided redesigning the residues, but mutations at E93, A98, and K100 were tested. The K100E–D652R mutants were previously tested for a charge swap interaction and the mutant complex was slightly more destabilizing than either single mutation²³. RosettaDesign predicted a cluster of mutations around A98 would form an orthogonal interface. The three mutations (A98W–Y645W–D652W) were all to Trp and an increase in buried hydrophobic surface area upon binding was the physical basis for the predicted gain in binding energy. We first tested the A98W–Y645W pair for an orthogonal interface and found that the mutant interaction indeed bound tighter than the WT interaction ($K_D = 480$ nM) (**Figure 4.1**). This gain in binding energy was entirely attributed to A98W as this mutant bound WT-E6AP with a K_D of 190 nM²⁵ while the Y645W-E6AP protein bound WT-UbcH7 with WT affinity. The D652W mutation was tested in combination with Y645W and it proved to provide a more orthogonal interface as it destabilized binding to both WT and A98W-UbcH7 by ~ 1.5 kcal/mol.

In the UbcH7–E6AP crystal structure, coordinates for the E93 side-chain are absent. This is likely the result of a high temperature factor and inconclusive electron density. We used RosettaDesign to model this side-chain and found no contacts to E6AP. This was a surprising result given the E93A and E93R mutations were both found to stabilize binding to E6AP ($K_D = 2.4$ and 0.92 μ M respectively)²³. To test whether E93 may be engaged in an interaction with Q637 of E6AP, the Q637A and Q637R mutant proteins were tested with WT-UbcH7. We found these mutations displayed similar affinities as E93A and E93R (**Figure 4.1**). This finding suggested that the E93A and Q637A mutations were either relieving an unfavorable interaction (steric or electrostatic clashes) or that they were allowing alternate structural arrangements. The E93R and Q637R mutations may allow for a new salt-bridge/hydrogen bond interaction across the interface. We tested this interpretation by measuring the affinity of the E93A–Q637R and E93R–Q637A interactions. In both

cases, the measured change in binding energy was roughly the sum of the change of the individual mutations (**Figure 4.1**). The additive effects argues against these side-chains forming interactions when either is mutated to an arginine. The changes in interface interactions imposed by the E93A/R and Q637A/R mutations remain unknown. The Q637W mutation was identified in search of mutations that enhance affinity by increasing buried hydrophobic surface area. This mutant was found to bind WT-UbcH7 with a slightly improved affinity ($K_D = 1.7 \mu\text{M}$)²⁵.

Manipulating loop 4 of UbcH7

The most important contact at the UbcH7–E6AP interface arises from a F63 which is situated at the tip of loop 4. All E2s that interact with HECT E3s contain a phenylalanine at this position^{23; 26; 27}. Roughly half of the human E2s have a phenylalanine at this position whereas the rest possess a mixture of polar, charged, aromatic, and hydrophobic amino acids. We tested the effects of mutating F63-UbcH7 on binding E6AP. The F63A and F63D mutations were previously shown to abolish binding to E6AP^{23; 24}. More conservative substitutions at this position (F63Y, F63H, and F63W) led to less pronounced destabilizations (**Table 4.1**). The F63W mutant, which was predicted by RosettaDesign to slightly improve E6AP binding has the least effect ($\Delta\Delta G^\circ_{\text{bind}}$ of +0.7 kcal/mol)²⁵. The F63H and F63Y mutants bound much weaker with destabilizations of 2.0 and 1.3 kcal/mol respectively. The F63H–F690Y design was predicted as orthogonal by RosettaDesign, but these mutants failed to form a favorable interaction. These results, along with others, emphasize the importance of the tightly packed hydrophobic interface core.

Flanking the F63 residue are the E60 and K64 side-chains. These residues form a salt-bridge interaction with each other and E60 also forms a hydrogen bond with T662-E6AP. The E60A and E60R mutations have been shown to have a small effect on E6AP affinity, while K64A and K64R displayed more pronounced destabilizations²³. We used RosettaDesign to redesign interactions at these two positions. For the E60 position, RosettaDesign predicted a cluster of mutations to

hydrophobic residues in place of the E60–T662 hydrogen bond (E60L–T662F–Q661F). We tested for orthogonal interactions and found that the E60L–T662F and E60L–T662F–Q661F proteins bound slightly weaker than the WT interaction (**Figure 4.1**). Furthermore, the T662F and T662F–Q661F proteins bound WT-UbcH7 with WT affinity while the E60L effect was more destabilizing ($\Delta\Delta G^{\circ}_{\text{bind}}$ of +0.6 kcal/mol). The K64L mutation was successfully predicted by RosettaDesign to enhance affinity for E6AP²⁵. The aliphatic portion of the K64 side-chain is in the vicinity of V634 and RosettaDesign predicted an orthogonal K64E–V634R interaction. When tested the V634R–E6AP mutant with WT-UbcH7 and found a loss in binding energy of 0.5 kcal/mol (**Figure 4.1**). Unfortunately the K64E–V634R interaction was more unfavorable than either single mutation ($\Delta\Delta G^{\circ}_{\text{bind}}$ of +1.0 kcal/mol). A similarity in these findings is that RosettaDesign is capable of destabilizing interactions but has difficulty in recovering the lost binding energy.

Combining mutations to generate orthogonal UbcH7–E6AP pairs

Using the results from these redesign efforts we sought to combine mutations to generate high affinity and orthogonal UbcH7–E6AP pairs. We first tested whether affinity enhancements observed with loop 7 mutations could be combined for additive stabilizations. The K96S–D641K pair was tested with additional E93R and A98W mutations. We found that indeed both mutations were able to significantly enhance binding affinity. The E93R–K96S–D641K pair interacted so strongly that it was difficult to measure the affinity with precision in our FP assay. A good estimate of this affinity (K_D of ~2 nM) indicates greater than additive effects to the binding affinity (**Figure 4.1**). The K96S–A98W–D641K pair bound with a K_D of 12 nM and slightly less than additive effects. We next tested the E93R–K96S–A98W–UbcH7 protein with D641K and found that the additional mutation slightly weakened binding displaying a K_D of 27 nM. Interestingly the K96S–A98W–UbcH7 protein bound WT-E6AP with a K_D of 4.2 μM , an affinity much weaker than expected based on the results from each single mutation.

Given the significant gains in binding affinity observed with E93R-K96S-D641K and K96S-A98W-D641K pairs, we next tested whether adding F63A/H/Y would help in achieving an orthogonal interaction. Our findings (**Table 4.1**) show that the loop 7 mutations indeed can compensate for lost binding energy from the F63A/H/Y mutations. The F63Y mutation which was the least destabilizing of the three bound with K_D of 600–850 nM when combined with loop 7 mutations. The F63H mutation with loop 7 mutations bound with WT affinity (K_D of 2.5–4.3 μ M) while F63A binding was much weaker (92–120 μ M). These Ubch7 mutants were tested with WT-E6AP and found to bind much weaker relative to D641K-E6AP ($\Delta\Delta G^\circ_{\text{bind}}$ of 1–2.5 kcal/mol). Because the D641K mutation is not destabilizing relative to WT binding²³, these mutant pairs should not be considered orthogonal. Given E6AP only binds tightly to Ubch7 and Ubch8 while Ubch7 functions with many E3s, we are more concerned with disrupting natural Ubch7–E3 interactions. Specificity in this direction is also more important in our system because we are more concerned with our redesigned E2s not being able to pass Nedd8 onto naturally occurring E3s. Redesigned E3s interacting with natural E2s is tolerable because the outcome is that these E3s will ubiquitinate their natural substrates.

DISCUSSION

In this study we have used a combination of computational interface design and rational engineering to modulate the binding affinity of the UbcH7–E6AP interaction. Our findings suggest that UbcH7 loop 7 is most amenable to reengineering because it lies on the periphery of the interface and forms many contacts to E6AP. Using RosettaDesign to engineer orthogonal and enhanced affinity interactions we were able to find several mutations that stabilized binding. Though not completely successful at generating orthogonal interfaces, RosettaDesign in most cases showed success in either stabilizing or destabilizing interactions. By combining results from both computational and rational engineering we were able to create a UbcH7–E6AP pair that bound roughly 1000 times stronger than the WT interaction (5.0 μ M versus \sim 2 nM). Using this approach we were also able to generate a pseudo-orthogonal interaction around F63Y and F63H of UbcH7. Because few E2s possess Tyr and His at this position, this mutant UbcH7 may prove quite effective at disfavoring interactions with other natural E2s. An interesting question that remains is whether the effects seen for A98W, E93R, and K96S–D641K will translate to other E2–HECT interactions.

FIGURES

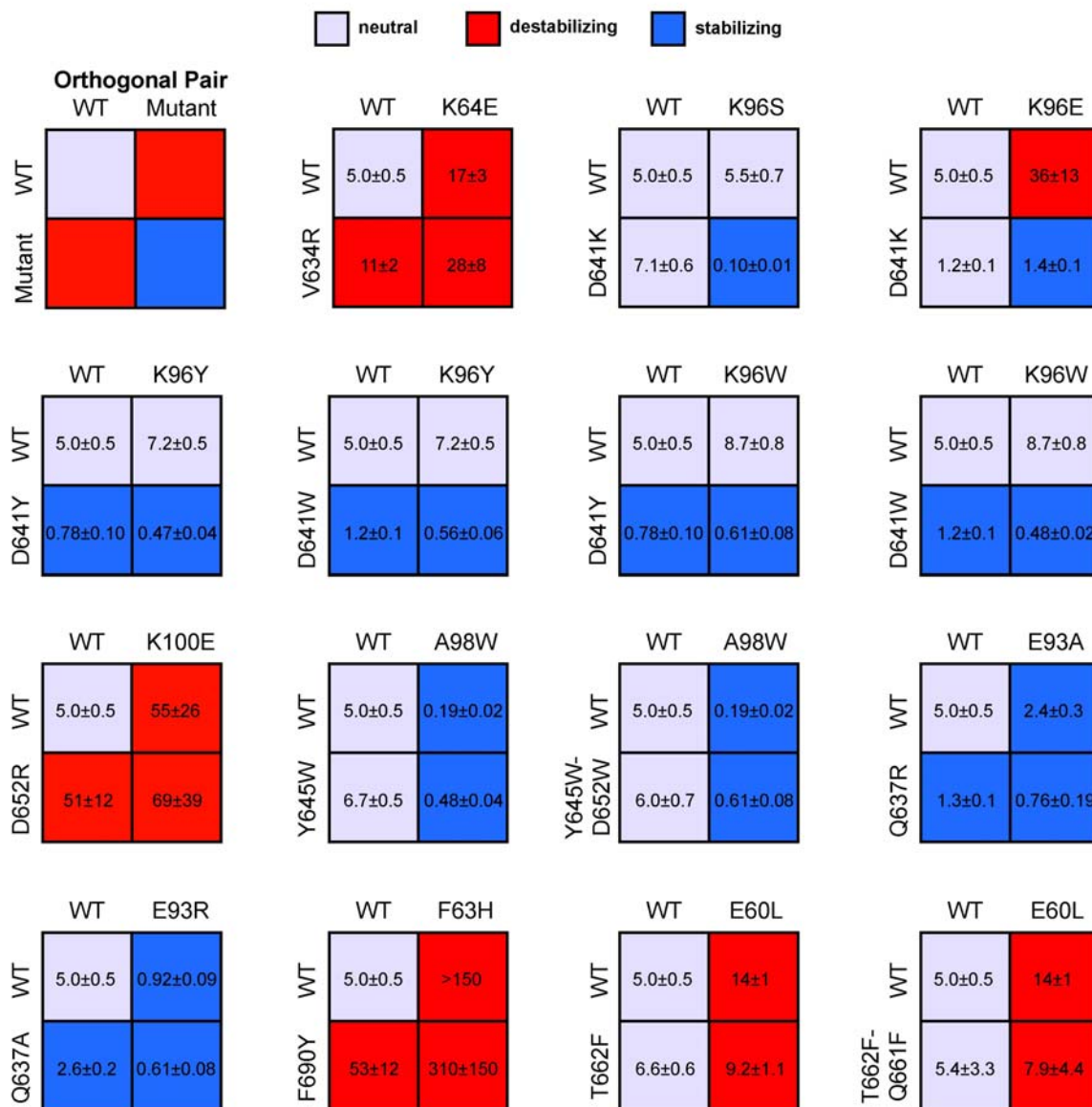


Figure 4.1. Binding results from orthogonal and rational designs of the Ubch7–E6AP complex. Values are measured dissociations (μM) and the associated standard error.

TABLES

Table 4.1. Measured dissociation for mutant UbcH7–E6AP interactions.

UbcH7	WT-E6AP		D641K-E6AP	
	K_D (μM)	$\Delta\Delta G^\circ_{\text{bind}}$	K_D (μM)	$\Delta\Delta G^\circ_{\text{bind}}$
WT	$5.0 \pm 0.5^\dagger$		ND	ND
F63A	$810 \pm 550^\ddagger$	3.0	ND	ND
F63H	>150	>2	ND	ND
F63Y	47 ± 11	-1.3	ND	ND
E93R	$0.92 \pm 0.09^\ddagger$	-1.0	ND	ND
K96S	$5.5 \pm 0.7^\dagger$	0.05	$0.10 \pm 0.01^\dagger$	-2.3
A98W	$0.19 \pm 0.02^\S$	-1.9	ND	ND
E93R-K96S	ND	ND	~ 0.002	-4.7
K96S-A98W	4.2 ± 0.6	-0.10	0.012 ± 0.004	-3.6
E93R-K96S-A98W	ND	ND	0.027 ± 0.003	-3.1
E93R-K96S-F63A	550 ± 190	2.8	120 ± 10	1.9
E93R-K96S-F63H	97 ± 12	1.8	4.3 ± 0.3	-0.09
E93R-K96S-F63Y	25 ± 3	1.0	0.60 ± 0.05	-1.3
K96S-A98W-F63A	450 ± 120	2.7	92 ± 15	1.7
K96S-A98W-F63H	100 ± 34	1.8	2.5 ± 0.2	-0.41
K96S-A98W-F63Y	75 ± 8	1.6	0.85 ± 0.09	-1.1

† Reproduced from (24), ‡ reproduced from (23), and § reproduced from (25).

MATERIALS AND METHODS

Protein purification and FP binding assays

The protocol for expression and purification of UbcH7 and E6AP has been described²⁴. UbcH7 and E6AP mutations were generated using the QuickChange® site-directed mutagenesis protocol (Stratagene). A detailed method describing the labeling of E2s with bodipy (507/545)-iodoacetamide (Molecular Probes) has been described^{23; 24}. The FP binding assay has also been described in detail in previous reports^{23; 24}.

RosettaDesign

Predictions for the K64L, F63W, and Q637W affinity enhancing mutations were carried out by Deanne Sammond and has been previously described²⁵. The interface mode of RosettaDesign was used to predict orthogonal interactions. The protocol is based on a ‘computational second-site suppressor’ method developed by Kortemme *et al.*²⁸. Briefly, the atomic coordinates of the UbcH7–E6AP crystal structure²⁶ were read by RosettaDesign. All interface positions are identified by the algorithm.. Negative design ensues as the algorithm tests all amino acids at each interface position to find destabilizing mutations. Positive design follows for each destabilizing point mutation in attempt to restore or increasing binding affinity. The final step is the calculation of energies for the free proteins (WT and mutants) as well as the complexes (WT–WT, WT–MUT, MUT–WT, and MUT–MUT). From these energies the changes to the free energy of binding are calculated then ranked.

REFERENCES

1. Hershko, A. & Ciechanover, A. (1998). The ubiquitin system. *Annu Rev Biochem* **67**, 425-79.
2. Schwartz, A. L. & Ciechanover, A. (1999). The ubiquitin-proteasome pathway and pathogenesis of human diseases. *Annu Rev Med* **50**, 57-74.
3. Glickman, M. H. & Ciechanover, A. (2002). The ubiquitin-proteasome proteolytic pathway: destruction for the sake of construction. *Physiol Rev* **82**, 373-428.
4. Kishino, T., Lalonde, M. & Wagstaff, J. (1997). UBE3A/E6-AP mutations cause Angelman syndrome. *Nat Genet* **15**, 70-3.
5. Matsuura, T., Sutcliffe, J. S., Fang, P., Galjaard, R. J., Jiang, Y. H., Benton, C. S., Rommens, J. M. & Beaudet, A. L. (1997). De novo truncating mutations in E6-AP ubiquitin-protein ligase gene (UBE3A) in Angelman syndrome. *Nat Genet* **15**, 74-7.
6. Shimkets, R. A., Warnock, D. G., Bositis, C. M., Nelson-Williams, C., Hansson, J. H., Schambelan, M., Gill, J. R., Jr., Ulick, S., Milora, R. V., Findling, J. W. & et al. (1994). Liddle's syndrome: heritable human hypertension caused by mutations in the beta subunit of the epithelial sodium channel. *Cell* **79**, 407-14.
7. Kitada, T., Asakawa, S., Hattori, N., Matsumine, H., Yamamura, Y., Minoshima, S., Yokochi, M., Mizuno, Y. & Shimizu, N. (1998). Mutations in the parkin gene cause autosomal recessive juvenile parkinsonism. *Nature* **392**, 605-8.
8. Shimura, H., Hattori, N., Kubo, S., Mizuno, Y., Asakawa, S., Minoshima, S., Shimizu, N., Iwai, K., Chiba, T., Tanaka, K. & Suzuki, T. (2000). Familial Parkinson disease gene product, parkin, is a ubiquitin-protein ligase. *Nat Genet* **25**, 302-5.
9. Staub, O., Dho, S., Henry, P., Correa, J., Ishikawa, T., McGlade, J. & Rotin, D. (1996). WW domains of Nedd4 bind to the proline-rich PY motifs in the epithelial Na⁺ channel deleted in Liddle's syndrome. *Embo J* **15**, 2371-80.
10. Staub, O., Gautschi, I., Ishikawa, T., Breitschopf, K., Ciechanover, A., Schild, L. & Rotin, D. (1997). Regulation of stability and function of the epithelial Na⁺ channel (ENaC) by ubiquitination. *Embo J* **16**, 6325-36.
11. Laan, L. A., v Haeringen, A. & Brouwer, O. F. (1999). Angelman syndrome: a review of clinical and genetic aspects. *Clin Neurol Neurosurg* **101**, 161-70.
12. Cooper, E. M., Hudson, A. W., Amos, J., Wagstaff, J. & Howley, P. M. (2004). Biochemical analysis of Angelman syndrome-associated mutations in the E3 ubiquitin ligase E6-associated protein. *J Biol Chem* **279**, 41208-17.
13. Nawaz, Z., Lonard, D. M., Smith, C. L., Lev-Lehman, E., Tsai, S. Y., Tsai, M. J. & O'Malley, B. W. (1999). The Angelman syndrome-associated protein, E6-AP, is a coactivator for the nuclear hormone receptor superfamily. *Mol Cell Biol* **19**, 1182-9.

14. Scheffner, M., Huibregtse, J. M., Vierstra, R. D. & Howley, P. M. (1993). The HPV-16 E6 and E6-AP complex functions as a ubiquitin-protein ligase in the ubiquitination of p53. *Cell* **75**, 495-505.
15. Kuhne, C. & Banks, L. (1998). E3-ubiquitin ligase/E6-AP links multicopy maintenance protein 7 to the ubiquitination pathway by a novel motif, the L2G box. *J Biol Chem* **273**, 34302-9.
16. Kumar, S., Talis, A. L. & Howley, P. M. (1999). Identification of HHR23A as a substrate for E6-associated protein-mediated ubiquitination. *J Biol Chem* **274**, 18785-92.
17. Oda, H., Kumar, S. & Howley, P. M. (1999). Regulation of the Src family tyrosine kinase Blk through E6AP-mediated ubiquitination. *Proc Natl Acad Sci U S A* **96**, 9557-62.
18. Li, L., Li, Z., Howley, P. M. & Sacks, D. B. (2006). E6AP and calmodulin reciprocally regulate estrogen receptor stability. *J Biol Chem* **281**, 1978-85.
19. Lucking, C. B., Durr, A., Bonifati, V., Vaughan, J., De Michele, G., Gasser, T., Harhangi, B. S., Meo, G., Deneffe, P., Wood, N. W., Agid, Y. & Brice, A. (2000). Association between early-onset Parkinson's disease and mutations in the parkin gene. *N Engl J Med* **342**, 1560-7.
20. Kahle, P. J. & Haass, C. (2004). How does parkin ligate ubiquitin to Parkinson's disease? *EMBO Rep* **5**, 681-5.
21. Mata, I. F., Lockhart, P. J. & Farrer, M. J. (2004). Parkin genetics: one model for Parkinson's disease. *Hum Mol Genet* **13 Spec No 1**, R127-33.
22. Winkler, G. S., Albert, T. K., Dominguez, C., Legtenberg, Y. I., Boelens, R. & Timmers, H. T. (2004). An altered-specificity ubiquitin-conjugating enzyme/ubiquitin-protein ligase pair. *J Mol Biol* **337**, 157-65.
23. Eletr, Z. M. & Kuhlman, B. (2007). Sequence Determinants of E2-E6AP Binding Affinity and Specificity. *J Mol Biol* **369**, 419-28.
24. Eletr, Z. M., Huang, D. T., Duda, D. M., Schulman, B. A. & Kuhlman, B. (2005). E2 conjugating enzymes must disengage from their E1 enzymes before E3-dependent ubiquitin and ubiquitin-like transfer. *Nat Struct Mol Biol* **12**, 933-4.
25. Sammond, D. W., Eletr, Z. M., Purbeck, C., Kimple, R. J., Siderovski, D. P. & Kuhlman, B. (2007). Structure-based Protocol for Identifying Mutations that Enhance Protein-Protein Binding Affinities. *Journal of Molecular Biology* **Article in Press**.
26. Huang, L., Kinnucan, E., Wang, G., Beaudenon, S., Howley, P. M., Huibregtse, J. M. & Pavletich, N. P. (1999). Structure of an E6AP-UbcH7 complex: insights into ubiquitination by the E2-E3 enzyme cascade. *Science* **286**, 1321-6.
27. Nuber, U. & Scheffner, M. (1999). Identification of determinants in E2 ubiquitin-conjugating enzymes required for E3 ubiquitin-protein ligase interaction. *J Biol Chem* **274**, 7576-82.

28. Kortemme, T., Joachimiak, L. A., Bullock, A. N., Schuler, A. D., Stoddard, B. L. & Baker, D. (2004). Computational redesign of protein-protein interaction specificity. *Nat Struct Mol Biol* **11**, 371-9.

CHAPTER V

E2 CONJUGATING ENZYMES MUST DISENGAGE FROM THEIR E1 ENZYME BEFORE E3-DEPENDENT UBIQUITIN AND UBIQUITIN-LIKE TRANSFER

Ziad M Eletr^{1,3}, Danny T Huang^{2,3}, David M Duda², Brenda A Schulman² & Brian Kuhlman¹

¹ Department of Biochemistry and Biophysics, University of North Carolina, Chapel Hill, North Carolina 27599-7260, USA.

² Department of Structural Biology and Department of Genetics and Tumor Cell Biology, St. Jude Children's Research Hospital, Memphis, Tennessee 38105, USA.

³ These authors contributed equally to the work.

Correspondence should be addressed to Brian Kuhlman bkuhlman@email.unc.edu

This work was published in Nature Structural and Molecular Biology (2005) 12, 933–934.

Reproduced with permission from the Nature Publishing Group.

ABSTRACT

During ubiquitin ligation, an E2 conjugating enzyme receives ubiquitin from an E1 enzyme and then interacts with an E3 ligase to modify substrates. Competitive binding experiments with three human E2-E3 protein pairs show that the binding of E1s and of E3s to E2s are mutually exclusive. These results imply that polyubiquitination requires recycling of E2 for addition of successive ubiquitins to substrate.

MAIN TEXT

Post-translational modification by ubiquitin and ubiquitin-like proteins (ubls) regulates almost all aspects of cellular function. Although it is known that E1, E2 and E3 enzymes work together in a cascade to transfer ubiquitin and ubls, the mechanism and assembly of the cascade are incompletely understood. It is not known whether the process involves sequential E1-E2 and E2-E3 interactions, with E2 disengaging from E1 before it can interact with an E3, or whether the E1, E2 and E3 enzymes function as a single complex. The answer to this question has important implications for the nature and processivity of ubiquitin and ubl transfer.

Indirect evidence from structural studies indicates that the E3-binding site on ubiquitin E2s may partially overlap with the E1-binding site. Residues on the N-terminal helix of the E2 UbcH7 interact with the HECT domain E3 E6AP¹ and the RING domain E3 c-Cbl² and correspond with residues on Ubc12, the conjugating enzyme for the ubl NEDD8, that interact with its E1, APPBP1-UBA3 (ref. 3).

To determine whether a HECT E3 is capable of inhibiting the E1-E2 interaction, we examined the effects of increasing concentrations of the E6AP-HECT domain on the initial rate of E1-UbcH7 transthioylation. To simplify the reaction, we used a catalytically inactive variant of E6AP (C820A) that cannot receive ubiquitin from E2, but binds to E2 with wild-type affinity (**Fig. 5.1** and **Supplementary Data, Table 5.1**). Kinetic ubiquitination assays *in vitro* revealed that the initial rate of formation of the UbcH7-³²P]ubiquitin thioester depends on the concentration of C820A-HECT. A modified Michaelis-Menten scheme was derived and used to fit the kinetic data to determine an inhibition constant (K_i) of 3.1 μ M for the UbcH7-C820A-E6AP interaction (**Fig. 5.1b**, **Supplementary Data, Methods** and **Fig. 5.3**). To verify that the K_i corresponds to binding between E3 and E2, we monitored binding directly by fluorescence polarization of BODIPY-labeled UbcH7 as a function of E6AP concentration. The measured K_d , 6.0 μ M, is very similar to the K_i . In a second set of experiments, we assessed the changes in the kinetic parameters k_{cat} and K_m for E1-E2 transthioylation in the presence of high concentrations of C820A-HECT and found that inhibition is

due to competitive binding, as the K_m for the E1-E2 interaction was compromised (1.7 μM versus 18 μM), whereas k_{cat} was largely unchanged (0.4 s^{-1} versus 0.5 s^{-1} ; **Supplementary Data, Fig. 5.4**).

To further confirm that the HECT domain is capable of inhibiting UbcH7 transthiolation, we used RosettaDesign⁴ to engineer an enhanced affinity UbcH7-E6AP pair (K96S-UbcH7 and D641K-E6AP, $K_d = 0.10 \mu\text{M}$; **Supplementary Data, Methods**). With the designed E2-E3 pair, the E3 inhibits UbcH7 transthiolation at lower concentrations of E3 ($K_i = 0.33 \mu\text{M}$). Additionally, a UbcH7 variant (F63D) that binds very weakly to E6AP ($K_d > 100 \mu\text{M}$) did not inhibit the conjugation of ubiquitin to UbcH7. Because E2s do not change conformations substantially upon binding E3s or E1s (refs. 1–3,5,6), our results suggest that UbcH7 contains overlapping binding sites for E1 and E3 that prevent the formation of a ternary E1–UbcH7–HECT complex.

To determine whether E1-binding sites on E2s are also involved in downstream interactions in RING E3-dependent ubiquitin and ubl transfer, we studied the effects of adding E2-binding domains from E1s to chase assays examining ubiquitin and NEDD8 transfer from their respective E2s to targets. For a RING E3 in the ubiquitin pathway, we examined SCF ^{β -TRCP}-mediated transfer of ubiquitin from the ubiquitin E2, UbcH5b, to a target peptide from β -catenin. For the NEDD8 pathway, we looked at Rbx1- or Roc1- mediated transfer of NEDD8 from the NEDD8 E2, Ubc12, to Cull1. Because the isolated fragments corresponding to the E2-binding domains from ubiquitin's and NEDD8's E1s bind UbcH5b and Ubc12, respectively (ref. 3 and D.M.D., unpublished results), these domains from E1s inhibit transfer of ubiquitin or NEDD8 from their E1s to their specific E2s (ref. 3; **Fig. 5.2**). Therefore, chase assays, which are not sensitive to inhibition of E1-mediated transfer of ubiquitin or NEDD8 to E2, must be used to monitor transfer of ubiquitin or NEDD8 to their targets. These assays require two steps. First, the UbcH5b- ^{32}P ubiquitin or Ubc12- ^{32}P NEDD8 thioester intermediate is generated by mixing the appropriate E1 and E2, MgATP, and ^{32}P ubiquitin or ^{32}P NEDD8, respectively. This first reaction is quenched, so that the chase reaction is not sensitive to any effects on E1-E2 interactions. In the second step, after formation of the UbcH5b- ^{32}P ubiquitin or

Ubc12- ^{32}P NEDD8 thioester complex is quenched, we add the E3 and target and monitor the transfer of ^{32}P ubiquitin or ^{32}P NEDD8 from E2 to the target. Addition of the ubiquitin E1's E2-binding domain inhibited SCF $^{\beta\text{-TRCP}}$ -mediated transfer of ubiquitin from UbcH5b to the β -catenin peptide target (**Fig. 5.2b**). The control containing the Ubc12-binding domain from NEDD8's E1 indicated that this inhibition is specific for ubiquitin E1-E2 interactions (**Fig. 5.2b**). Parallel results were obtained with the NEDD8 pathway. Addition of the NEDD8 E1's E2-binding domain inhibited Rbx1- or Roc1-mediated transfer of NEDD8 from Ubc12 to Cul1 (**Fig. 5.2d**), with the control containing the ubiquitin E2-binding domain from ubiquitin's E1 indicating that this inhibition is specific for NEDD8 E1-E2 interaction (**Fig. 5.2d**).

In these studies we probed the two most common types of E3 ubiquitin ligases, HECT and RING, and three different E2 conjugating enzymes. In each case we found that the binding of E1 or E3 to an E2 is mutually exclusive. This result has important implications for the nature and processivity of ubiquitin and ubl modification. One prediction is that an efficient conjugation pathway requires an E3 to have higher affinity for E2-ubiquitin or E2-ubl thioester, and indeed this has been observed for interactions between HsUbc2b and E3 α (ref. 7), as well as Ubc4 with SCF $^{\beta\text{-TRCP}}$ (ref. 8).

Because an E2 cannot be reactivated by an E1 while it is bound to E3, polyubiquitination probably requires multiple E2-E3 binding events. Indeed, a study of the anaphase-promoting complex (APC), a multisubunit E3, indicated that multiple E2 molecules are needed to label substrate with multiple ubiquitins⁹. These previous results could reflect multiple E2 molecules binding the APC complex simultaneously, or they could indicate that E2s must be released from the APC before they can be reactivated with ubiquitin by an E1, consistent with our findings here. A recent study reports that multiple E2-E3 binding events are needed for Cdc34p-mediated polyubiquitination; however, they also propose a model that involves ubiquitin-conjugated E2 dissociating from its RING E3 before modifying the substrate with ubiquitin¹⁰. Our studies do not address this aspect of their model. Our studies do suggest a possible mechanism for the difference between mono- and polyubiquitinating

enzymes: a difference in turnover rates for substrate binding and E2 binding. E3s that release product quickly and turn over E2 slowly may catalyze monoubiquitination, whereas E3s that release product slowly and turn over E2 quickly may catalyze polyubiquitination.

FIGURES

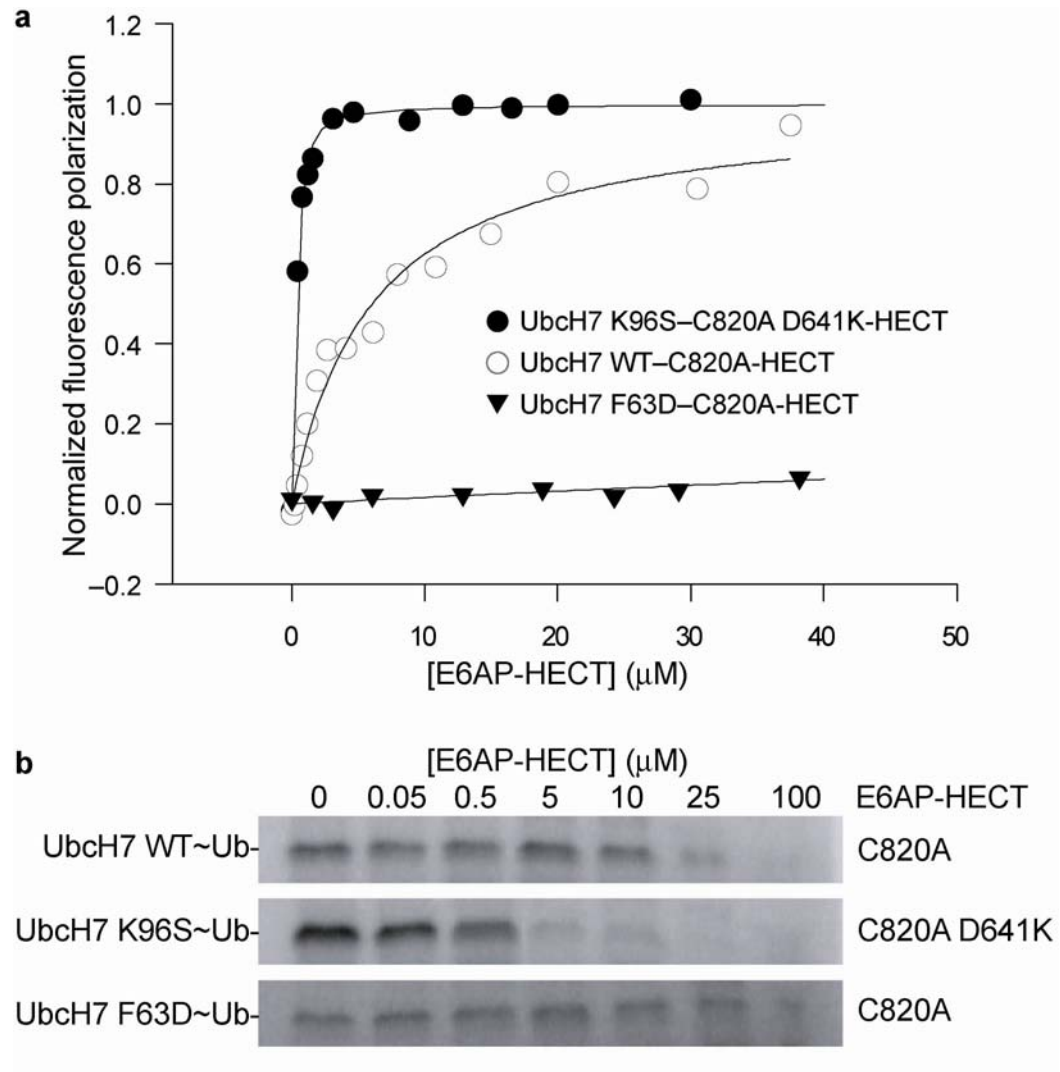


Figure 5.1. An E2 binding to E1 and to a HECT E3 are mutually exclusive. (a) The change in fluorescence polarization of BODIPY-Ubch7 was measured upon titration of E6AP-HECT into Ubch7. (b) The initial rate of formation of Ubch7- ^{32}P -ubiquitin was measured at increasing concentrations of E6AP-HECT for the Ubch7-HECT interactions described.

SUPPLEMENTARY METHODS

Proteins for Biophysical and Biochemical Assays of E6AP(HECT)

E6AP-HECT domain and UbcH7 single amino acid substitutions were generated using QuikChange site-directed mutagenesis kit (Stratagene). All proteins were overexpressed in *E.coli* BL21(DE3) pLysS cells (Stratagene). *E.coli* cultures were grown to an OD₆₀₀ of 0.8 - 1.0 at 37 °C then induced with 0.33 mM IPTG for 6-8 hours at 25 °C. Human UbcH7 was overexpressed with an N-terminal His₆•tag from a pET vector then purified using metal chelating sepharose followed by cation exchange. The HECT domain of human E6AP (residues 492-852) was overexpressed as a glutathione S-transferase (GST) fusion using pGEX-4T vector and was purified according to a previously described method¹ with a single modification. Following thrombin cleavage to remove the GST moiety, an irreversible thrombin inhibitor (PPACK dihydrochloride, EMD Biosciences) was added at a 5-fold molar excess. Ubiquitin was overexpressed with an N-terminal His₆•tag in a modified pET vector containing a protein kinase A (PKA) recognition sequence¹¹. Recombinant ubiquitin was purified using metal chelating sepharose followed by gel filtration. Labeling of ubiquitin with ³²P was carried out using a PKAce kit (EMD Biosciences) and the manufacturer's recommended protocol. The labeling reaction was terminated with a 10-fold molar excess of protein kinase A inhibitor (PKI 6-22 Amide, EMD Biosciences). UbcH7 and E6AP-HECT domain were dialyzed into the appropriate buffer then concentrated using centrifugal concentrators and quantitated according to the procedure given below. Molar extinction coefficients for all proteins were predicted from the ExPASy ProtParam tool (www.expasy.org). Quantification was carried out in 20 mM KH₂PO₄ and 6.0 M guanidinium hydrochloride pH 6.5 using the absorbance value at 280 nm. Protein concentrations determined using molar extinction coefficients were confirmed using a Bradford assay.

RosettaDesign

Mutations that enhance the affinity between Ubch7 and E6AP were identified using the RosettaDesign algorithm for protein design¹² (rosettadesign.med.unc.edu). To identify a small set of mutations that would increase binding affinity, a large set of independent simulations were performed. In each simulation small clusters of residues at the interface were redesigned and ranked based on their effect on binding affinity and specificity and K96S-Ubch7 and D641K-E6AP ranked highly in both categories. RosettaDesign attributes the enhanced affinity to the formation of an ideal hydrogen bond between Ser96-Ubch7 and Lys641-E6AP when they adopt their most favorable side chain conformations, while the wild type pair, lysine 96-Ubch7 and aspartate 641-E6AP, can only form a weak hydrogen bond when less favorable conformations are adopted.

Fluorescence Polarization Assay

The thiol-reactive fluorescent probe bodipy(507/545)-iodoacetamide (Molecular Probes) was conjugated to Ubch7 using the manufactures recommended protocol. Ubch7 was concentrated to ~100 μ M then buffer exchanged into 50 mM Tris·Cl pH 7.5 and 1 mM TCEP using a PD10 desalting column. The PD10 eluate was stirred for one hour at room temperature. A 20 mM stock solution of bodipy(507/545-IA) suspended in dimethyl sulfoxide (DMSO) was diluted into the Ubch7 solution to a 10-fold molar excess and the conjugation reaction was allowed to proceed overnight, in the dark at 4 °C. The precipitate was pelleted and discarded then 5 mM β -mercaptoethanol (β -ME) was added to quench the reaction. The supernatant containing bodipy-Ubch7 was diluted and run over a PD10 column to separate free probe from labeled protein. Bodipy-Ubch7 was quantified using UV/Vis and a correction factor ($Ab_{S_{280\text{ nm}}}/Ab_{S_{508\text{ nm}}}$) of 0.03 was used to correct for the absorption of the conjugated probe at 280 nm. In brief, the correction factor was determined by conjugating bodipy to a heptapeptide, NH_2 -KGACAGK-COOH (Sigma-Genosys), lacking absorbance at 280 nm then determining the ratio of absorbance at 280 nm and 508 nm of this bodipy conjugated peptide.

Fluorescence polarization assays were carried out on a Jobin Yvon Horiba Spex FluoroLog-3 instrument (Jobin Yvon Inc.) performed in L-format with the excitation wavelength set at 508 nm and the emission wavelength set at 545 nm. Bodipy-UbcH7 and HECT domain were dialyzed versus 20 mM KH₂PO₄ pH 7.0, 150 mM NaCl and 5 mM β-ME. Titrations were performed using a 3 x 3-mm quartz cuvette with a starting volume of 150 μL of wild type or mutant bodipy-UbcH7. Bodipy labeled wild type or mutant UbcH7 was diluted to 100 or 500 nM and the excitation and emission slit widths adjusted between 3.0 and 4.2 nm to give a fluorescence intensity >100,000 counts per second. Wild type or mutant HECT domain was added in increasing volumes from a stock solution of 60 μM or 120 μM. Three polarization readings consisting of 3 averaged measurements were collected for 13-18 concentrations of HECT domain. Data was averaged and analyzed using a model for single site binding according to Equation 1 which was incorporated into Equation 2 to account for the observed polarization.

$$[E2 : E3] = \frac{([E2_t] + [E3_t] + K_d) - \sqrt{([E2_t] + [E3_t] + K_d)^2 - 4 \cdot [E2_t] \cdot [E3_t]}}{2} \quad (1)$$

$$P_{obs} = \frac{(P_{max} - P_o) \cdot [E2 : E3]}{[E2_t]} + P_o \quad (2)$$

where $[E2:E3]$ is the concentration of bodipy-UbcH7 and HECT complex formed, $[E2_t]$ is the total concentration of bodipy-UbcH7, $[E3_t]$ is the concentration of HECT domain from E6AP, K_d is the dissociation constant for the interaction, P_o is the polarization in the absence of HECT domain, P_{max} is the maximum polarization observed when all bodipy-UbcH7 is bound to HECT domain, and P_{obs} is the measured polarization at a given concentration of HECT domain. The data was fit according to

Equation 2 using nonlinear regression with SigmaPlot software to obtain fitted parameters for K_d , P_{\max} , and P_o .

Determination of k_{cat} and K_m for E1-mediated E2 transthioylation

Determination of the kinetic parameters k_{cat} and K_m for the interaction between the human ubiquitin activating enzyme and UbcH7 was performed using slight modifications of a previously published method⁷. The assays were carried out in 100 μ L volumes containing 20 mM Tris-Cl pH 7.5, 50 mM NaCl, 10 mM MgCl₂, 0.2 mM β -ME, 2 mM ATP, 10 mM creatine phosphate, 10 U/ml creatine kinase, 5 μ M ³²P-ubiquitin, 1 nM human ubiquitin E1 (Boston Biochem Inc.), and varying concentrations of UbcH7. The E6AP-HECT domain active site point mutant C820A that lacks the ability to form a HECT~ubiquitin thiolester was used in experiments performed in the presence of high concentrations of HECT domain. These kinetic assays were performed with 200 μ M C820A-HECT or 80 μ M C820A-D641K-HECT. Reaction components minus ubiquitin were allowed to equilibrate 10 minutes before initiating the reaction by the addition of ³²P-ubiquitin. Over the course of four minutes (before significant product accumulation), four aliquots of 20 μ L were removed and quenched in 4X gel loading buffer lacking a reductant. Proteins were separated by SDS-PAGE at room temperature and the gels were dried and exposed to a phosphor screen. ³²P-ubiquitin bands were visualized by autoradiography using a phosphorimager and quantitation of data was performed using ImageQuant 5.0 software (Molecular Dynamics). Background correction for each band was performed by subtracting the volume of counts from a box of equal area in the same gel lane. A lane containing only ³²P-ubiquitin was included on the gel to convert the observed volume of counts to a concentration value. The concentration of active E1 enzyme was determined from a lane lacking UbcH7. Concentrations of UbcH7~³²P-ubiquitin were measured and then plotted to determine the initial rates of thiolester formation. Kinetic parameters k_{cat} and K_m were determined by fitting data to the Michaelis-Menton equation using nonlinear regression (SigmaPlot software). For the assay

containing K96S-UbcH7 and C820A-D641K-HECT, the initial rates of E2~³²P-ubiquitin formation remained linear over the range of K96S-UbcH7 concentrations tested. To set a lower limit for K_m (to 95% confidence), a statistical F test was performed using χ^2 values obtained from the residuals to the fit¹³.

Determination of K_i for HECT inhibition of E1-mediated E2 transthiolation

Reactions were carried out as described above except the E1 concentration was increased to 3 nM, the wild type and mutant UbcH7 concentration was fixed at 500 nM, and the wild type and mutant inactive HECT domain concentration varied from 0 to 100 μ M. Experiments were performed at E1 concentrations below the K_m of the E1-E2 interaction to ensure UbcH7 is not saturated with E1 enzyme. Single time points were taken at 2.5 minutes and data was analyzed as described above. A modified Michaelis-Menton equation (Equation 3) was derived to model competitive inhibition by inactive HECT domain for the E1-E2 interaction. Equation 3 incorporates an E2-E3 binding equilibrium (Equation 4) that is reflected in an apparent inhibition constant, K_i . A baseline offset parameter, b , was also incorporated to account for error in background correction. In Equation 3, the catalytic constant determined from the E1-E2 transthiolation assays in the absence of HECT domain was substituted and the data was fit to K_i , K_m , and b using nonlinear regression (SigmaPlot software).

$$v_0 = \frac{k_{cat} \cdot [E1] \cdot ([E2]_t - [E2 : E3^*])}{K_m + ([E2]_t - [E2 : E3^*])} + b \quad (3)$$

$$[E2 : E3^*] = \frac{([E2]_t + [E3^*]_t + K_i) - \sqrt{([E2]_t + [E3^*]_t + K_i)^2 - 4 \cdot [E2]_t \cdot [E3^*]_t}}{2} \quad (4)$$

where $[E2:E3^*]$ is the concentration of E2 enzyme bound to catalytically inactive HECT domain from E6AP (C820A), $[E3^*]$ is the total concentration of catalytically inactive HECT and K_i is the apparent inhibition constant.

Biochemical Assays of RING E3s

Proteins for biochemical assays of RING E3s were expressed and purified as described previously¹⁴⁻¹⁷. Biochemical assays were performed in 10 μ l in 50 mM Tris-HCl (pH 7.6-8.0), 50 mM NaCl, 10 mM MgCl₂, 5 mM ATP, 1-1.5 mM DTT, 0.3 U/ml inorganic pyrophosphatase, 0.3 U/ml creatine phosphatase, 5 mM creatine phosphate, 2 mg/ml ovalbumin, and NEDD8 or ubiquitin K>R (all lysines mutated to arginines) phosphorylated at the N-terminal PKA site (from pGEX2TK) with $[\gamma\text{-}^{32}\text{P}]\text{ATP}$, at 18°C. Reactions were quenched with an equal volume of 2X SDS sample buffer, proteins were resolved by SDS-PAGE, dried and visualized by autoradiography.

For ubiquitin pathway experiments, inhibition of E1-E2 transthiolation reactions used 5 nM Ube1, 0.5 μ M UbcH5b, 7 μ M ^{32}P -ubiquitin and 250 μ M of the E2-binding domain from ubiquitin's or NEDD8's E1s (termed Ube1^{ufd} and NE1^{ufd}, respectively) for 2 minutes. Ubiquitin modification on the β -catenin peptide (sequence Ac- KAAVSHWQQSYLDSGIHSGATTTAP-NH₂) was examined using pulse-chase. The pulse contained 18 nM APPBP1-UBA3, 0.9 μ M UbcH5b and 2.5 μ M ^{32}P -ubiquitin R7, and formation of the UbcH5b~ ^{32}P -ubiquitin thioester complex was quenched after 1 hour with 230 μ M cold ubiquitin and 90 mM EDTA. The reactions were chased with 0.25 μ M E3 (neddylated split Cul1/Rbx1/ β TCRP1/Skp1), 30 μ M β -catenin peptide and 250 μ M of either NE1^{UFD} or Ube1^{UFD} for 1 min.

For NEDD8 pathway experiments, inhibition of E1-E2 transthiolation reactions used 1 nM APPBP1-UBA3, 0.2 μ M Ubc12, 5 μ M ^{32}P -NEDD8 and 250 μ M NE1^{ufd} or Ube1^{ufd} for 90 seconds. NEDD8 modification of Cul-1 was examined using pulse-chase. The pulse contained 1 nM APPBP1-UBA3, 0.2 μ M Ubc12 and 1 μ M ^{32}P -NEDD8, and formation of the Ubc12~ ^{32}P -NEDD8 thioester

complex was quenched after 7 min with 50 μ M NEDD8, 50 mM EDTA and 0.8 mM Ubc12N26 peptide. The Ubc12N26 peptide was shown previously to efficiently inhibit Ubc12~NEDD8 thioester formation, with no effect on Rbx1-mediated transfer of NEDD8 to Cul1⁶ (and DH and BAS, unpublished results). The reactions were chased with 1 μ M Rbx1-Cul1 and 250 μ M NE1^{ufd} or UbE1^{ufd} for 1 min.

SUPPLEMENTARY DATA

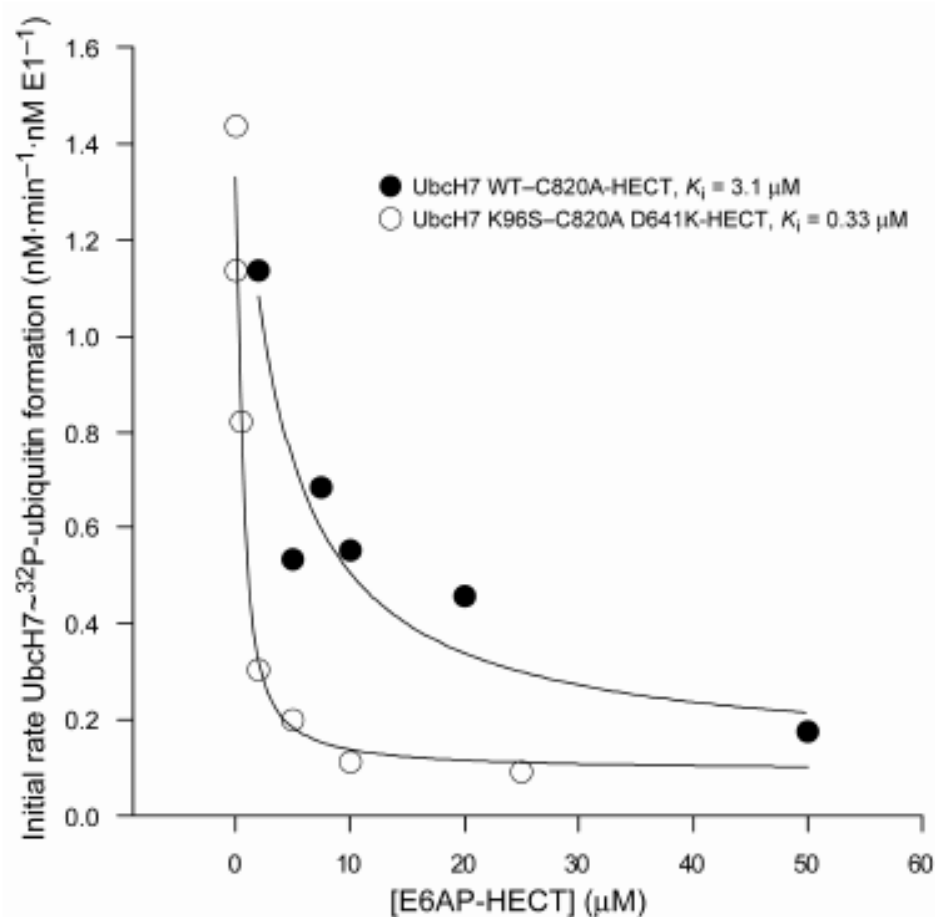


Figure 5.3. Enhanced affinity UbchH7–E6AP-HECT pair inhibits E1-mediated UbchH7 transthiolation at lower E6AP-HECT concentrations. UbchH7~[³²P]-ubiquitin bands were quantitated from kinetic inhibition assays performed in **Figure 5.1b** to determine initial rates of UbchH7~[³²P]-ubiquitin formation. Initial velocity data were fit to a modified Michaelis-Menton scheme to determine an apparent inhibition constant, K_i , for the UbchH7–E6AP-HECT interactions. Kinetic parameters k_{cat} and K_m for the E1–UbchH7 interaction were determined from independent experiments (see **Supplementary Data, Fig. 5.4**) and used in the fitting process. The apparent inhibition constants are consistent with the dissociation constants determined using the fluorescence polarization assay.

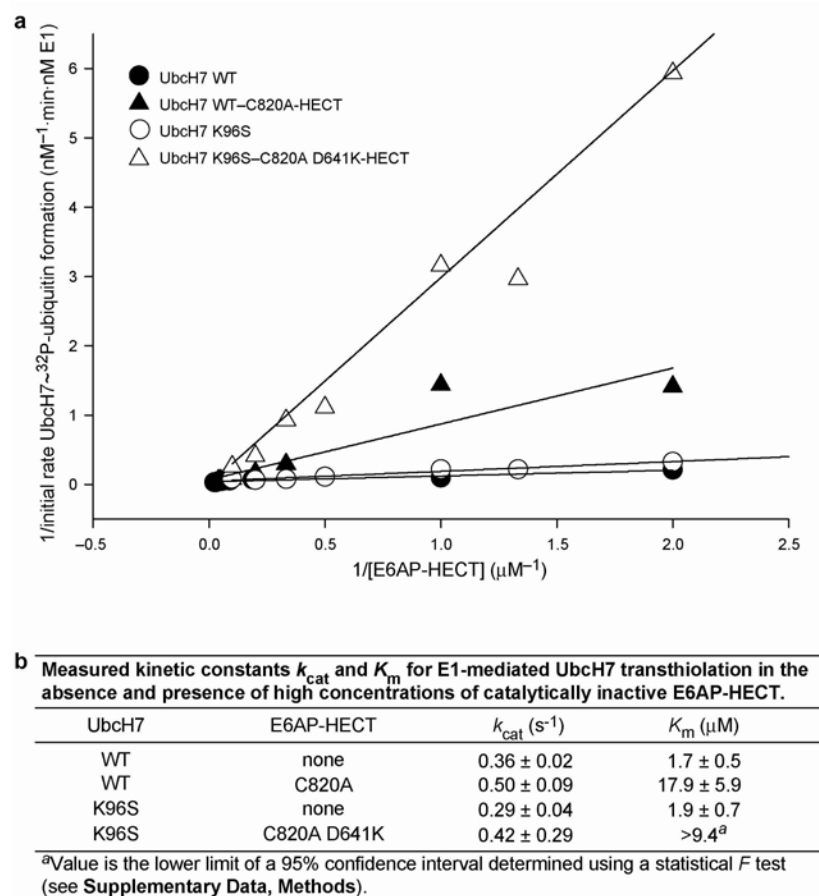


Figure 5.4. Kinetics of E1-mediated UbchH7~[³²P]-ubiquitin formation in the presence and absence of high concentrations of E6AP-HECT. (a) *In vitro* ubiquitination reactions were performed with 1 nM E1, 5 mM [³²P]-Ubiquitin, 2 mM ATP and an ATP regenerating system. Assays were performed at varying E2 concentrations for UbchH7 WT in absence (closed circles) and presence of 200 mM C820A-HECT (closed triangles), and for UbchH7 K96S in absence (open circles) and presence of 80 mM C820A D641K-HECT (open triangles). UbchH7~[³²P]-ubiquitin bands were resolved by SDS-PAGE and quantified to determine the initial velocities of UbchH7~[³²P]-ubiquitin formation. Initial velocities were fit to the Michaelis-Menton equation to determine the kinetic parameters k_{cat} and K_m . (b) Table of fitted kinetic parameters k_{cat} and K_m . Uncertainties in kinetic parameters are reported as standard errors.

Table 5.1 Measured dissociation and inhibition constants for wild type and mutant UbchH7–E6AP-HECT interactions.

UbchH7	E6AP-HECT	K_d (μ M)	K_i (μ M)
WT	WT	5.4 ± 0.8	ND
K96S	D641K	0.10 ± 0.02	ND
WT	C820A	6.0 ± 1.3	3.1 ± 2.7
K96S	C820A D641K	0.12 ± 0.02	0.33 ± 0.12
F63D	C820A	>100	ND

Uncertainties are reported as standard errors. ND, not determined.

REFERENCES

1. Huang, L. et al. Structure of an E6AP-UbcH7 complex: insights into ubiquitination by the E2-E3 enzyme cascade. *Science* **286**, 1321-6 (1999).
2. Zheng, N., Wang, P., Jeffrey, P. D. & Pavletich, N. P. Structure of a c-Cbl-UbcH7 complex: RING domain function in ubiquitin-protein ligases. *Cell* **102**, 533-9 (2000).
3. Huang, D. T. et al. Structural basis for recruitment of Ubc12 by an E2 binding domain in NEDD8's E1. *Mol Cell* **17**, 341-50 (2005).
4. Kuhlman, B. et al. Design of a novel globular protein fold with atomic-level accuracy. *Science* **302**, 1364-8 (2003).
5. Hamilton, K. S. et al. Structure of a conjugating enzyme-ubiquitin thiolester intermediate reveals a novel role for the ubiquitin tail. *Structure* **9**, 897-904 (2001).
6. Pickart, C. M. & Eddins, M. J. Ubiquitin: structures, functions, mechanisms. *Biochim Biophys Acta* **1695**, 55-72 (2004).
7. Siepmann, T. J., Bohnsack, R. N., Tokgoz, Z., Baboshina, O. V. & Haas, A. L. Protein interactions within the N-end rule ubiquitin ligation pathway. *J Biol Chem* **278**, 9448-57 (2003).
8. Kawakami, T. et al. NEDD8 recruits E2-ubiquitin to SCF E3 ligase. *Embo J* **20**, 4003-12 (2001).
9. Carroll, C. W. & Morgan, D. O. The Doc1 subunit is a processivity factor for the anaphase-promoting complex. *Nat Cell Biol* **4**, 880-7 (2002).
10. Deffenbaugh, A. E. et al. Release of ubiquitin-charged Cdc34-S - Ub from the RING domain is essential for ubiquitination of the SCF(Cdc4)-bound substrate Sic1. *Cell* **114**, 611-22 (2003).
11. Tan, P. et al. Recruitment of a ROC1-CUL1 ubiquitin ligase by Skp1 and HOS to catalyze the ubiquitination of I κ B α . *Mol Cell* **3**, 527-33 (1999).
12. Kuhlman, B. & Baker, D. Native protein sequences are close to optimal for their structures. *Proc Natl Acad Sci U S A* **97**, 10383-8 (2000).
13. Shoemaker, D. P., Garland, C. W., and Nibler, J. W. *Experiments in Physical Chemistry* (McGraw-Hill, Inc., 1989).
14. Huang, D. T. et al. A unique E1-E2 interaction required for optimal conjugation of the ubiquitin-like protein NEDD8. *Nat Struct Mol Biol* **11**, 927-35 (2004).
15. Zheng, N. et al. Structure of the Cul1-Rbx1-Skp1-F box^{Skp2} SCF ubiquitin ligase complex. *Nature* **416**, 703-9 (2002).
16. Wu, G. et al. Structure of a β -TrCP1-Skp1- β -catenin complex: destruction motif binding and lysine specificity of the SCF(β -TrCP1) ubiquitin ligase. *Mol Cell* **11**, 1445-56 (2003).

17. Walden, H., Podgorski, M. S. & Schulman, B. A. Insights into the ubiquitin transfer cascade from the structure of the activating enzyme for NEDD8. *Nature* **422**, 330-4 (2003).

CHAPTER VI

CONCLUSIONS AND FUTURE DIRECTIONS

In our studies on the UbcH7–E6AP interface we found 10 side-chains that were important for maintaining a high affinity interaction. Eight of these side-chains are cluster together at the center of the interface and form a hydrophobic interface core. The single residue that contributes most to binding is F63-UbcH7 which provides about 3 kcal/mol to the free energy of binding. This in fact is the primary specificity determining residue for HECT E3s because all E2s known to function with HECT E3s possess a phenylalanine at this position. We found three additional UbcH7–E6AP specificity determining residues at S4, K96, and K100 of UbcH7. Though not determined at the time, the role of K96 and K100 in E6AP specificity could be deduced from a multiple sequence alignment and the UbcH7–E6AP crystal structure. We stumbled upon S4 in attempt to reengineer UbcH5b to interact with E6AP with UbcH7-like affinity. The S4A-UbcH7 mutant was not largely unfavorable for E6AP binding so we had little reason to expect it was dictating specificity. It was the L3S-UbcH5b mutant that ultimately led to generating a high affinity UbcH5b–E6AP interaction. An interesting finding from these studies was that the S94K-UbcH5b protein was unable induce a tighter association with E6AP; this suggests that loop 7 in UbcH7 has an optimal orientation for interacting with E6AP.

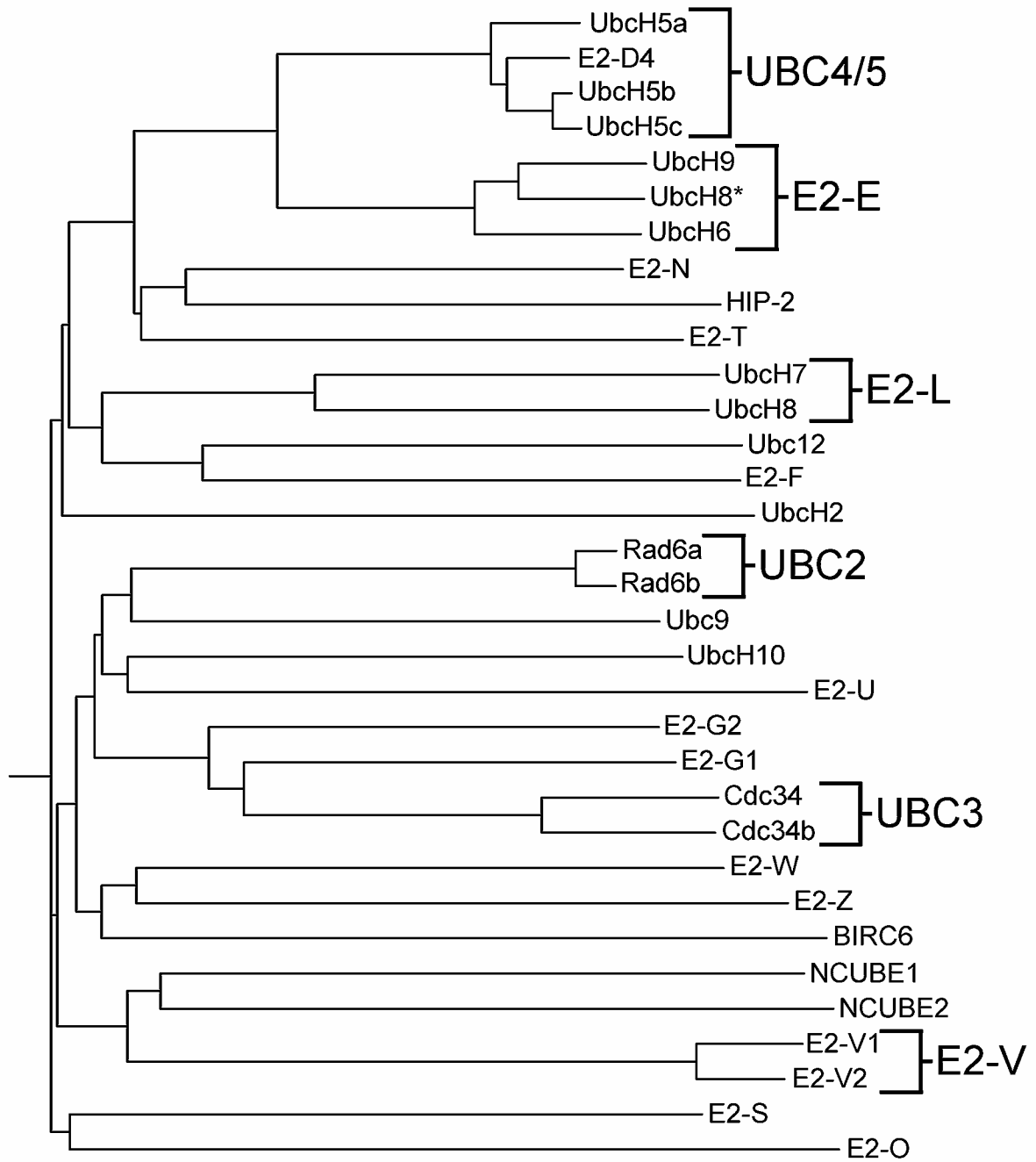
Our results assessing E2–HECT specificity agrees with previous findings. The E6AP protein selectively interacts with the E2-L subfamily while Nedd4L prefers the E2-E and UBC4/5 subfamilies. The basis for Nedd4L selectivity may stem in part from a hydrogen bond interaction not present in E6AP (T58-UbcH5b–D778-Nedd4L). Nedd4L in part disfavors binding UbcH7 because the K96 side-chain sterically clashes with W762 of Nedd4L. More mutations to both Nedd4L and UbcH7 will be tested address some of these interpretations. Smurf2 and Huwe1 were incapable of forming high affinity interactions with E2s. This result for Smurf2 is consistent with previous finding that it possesses side-chains that disfavor E2-binding.

Indeed Smurf2 requires a tertiary protein capable of recruiting and E2 for increased activity. The Huwe1 protein has many additional domains that may facilitate interactions with tertiary, E2-recruiting proteins. Less is known about E2–Huwe1 specificity but our results suggest it functions in a manner similar to Smurf2. Both Huwe1 and Smurf2 express well in *E.coli* and are very soluble so an interesting project in my view would be attempting to enhance an E2–Huwe1 or E2–Smurf2 interaction. I have retrieved and subcloned many other HECT domains that have not yet been characterized. These include the five yeast HECT domains as well as human Itch, WWP1, and Herc5 (an ISG15 HECT E3). In humans there are ~27 HECT E3s and ~33 E2s so ~900 interactions of which I have characterized 60 (~7%).

Manipulating UbcH7–E6AP interactions led to some very interesting findings. We found that just three mutations to these proteins were needed to gain ~1000-fold increase in affinity. I was able to create UbcH7–E6AP pairs containing F63Y and F63H mutations that bound with wild-type or tighter affinity. These could prove useful in the cell because no E2 with a Tyr or His at this position has been shown to function with a HECT E3. The K96S–D641K pair proved quite useful in answering an important question pertaining to the mechanism of poly-ubiquitination. In collaboration with Brenda Schulman's group we were able to show that E2s cannot simultaneously bind E1 and E3 enzymes. This implies that for poly-ubiquitination the E2 must release from the E3 to become recharged with ubiquitin. This study also suggests that nanomolar E2–E3 binding affinities may have adverse effects inside the cell. Other studies which are ongoing aim to better assess whether an increase in E2–E3 binding affinity directly correlates to an increase in E2–E3 activity. This has been a challenging question to answer because ubiquitin transfer from E1 to E2 is slow while E2

transfer to E3 is very fast. The E1 enzyme is currently being purchased from Boston Biochem so creating conditions where E2-E3 transfer is the rate-limiting step has proven difficult. The work conducted in this dissertation has shed insights into many aspects of the ubiquitin pathway and will certainly aid efforts to manipulate E2–E3 interactions and dissect the ubiquitin pathway.

APPENDIX I:
PHYLOGENETIC TREE OF HUMAN E2s



APPENDIX II:
PHYLOGENETIC TREE OF HUMAN HECT E3s

